Catchment-wide evaluation of saturated areas using LIDAR data

Volker Rothmund

Diplomarbeit unter Leitung von Prof. Dr. Markus Weiler

Freiburg im Breisgau

April 2010

Catchment-wide evaluation of saturated areas using LIDAR data

Volker Rothmund

Supervisor: Prof. Dr. Markus Weiler
Co-supervisor: PD Dr. Klaus-Hermann von Wilpert

Diplomarbeit unter Leitung von Prof. Dr. Markus Weiler
Freiburg im Breisgau
April 2010

Dedicated to my father
Werner Rothmund †

Table of contents

List of figures

List of tables

List of symbols

a	Specific catchment	[m]
A	catchment	[m^2]
A_R	Amplitude of the reflection	[W]
A_T	Amplitude of the transfer	[W]
β	Slope in degree	[°]
CIT	Channel initiation threshold	[m^2]
h	convergence factor after HOLMGREN (1994)	[ ]
f_s	Scaling parameter	[m^{-1}]
F_i	Proportion of the area that drains into direction i	[ ]
k_a	Proportion of agreement of all three classes	[ ]
k_s	Proportion of agreement only for the saturated area	[ ]
k_t	Proportion of agreement only for transitional area	[ ]
k_{as}	Proportion of agreement of the aggregated saturated area	[ ]
k_{s+t}	Proportion of agreement of transitional and saturated area	[ ]
λ	Average of TI of the catchment	[ ]
L_i	Contour length	[m]
m	Model parameter for TOPMODEL	[m]
m a.s.l.	Meter above sea level	[m]
n_{eff}	Effective porosity	[ ]
p	Convergence factor after FREEMAN (1991)	[ ]
q	Downslope saturated subsurface flow rate	[m^2/h]
r	Spatially homogeneous recharge rate	[m/h]
SD	Storage deficit	[m]
$\overline{SD}$	Average storage deficit	[m]
S^p	Calculated slope with convergence factor p	[ ]
T_0	Lateral transmissity	[m^2/h]
T	Transmissity	[m^2/h]
TI	Topographic Index	[ ]
z	water depth	[m]
z_i	Local water depth	[m]
$\bar{z}$	Average water depth	[m]

Abbreviations

ArcGis	ESRI ArcGis 9.3, GIS software
CIT / C	Channel Initiation Threshold
D8	Flow direction algorithm after O'CALLAGHAN and MARK 1984
Dinf	Flow direction algorithm after TARBOTON 1997
DEM	Digital Elevation Model
dGPS	Differential Global Positioning System
DTW	Depth-To-Water index after MURPHY et al. 2009
DWD	Deutscher WetterDienst, German National Meteorologie Service
FHM	Forest Habitat Map (FVA)
FVA	Forstliche Versuchs- und Forschungsanstalt Baden-Württemberg
GIS	Geographic Information System
GPS	Global Positioning System
HIT	Hortonian Infiltration Theory
INS	Inertial Navigation System
LGL	Landesamt für Geoinformation und Landentwicklung, Baden-Württemberg
LIDAR	LIght Detection And Radar
MD	Flow direction algorithm after QUINN et al. 1991
MDinf	Flow direction algorithm after SEIBERT and MCGLYNN 2007
SAGA	System for Automated Geoscientific Analyses, GIS Software
Sg	Slope after the global method
St	Slope after the method of TARBOTON (1997)
Sz	Slope after the method of ZEVENBERGEN and THORNE (1987)
TI	Topographic Index of TOPMODEL (BEVEN and KIRKBY 1979)
TOPMODEL	TOPography based hydrological MODEL (BEVEN and KIRKBY 1979)
VDG	Vertical Distance to potential Groundwater table
VSC	Variable Source Concept

Acknowledgements

First, I would like to thank my supervisor Prof. Dr. Markus Weiler for his guidance throughout this research. During my work his advices, discussions and practical support were very helpful. But also his understanding on a personal level helped me a lot.

I would also like to thank PD Dr. Klaus-Hermann von Wilpert for the co-supervising and the institution FVA for making this work possible.

Thanks also to Volker and Olaf from the SAGA user forum, for their essential help with my problems with the software. I strongly recommend everybody who works with SAGA to be part of this forum, reachable on the official SAGA webpage. You get excellent help there!

I also would like to thank my friends for their support especially those who did the proofreading.

Finally, I would like to thank my family and especially my love Maria, for their all-around support which contributed a lot to this work.

Abstract

With their ability to generate saturation overland flow saturated areas are a very sensitive and important factor in hydrology. When occurring they can majorly influence the water quantity and quality. Therefore, a correct prediction of their spatial pattern is of utmost importance.

The major influence on generating saturated areas is the topography making its attributes useful for modeling saturated areas. For this purpose the Topographic Index (TI), which is part of TOPMODEL (BEVEN and KIRKBY 1979), was applied as a predictor in many preceding studies. However, in none of them a satisfying modeling of saturated areas was possible. A reason for that was the poor quality of the digital elevation model (DEM) on which the calculations of the TI are based in many of these studies.

For this study a new level of quality for the DEM was available, the LIDAR DEM. It is a high resolution DEM with improved horizontal and vertical accuracy. The aim of the study was to analyze if better information about the topography also results in better modeling of the spatial pattern of saturated areas. For this purpose many variations of the TI and an additional approach, the vertical distance to groundwater table, were tested on three different catchments in South-Western Germany

However, with its detailed information about the topography, the LIDAR DEM led to new problems for modeling hydrologic applications, like calculating flow paths. Additionally, the groundwater table might have been better related to a smoothed topography than to the detailed LIDAR DEM, since best results were obtained for a coarsened 10 m grid DEM which was based on the original 1 m LIDAR DEM. With it, the most divergent variation of the TI emerged to perform best and a transfer of the method for ungauged catchments seems to be possible.

Compared to earlier studies the new DEM data slightly improved the performance, but the results remain bipolar: whereas approximately half of the saturated areas of the three catchments could be well modeled it was not possible for the rest. Thereby, the results of the study indicate that there are more driving forces on generating saturated areas than only the topography and the methods applied in this study might have conceptual errors. These factors should be considered in further examination. To implement them in the method which was found to be best in this study and finally to model the spatial patterns of saturated areas correctly, provides a further challenge for research.

Keywords: saturated areas, Topographic Index, Vertical Distance to Groundwater Table, LIDAR DEM

Zusammenfassung

Da auf gesättigten Flächen Sättigungsoberflächenabluss entstehen kann, stellen diese eine sehr sensible und einflussreiche Größe in der Hydrologie dar. Dort wo sie auftreten, können sie die Wasserquantität und –qualität entscheidend beeinflussen. Daher ist eine genaue Vorhersage ihrer räumlichen Ausdehnung von größtem Wert.

Den Haupteinfluss auf die Entstehung von Sättigungsflächen hat die Topographie, welche den wichtigsten Faktor für die Modellierung von Sättigungsflächen darstellt. Aus diesem Grund wurde der Topographische Index (TI), ein Teil des Modells TOPMODEL (BEVEN and KIRKBY 1979), von vielen vorherigen Studien als Werkzeug zur Modellierung von Sättigungsflächen verwendet. Jedoch war es in keiner dieser Studien möglich, die räumliche Ausbreitung von Sättigungsflächen korrekt widerzugeben. Ein Grund dabei war die schlechte Qualität der digitalen Höhenmodelle (DEM), worauf die Berechnungen der TIs basierten.

Für diese Arbeit stand ein DEM mit einem neuen Qualitätsniveau zur Verfügung, das LIDAR DEM. Dieses hochaufgelöste DEM verfügt sowohl über eine verbesserte horizontale als auch vertikale Genauigkeit. Das Ziel dieser Arbeit war es nun, zu untersuchen, ob diese verbesserte Datengrundlage auch zu einer verbesserten Modellierung der räumlichen Ausdehnung von Sättigungsflächen führt. Dafür wurden verschiedene Variationen des TI und ein zusätzlicher Ansatz, der „Vertikale Distanz zum Grundwasserspiegel-Index“, in drei verschiedenen Einzugsgebieten in Südwestdeutschland getestet.

Das LIDAR DEM mit einer Rasterbreite von 1 m führte mit seinen detaillierten Geländeinformationen jedoch zu neuen Problemen bei hydrologischen Anwendungen, wie z.B. bei dem Bestimmen von Fließwegen. Zusätzlich schien der Grundwasserspiegel besser mit einer geglätteten Geländeoberfläche übereinzustimmen: Die besten Ergebnisse lieferten Modellierungen für ein von 1 m auf 10 m Rasterbreite vergröbertes DEM. Dabei kristallisierte sich die divergierendste Variation des TI als beste Methode heraus und eine Anwendung dieser für ungemessene Einzugsgebiete scheint möglich.

Verglichen mit vorangegangenen Arbeiten führte die neue Datengrundlage zu leicht besseren Ergebnissen, jedoch blieben diese zwiespältig. So war es nur möglich, ungefähr die Hälfte aller Sättigungsflächen der drei Einzugsgebiete zu modellieren. Dabei deuten die Ergebnisse an, dass für einen Teil der Sättigungsflächen andere Einflussfaktoren als die Topographie alleine mitentscheidend sind und die angewendeten Methoden möglicherweise konzeptionelle Fehler beinhalten. Diese Faktoren sollten in weitergehenden Untersuchungen berücksichtigt werden. Es stellt

eine weitere Herausforderung für die Wissenschaft dar, diese Faktoren in die in dieser Arbeit als beste befundene Methode einzufügen, um schließlich zu einer korrekten Modellierung der räumlichen Ausdehnung von sättigungsflächen zu gelangen.

Schlüsselbegriffe: Sättigungsflächen, Topographischer Index, Vertikale Distanz zum Grundwasserspiegel-Index, LIDAR DEM

1 Introduction

Overland runoff is a very sensitive variable in catchment hydrology. Its velocity can be much higher than it is possible for water moving within the soil and it so can influence the water quantity and quality at specific points strongly.

In humid regions, the infiltration capacity of the soil remains high unless the dense vegetation cover is disturbed or the soil is compacted. Hence, Horton overland flow is confined to such locations as roads and parking lots, skid trails in forests, some ploughed fields, artificial fills, and other areas that have been denuded of their vegetation. In those regions, however, that have not been severely disturbed, Horton overland flow does not occur (DUNNE et al. 1975). A major process that generates storm runoff in these regions is saturation overland flow which is a combination of return flow and direct precipitation on saturated areas. The importance of saturation overland flow was suggested by DUNNE and BLACK (1970a,b) from field studies in northeastern Vermont (DUNNE et al. 1975).

Although saturated areas often cover only a few percent of a whole catchment they can control its reactions. For instance UHLENBROOK and DIDSZUN (2005) showed that runoff from saturated areas has major influence on generating stormflows, even though the saturated areas covered only about 8% of the study area. With the help of tracers they could prove that the quick and strong reaction in hydrographs to precipitation events was mainly related to overland flow generated on saturated areas. It is therefore obvious that for flood management the knowledge about extent and location of saturated areas is essential.

With their ability to generate overland flow saturated areas are also enhanced hydrological sensitive with respect to their potential to transport contaminants with quick runoff to perennial water bodies. In a study of WALTER (2000) for example they could reduce water pollution risk for a New York City water supply watershed by 20%. They could manage that as the agriculture manure was excluded for sensitive saturated areas which only covered 10% of the whole catchment. Knowing the location and extent of saturated areas provides therefore a basis or a starting point for water quality risk assessment and developing water quality management practices for example for non-point source pollution.

Regarding the importance of saturated areas highlighted above it is obvious that it would be of great value to know their location and dimension. However, apart from areas where intensive studies are conducted, for large wetlands (saturated areas) or for wetlands of ecological interest, the spatial distribution of wetlands, especially for small wetlands scattered in the landscape, is not well known (MEROT et al. 2003). As topography is a major factor for the development of saturated areas and digital elevation models (DEM) with increasing data quality become more and more available, it is therefore proposed to evaluate spatial patterns of saturated areas on basis of the catchment's topography.

1.1 State of the art

From the beginning of the history of hydrology there was no agreement about saturated areas and its effects on a catchment. Thus, in the first part the discovery of the importance of saturated areas for hydrology is shortly outlined. In the following the evolution of topographic methods for evaluating saturated is summarized and several studies will be presented which all use topographic information as an indicator of soil wetness or saturated areas.

1.1.1 Saturated areas

The first traditional concept how stormflow is generated was introduced by HORTON (1933, 1945). The Hortonian Infiltration Theory (HIT) says that overland flow is generated when the effective precipitation rate exceeds the infiltration rate of the soil. When this Hortonian overland flow reaches a river quickly a stormflow might develop.

One of the first studies where it was shown that the traditional HIT was not applicable for humid regions was BETSON (1964). He tried to develop a mathematical model based on the HIT which calculates storm runoff from precipitation data. This resulted in large errors comparing observed with predicted results. He revised his model so that the runoff is generated only by a small part of the catchment. This approach maintained unusual good statistical control and the low percentage of the contributing area of only a few percent of the whole catchment is surprising (BETSON 1964). This so called partial area concept is confirmed in a study of RAGAN (1968). He analyzed a series of storms which showed that only a small portion of the watershed ever contributed flow to the storm hydrograph. The contributing area was found to be a function of storm duration and intensity and, rather than being uniformly distributed along the length of the channel, it existed in the form of localized zones of intense contribution. The results of the study illustrated that there was a need for a re-evaluation of some of the traditional methods used for runoff computations. Further, any parametric model developed for the synthesis of hydrologic events should be able to reflect partial area contributions (RAGAN 1968).

It was then HEWLETT and HIBBERT (1967), who proposed a new conceptual model which is an independent and new approach compared to the HIT. They assumed that subsurface flow regulates the fast response of a catchment and is responsible for generating a stormflow event. According to the theory that happens when subsurface water moves downhill and gets concentrated at some areas near a river. When this water coming from upper regions exceeds the capacity of the area to transmit it, the water will come to the surface and overland flow will be generated which they call a growing of channel length. A fraction of the direct runoff produced on these areas consisted of the actual drops falling on the saturated area during the event and the other fraction was return flow of water already stored in the soil mantle before the event. Because this overland flow is produced by saturated areas that, according to their theory, are varying rapidly in size this concept is called variable source concept (VSC) (HEWLETT and HIBBERT 1967).

Experimental work by DUNNE and BLACK (1970a) has thrown doubt on the role of subsurface stormflow from hillsides as major contributor to storm hydrographs in upland watersheds of northern Vermont (DUNNE and BLACK 1970b). The main findings of their studies were first, that there was no Hortonian overland flow as the rainfall intensity did not exceed the infiltration capacity of the soils. Second, that subsurface stormflow was not an important contributor to the storm hydrograph in their watershed, despite soil conditions that are generally considered ideal for such mechanism. Third, that the major portion of storm runoff is produced as overland flow on small saturated areas close to streams. The remainder of the watershed acts mainly as a reservoir during storms, and between storms it supplies base flow and maintains the wet areas that produce storm flow. Compared to the variable source theory of HEWLETT and HIBBERT (1967) this would be the subsurface flow which regulates the behavior of the small runoff producing wet areas. Runoff from these wet areas is supplied by water escaping from the ground surface (return flow) to reach the channel as overland flow and by direct precipitation onto saturated area which is essentially an expanded stream system (DUNNE and BLACK 1970a; DUNNE and BLACK 1970b). It is the ability to generate saturated overland flow which makes an area important for generating stormflow. The location of the saturated areas was found to depend on the topographic position, soil profile characteristics, depth to water table, antecedent condition of the topsoil, and the intensity and duration of rainfall. Comparing three plots located in a concave, planar and convex hillside it was the concave plot which distributed saturation overland flow. As these saturated areas were only on small areas of the catchment and they did expand and contract during the time their findings confirmed the partial area concept (BETSON 1964; RAGAN 1968) and the variable source area concept (HEWLETT and HIBBERT 1967). This new concept provides an attractive alternative to the Horton and subsurface storm flow models as the basis for a study of storm runoff production in an area such as Vermont. It also provides a point of departure for models of catchment behavior not based on infiltration theory (DUNNE and BLACK 1970a; DUNNE and BLACK 1970b).

In the study of DUNNE et al. (1975) they tried to combine the concepts of HEWLETT and HIBBERT (1967) and DUNNE and BLACK (1970b). There is a general consensus that in humid regions storm runoff is generated on relatively small areas of the catchment, and that these areas vary during and between storms. They so confirmed that in humid regions the infiltration capacity of the soil remains high unless the dense vegetation cover is disturbed. Hence, Horton overland flow is confined to such locations as roads and parking lots, skid trails in forests, some ploughed fields, artificial fills, and other areas that have been denuded of their vegetation. But there are at least three processes that generate storm runoff and their relative importance varies with topography, soil, antecedent wetness and storm size. These sources of storm runoff are subsurface storm flow, return flow, and direct precipitation onto saturated areas. These last two processes may be grouped together under the title, saturation overland flow. (DUNNE et al. 1975). Where soils are well-drained, deep and permeable, and steep hillsides border a narrow valley floor, subsurface stormflow dominates the hydrograph volumetrically, but emerges from the ground surface over only limited zones of the catchment. The area that can supply saturation overland flow, therefore, is small. When on the other hand slopes are gentler, soils are thinner and valley bottoms are more extensive also the saturation overland flow is more extensive, and becomes the primary contributor of storm runoff. It is obvious that it would be valuable to be able to recognize and predict which processes influence the stormflow in which amount and where. They so presented a few suggestions of methods that are being used to recognize and predict the size and location of variable saturated areas. The best method of evaluating the size, location and variation of saturated zones is by repeat field mapping, but that is only possible for small catchments. They purpose soil characteristics, vegetation and topography as indicators for saturated areas. Among them topography is the most obvious feature as you can find saturated areas in flat valleys or swales. There is a probability of developing a saturated zone on low lying ground with a considerable drainage area above it to supply seepage throughout the year. But by that time they had to confess that it is difficult to develop quantitative prediction from topography (DUNNE et al. 1975).

However, HEWLETT and TROENDLE (1975) outlined the importance of the right interpretation of the variable source concept and separated the concept strict from others as the HIT or the partitial area concept of BETSON (1964). Regarding problems like the non-point water pollution it is not enough to know how rain is transferred to stormflow but also the flow paths are important. If the basic core of the simulation model does not accommodate the variable source concept, but is rather made up from linear-distributed, Hortonian theory with modifications, the fitting process will most likely not reveal the physical discrepancy. Such models may predict mass outputs satisfactorily, but the hazard will lie in the interpretation of the management cause of the effect predicted (HEWLETT and TROENDLE 1975). Therefore they presented a variable source area model. The idea of that model is that every first order stream can be divided in little sections with each having its own subcatchment. The spatial pattern of stormflow source areas of each subcatchment is then strongly dependent on its topography in particular its slope. The variable source area concept and the model that eventually arises from it will provide an antidote to our historically strong dose of Hortonian runoff theory and will serve as a centralizing precept for relating management activities to stream water quality, quantity, timing and energy disposition (HEWLETT and TROENDLE 1975).

Subsequently, BEVEN and KIRKBY (1979) presented a physically based, variable contributing area model of basin hydrology. Later it became known as TOPMODEL which represents the importance of the topography for the model as it is the abbreviation for TOPography based hydrological MODEL (BEVEN 1997). One of the basic ideas is that areas with the same topography react to a given input also the same. For that characterization the Topographic Index (TI) was implemented in the model which is calculated as the natural logarithm of the quotient of the specific catchment and the slope. The specific catchment is an estimation of the accumulation of flow at any point as surface or shallow subsurface runoff on the landscape, and it integrates the effects of upslope contributing area and catchment convergence and divergence on runoff (MOORE et al. 1991). The slope represents the hydraulic gradient. The higher the TI is the less water is needed as an input to generate saturation overland flow. This TI can so be used as an indicator for saturated areas. It can be noted, that for a given input and with the assumption of homogeneous soils, it is then the topography only which is the responsible factor where there is a saturated area and saturation overland flow can occur. Hence, the TI supplies a basis for many studies which tried to evaluate saturated areas with topographic information. By that time there was no doubt on the importance of saturated areas anymore. The presented papers highlight the topography as a main factor for the location and size of these areas.

1.1.2 Evaluation of saturated areas with DEMs

When TOPMODEL was presented by BEVEN and KIRKBY (1979) it was still common to evaluate the topographic information manually out of maps. Therefore it was inconvenient and time intensive to calculate topographic attributes. With the upcoming availability of Digital Elevation Models (DEM) and the possibility to make quantitative analyses with computer software so called Geographic Information System (GIS) calculation of topographic information got much more comfortable and various approaches began to develop. HEERDEGEN and BERAN (1982) came to the conclusion that contour data by that time probably is the source of most potential information, but for catchment-wide calculation of topographic attributes, like plan and profile curvature, slope and slope vector, a more generalized approach would be useful. Therefore they suggested substituting the contours by spot heights for regular sized grids and create a uniform matrix. Mathematical algorithms can then be utilized to calculate topographic attributes. A method to calculate flow paths within a DEM was presented by

O'CALLAGHAN and MARK (1984). First sinks are filled in the original DEM to obtain a depressionless DEM. The flow direction of each grid cell is the direction to one of its eight nearest neighbors based on the direction of steepest descent. That is why it is often called D8 flow algorithm. Then a flow accumulation can be calculated which counts all the cells that drain into one. Multiplication with the grid area results in the specific catchment area for a cell. MOORE et al. (1991) give a review of hydrological, geomorphological, and biological applications of digital terrain analyses. One finding is that runoff from saturation zones is a threshold process and areas producing saturation overland flow can so be identified using a threshold wetness index. Thereby, the most commonly used topographic attributes as wetness indexes are slope, specific catchment area and, in particular, the TI. One study, which compared the TI with the curvature, was conducted by BURT and BUTCHER (1985). They analyzed a 1.4 ha hillslope which is characterized by steep slopes, large hollows, and permeable soils over impermeable bedrocks and high rainfall. Therefore 10 m gridded altitude data was created using a Nikon Electronic Distance Meter and the two topographic indexes were compared to soil moisture distribution which was measured in the instrumented hillslope. As a curvature index the plan curvature was used (EVANS 1980) which was later further developed by ZEVENBERGEN and THORNE (1987). Neither index is entirely satisfactory for predicting soil moisture on the hillslope, although the TI seemed to work better. As an alternative index the product of TI and plan curvature provides equally acceptable results. The indices, especially the alternative index, provide excellent predictions of soil moisture distributions when soils are wet, but are very poor predictors when the slope is much drier (BURT and BUTCHER 1985).

The major disadvantage of the D8 flow algorithm (O'CALLAGHAN and MARK 1984) is that the flow direction is limited to only one of the eight neighbor cells. This may be a maintainable limitation for the convergent flow of a river, but for the more divergent flow on hillslopes it seems to be a considerable limitation. Consequently, QUINN et al. (1991) presented a new flow algorithm (MD) which is focused on the divergent flow character. Here, a cell drains to all its lower neighbors weighted by the respective slope compared to the others. The specific catchment needed for the TI is then calculated by the summation of all the parts of the cells that drain into the cell of interest. The local slope is calculated as the average of all the downslopes. Comparing the two TIs calculated with the different flow algorithms (QUINN et al. 1991) it was found that on hillslopes the MD gives a more realistic pattern of accumulated area, but the D8 on the contrary is more suitable once the flow has entered a more permanent drainage system in the valley bottom. That is why they suggest overlying the MD method with a permanent drainage system, so that once hillslope flow reaches a channel the D8 method is be used to route it out of the catchment. They also compared two different grid sizes, 12.5 m and 50 m, and noticed that there is a shift to higher TI-values as the grid size increases. To avoid unrealistic high divergence flow calculated with the MD flow algorithm HOLMGREN (1994) modified the proportioning of outflow of a cell. Thereto an exponent h was implemented in the slope weighting function. For the value h=1 the weighting function is the same than in the original MD. The higher the exponent gets the more convergent the flow distribution will be. A value of around 100 is equivalent to the single flow direction algorithm (QUINN et al. 1995). As a result of their tests comparing different exponents they give the range 4 – 6 as a recommendation to get the most realistic flow distribution.

The effect of DEM grid size on the calculated TI and its elements was the central question of ZHANG and MONTGOMERY (1994). In order to analyze this effect they used a digitalized topographic map and a DEM obtained from low-altitude aerial photographs using a stereo digitizer at a density about every 10 m for two small catchments in the western United States. Out of the original DEMs they generated DEMs with the grid size of 2, 4, 10, 30, and 90 m and calculated the topographic attributes and the TIs for each dataset. As a result the slope and the specific catchment turned out to be sensitive to the grid size: whereas the mean slope got smaller as grid size increased the specific catchment area get normally larger as grid size increases. Consequently, the mean TI gets higher as grid size increases. The effect of grid size on spatial patterns of TI is even more striking. Detailed features that appear on finer grid DEMs are obscured on coarser grid DEM with a progressive loss of resolution for both the drainage network defined by the higher values TI and hillslopes associated with the lower values of TI (ZHANG and MONTGOMERY 1994). Summarizing they suggest that the most appropriate DEM grid size for topographically driven calculations should be somewhat finer than the hillslope scale identifiable in the field. Hence, they propose that for their catchments and for many others a 10 m grid size is most appropriate to use, as it offers a good compromise between increasing resolution and data handling requirements when modeling surface processes in a variety of landscapes (ZHANG and MONTGOMERY 1994). They also mention that decreasing the grid size beyond the resolution of the original DEM does not improve accuracy of the land surface representation, but instead offers potential interpolation errors. On this problem WOLOCK and PRICE (1994) paid additional attention and they also analyzed the effect of resolution. Thereto they used a 30 m and 90 m grid from a 1:24,000 and a 1:250,000 scale topographic map, respectively. On the effect of resolution they were in general agreement with ZHANG and MONTGOMERY (1994). The effect of the 1:250,000 scale compared to the 1:24,000 scale were similar compared to the effect of a coarser resolution to a finer resolution as it has also a smoothing effect on the DEM. Therefore the mean slope of the 1:250,000 scale was lower and the mean specific area was higher than at the 1:24,000 scale. Finally the mean TI of the 250,000 scale was higher than the one of the 1:24,000 scale. In the conclusion it is noted that a finer and more detailed DEM is not necessarily a better basis for estimating the water table for saturated areas as it gives only a more realistic representation of the real surface area. The water table configuration, however, may be smoother than the land surface topography and may be related more accurately to a coarser resolution or less accurate map scale DEM (WOLOCK and PRICE 1994).

The MD flow algorithm for computing the TI was used in the study of MEROT et al. (1995) to evaluate the location and extent of saturated areas in two contrasting catchments with different topography, geology and mean rainfall in Brittany, France. 40 m grid DEMs were created based on 1:25000 ordnance survey maps. A comparison to hydromorphic characteristics of waterlogged soils determined with 1:25000 soil survey maps was used for validation. The agreement between simulated and validation data was best for both end of the wetness scale whereas for the middle part poor results were obtained. They also found that for the steeper catchment the results were in general better than in the catchment with gentle slopes. With a cell by cell comparison they so obtained for the steeper catchment 84% agreement for the well drained soils and a 56% agreement for the poorest drained soils. As the TI is a continuous variable a threshold is needed which was defined so that the area of the simulated waterlogged soils was as big as that derived from the soil survey maps. These threshold values were different for the two catchments which lead to the conclusion that they are corresponding to the differences in catchment bedrock. In identical topographic conditions, the more permeable soils (Brioyerian shale) saturated earlier than the less permeable soils (on granite) (MEROT et al. 1995). Limitations in their study were found to be first, that the TI method does not account for some major factors leading to the development of waterlogging such as the amount of rainfall, soil surface properties and the structure of the agricultural landscape and drainage. Second, that as shown in WOLOCK and PRICE (1994) and ZHANG and MONTGOMERY (1994) the quality of the DEM with a 40 m grid size was just the minimum required for analyzing topographic information. Nevertheless the results emphasized the major role of topography for determining the positions of saturated areas.

QUINN et al. (1995) picked up the studies above and gave additional a new update for it. First, they confirmed the findings of WOLOCK and PRICE (1994) and ZHANG and MONTGOMERY (1994) that larger grid size DEMs exhibit a bias towards larger index values. Second, they also confirmed that the manipulation of the original MD algorithm by HOLMGREN (1994) offers a helpful tool for more realistic calculations of the TI. And third, they found that the channel initiation threshold (CIT) introduced by MORRIS and HEERDEGEN (1988) offers also a valuable tool to improve the calculation of the TI. The underlying idea is that the movement of water within a river is different than that in a hillslope. Most of the water will move out of a cell without interacting with the soil and so the assumption of homogeneous transmissibility in the whole catchment is not fulfilled. Water also tends to move in its given river network and is therefore strongly convergent. Reaching CIT the perennial rivers can be split from the rest of the catchment and have special treatment for river cells like reduction of specific catchment area, single flow algorithm (D8 or MD with a high h), or even exclusion. Finally, their main conclusions are that there is not only one solution for calculating the TI and in most catchment studies the pattern of the index will probably have to be optimized to fit the field observations. For those optimizations the user can use the h parameter as well as CIT, or combine them. However, h values and CITs are not transferable between grid resolution (QUINN et al. 1995).

THOMPSON and MOORE (1996) analyzed the relation between water table depth which was measured at 59 wells in a shallow forest soil and topographic characteristics derived from gridded DEMs. The study area was a catchment of about 0.04 km^2 located 80 km east of Vancouver, Canada. Three different DEMs with a resolution of 4, 8, and 16 m grid size were produced by ground survey with an average spacing of about 5 m with a higher density in topographically more complex areas and lower in smoother terrain. The calculated topographic characteristics were the curvature and the TI with its components. Those were calculated using a D8 flow algorithm. The TI provided generally more reliable classifications than the exclusive applying of the specific catchment, slope, and curvature as separate predictor variables (THOMPSON and MOORE 1996). It has to be mentioned that comparing the probability of saturation at a well with the topographic attributes had weak and nonlinear relation. They could only be used as threshold, e.g. there was no saturation where hillslope was convex or there was no saturation where TI was less than 6. But on the contrary not every concave hillslope or every point with TI more than 6 was saturated. It was notable that the results were bipolar: at some wells water tables were predicted accurately and at some completely wrong. This might either be caused by errors in the calculated TIs or phenomena not related to surface topography. Their recommendation of an optimum grid size is 10 m.

As studies like BURT and BUTCHER (1985) and THOMPSON and MOORE (1996) have shown, calculation of TI is very sensitive to the specific catchment area. It is therefore important that flow directions and therewith the specific catchment area are accurately determined. Both common flow algorithm by that time, D8 and MD, are restricted to the fact that the outflow of a cell can only occur in 8 possible directions. Therefore TARBOTON (1997) introduced a new flow algorithm Dinf with the advantage that the flow out of a cell can have any direction between 0° and 360°. The procedure is based on representing flow direction as a single angle taken as the steepest downward slope. If the steepest slope falls between two main directions the flow is apportioned between the two neighbor cells according to how close the flow direction angle is to the direct angle to those cells. The specific catchment area is calculated as in the MD flow algorithm. Results from the Dinf were compared to D8 and MD and performed better (TARBOTON 1997).

GÜNTNER (1997) used TOPMODEL in the 40 km^2 large Brugga catchment in the southern Black Forest, Germany, in his diploma thesis. One of the main subjects was a correct considering of saturated areas within the model. Therefore he did field observations and mapped all saturated areas and compared those with different calculation methods of TI. This central subject was later published in GÜNTNER et al. (1999). As QUINN et al. (1995) proposed he used the MD algorithm and used the Holmgren parameter and CIT as tools to optimize the calculation so that they fit best with the observed patterns of saturated area. Cells with an upslope area exceeding CIT and all following downslope cells in the direction of the steepest gradient are marked as channel cells. The specific catchment of these was set to CIT for the calculation of TI. The threshold for TI was set as in MEROT et al. (1995). As a result of the field observations 6.2 % of the whole catchment was mapped to be saturated areas. The optimized parameter set was found to be h = 10 and CIT = 100,000 m^2 which was related to a cell by cell agreement of 34.5 %. The poor agreement was explained by difficulties when comparing different data structures as TI was raster and field observation vector data. Furthermore, the assumptions for using the TI were not valid in the study area as soils are not homogeneous and different recharge areas exist as precipitation varies. The factor geology is also responsible for the appearance of some saturated areas which cannot be represented by topography only. Finally, the grid resolution of 50 m used in the study was too coarse to reflect adequately the small scale pattern of mapped saturated areas, especially in the steeply slope Brugga basin.

RODHE and SEIBERT (1999) wanted to evaluate the use of the TI for predicting the occurrence of mires, as they are the wetness end of a wetness spectrum, in two Swedish catchments. They only obtained poor agreement of predicted and observed mires especially in the catchment with small scale topographic features. This was mainly due to the too coarse DEM with a grid size of 50 m^2. Nevertheless, they introduced an interesting new way how to calculate the slope in the TI which is assumed to be more related to the hydraulic gradient. This is a global slope method which calculates the horizontal distance needed until a selectable vertical distance following the steepest direction is reached. The resulting slope of those two distances gives the global slope at the point of interest. This method is described more specific later in HJERDT et al. (2004) where they show that the global slope is less sensitive to grid size than the local slope.

A more general approach for deriving topographic characteristics along a river network was given by MCGLYNN and SEIBERT (2003) whose intention was to determine hydrologic characteristics comparing streams with different order. They studied the relation of riparian area and the respective hillslope area for specific stream reaches. They found for a catchment in New Zealand that the higher the stream order becomes the larger is the riparian width. On the contrary they found that the higher the stream order the smaller the local hillslope area is that contributes to the specific stream reach. Hence, the ratio of riparian area to hillslope area is smaller at the first order streams than at high order streams. That is an interesting finding and when it is compared to the theory of variable source area (HEWLETT and HIBBERT 1967) under the assumption of hydrologic homogeneity it leads to the conclusion that there should be more saturated areas where the ratio is small: at first order streams. This was later confirmed by MOURIER et al. (2008) where they found that the extent of hydromorphic zones remains similar for orders of 1 to 3, but decreases significantly for orders of 6 and 7. By contrast, simple TI modeling results in higher values for high order rivers. Therefore, TI modeling appears effective in upper catchment settings (1st, 2nd and 3rd order) but is limited in high order settings where the indices prove to be inappropriate (MOURIER et al. 2008).

In an extensive study of MEROT et al. (2003) they used a new climato-TI for predicting wetlands distribution along an European climate gradient. They weighted the specific catchment area, which was calculated with MD, with the effective rain for the area of concern. For one of the catchments where they knew that soils are highly heterogeneous and adequate data was available they used the soil-TI where the transmissivity is implemented. They also used a new way to calculate the hydraulic gradient and used instead of the local slope, the slope between the point of interest and the river following the flow path. The grid sizes of the DEMs varied from 10 m to 50 m. This climato-TI was able to predict the structure and general areal extent of wetlands without any local calibration of the model in many cases. Nevertheless, for geological complex area as sedimentary and morainic mountainous catchments with a soil surface permeability heterogeneity the climato-TI failed to predict the wetland location. The exact location of the wetland was often poor which was mostly due to the current poor quality of the DEM (MEROT et al. 2003). Whereas they tried to validate one approach of calculating a TI for evaluating saturated areas in different climate regions GÜNTNER et al. (2004) tried to validate many different approaches of TIs in one region and optimize them with additional data of soils and climate. They modeled the same catchment as in (GÜNTNER 1997; GÜNTNER et al. 1999) and its neighbor catchment also with a 50 m grid size DEM. They tested the radiation, curvature, local slope, slope after HJERDT et al. (2004), specific catchment area, different TIs, a soil-TI, and a climato-soil-TI for the ability to model spatial patterns of saturated areas. As validation data field survey and a forest habitat map was used. Of all the single topographic attributes it was the specific catchment area which performed best, followed by slope, then curvature and worst the radiation. The method which gave best prediction for the Brugga basin of about 50% agreement with observed saturated areas was a TI with a convergence factor of 8, a local slope, and a CIT of 8 ha. The climato-soil-TI with the same parameters than the best TI gave only an improvement of about 0 to 2%. The poor agreement was explained by the authors with scale problematic, poor data quality and that the geology could not be implemented in the calculation.

A comparable study was conducted by SØRENSEN et al. (2006). They studied two boreal forest sites in northern Sweden where they also compared a number of calculation methods for TI and evaluated them in terms of their correlation with following measured variables: vascular plant species richness, soil pH, groundwater level, soil moisture, and a constructed wetness degree. Beside the MD method they implemented a new flow direction algorithm method which was later published by SEIBERT and MCGLYNN (2007). The new triangular multiple flow direction algorithm (MDinf) is an evolution of the Dinf algorithm that allows multidirectional flow in any downslope direction, thereby combining the benefits of Dinf and MD (SEIBERT and MCGLYNN 2007). Although they found not one single method for calculating TI in the study of SØRENSEN et al. (2006) the new MDinf performed in general better than MD. For the Holmgren h, which is also used in MDinf, they found that values of 0.5 to 2 are most appropriate. And compared to GÜNTNER et al. (2004) who recommended values of 8 to 10, they suggested that h might decrease when going from mountainous to hilly areas. Both studies agreed in preferring the local slope than the slope method of HJERDT et al. (2004) and for CIT SØRENSEN et al. (2006) found values of 10 to 20 ha to be an optimum which is a little higher than GÜNTNER et al. (2004) which can be explained by more rainfall.

In a study of ERSKINE et al. (2006) the effect of grid size on different flow direction algorithms for calculating the specific catchment was evaluated. They found that the finer the DEM gets the more sensitive the calculation gets regarding the different methods. They therefore recommend that the finer the DEM resolutions gets the more important it is to use multiple flow direction algorithms for calculating the specific area on hillslopes.

A new level of DEM quality was used in the study of MURPHY et al. (2009) called light detection and ranging (LIDAR) DEM. Compared to a conventional photogrammetric DEM this improves the initial point density by two orders of magnitude and the vertical accuracy can be improved from 1 to 10 m to 0.15 to 1 m. They also used a new method for delineating saturated areas. They called it depth-to-water index (DTW). The value of that index approximates the elevation difference between the cell in the landscape and the nearest downslope surface water body, being a lake, stream, or river. It is then assumed that the smaller the value is the more probably saturation is. That new index was compared with the TI using D8 and Dinf for the LIDAR DEM with 1 m grid size and a conventional DEM with 10 m grid size. The new DTW index performed better with LIDAR compared to the conventional DEM and with a threshold of 1.5 m it had an agreement of 71% with observed saturated areas. This was not only a better performance than the used TI methods in the study but also to the other studies using TI presented earlier in this chapter. The relatively poor performance of the TI model results from over-dependence on flow accumulation, regardless of whether a unidirectional or multidirectional flow algorithm is used. It would appear that local downslope topography and hydrologic conditions may be more important in determining soil moisture conditions than the TI accounts for. The DTW model captures this effect which may account for its better performance (MURPHY et al. 2009).

1.2 Impulse for the study and its objectives

Is it possible to evaluate saturated areas solely with topographic information?

That is the central question of this study. In the previous chapter most studies (GÜNTNER 1997; GÜNTNER et al. 2004; GÜNTNER et al. 1999; MEROT et al. 1995; MEROT et al. 2003; RODHE and SEIBERT 1999) which tried to evaluate saturated areas on the basis of topographic information, claimed more or less that the poor quality of their DEMs was responsible for the poor agreement of modeled and observed data. For this study there is topographic information available with a new level of quality: the LIDAR DEMs derived from the Landesamt für Geoinformation und Landentwicklung, Baden-Württemberg (LGL). They offer a much better resolution in horizontal as well as in vertical direction.

The aim of this study is therefore to analyze if data with a new level of quality allows evaluating the spatial pattern of saturated areas correctly.

Nevertheless, in the previous chapter it was already intended that a finer resolution might not lead to a better prediction of saturated areas. Therefore the methods applied in this study to model the spatial patterns of saturated areas will not only be calculated for the original LIDAR DEM but also for coarser DEMs which will be aggregated from the LIDAR DEMs.

To find an answer to above mentioned question, saturated areas will be modeled for three catchments in Southwest Germany and validated with forest habitat maps which are derived from the Forstliche Versuchs- und Forschungsanstalt Baden-Württemberg (FVA), and field survey. They will be modeled for different grid sizes and most of the methods introduced in the previous chapter will be used for this. Besides the central question, an objective will be to examine which methods to evaluate the spatial patterns of saturated areas perform best at which regions or landscapes and at which DEM resolution. The ultimate goal would be to indentify one best method that then could be a standardized method for other regions.

2 Study areas

To evaluate the methods used for modeling saturated areas they are applied for three different catchments. This has the advantage that the obtained information are more independent from on specific environment but also that the methods can be tested for different conditions in geology and topography. The study areas are all located in Baden-Württemberg, South-West Germany. For this region LIDAR DEMs are available as input data and forest habitat maps for validation. As the name implies, the forest habitat map covers only forest stands, so the catchments were chosen to have large proportion of it. Additionally, the areas should be not that far away from each other so that field observation, within the time budget of a diploma thesis, was possible. Resulting from these several criteria the catchments Acher, Eyach, and Zastlerbach were chosen (figure 1). They are all located in the mountainous region of the Black Forest whereas the Zastlerbach is located in the south and Acher and Eyach in the north of it.

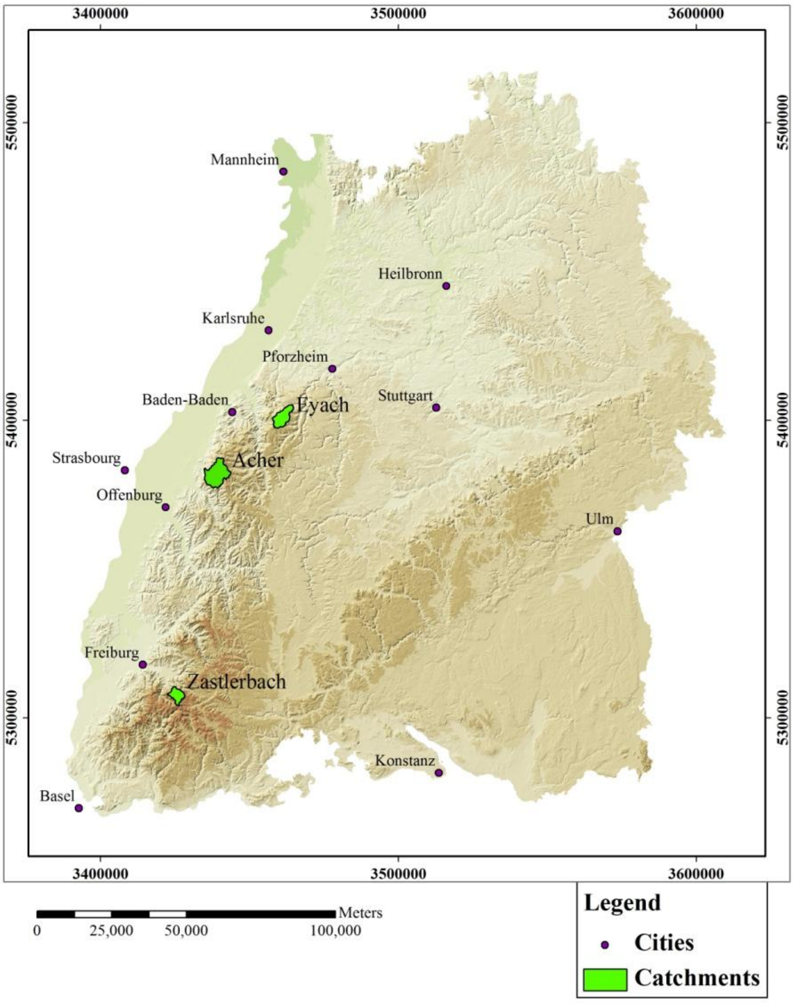

Figure 1: Location of the catchments in Baden-Württemberg

2.1 Acher

The largest of the three catchments is the Acher catchment with 53.4 km^2 which is also the most anthropologic influenced and several towns are located in it. As you can see in figure 2 the elevation ranges between 214 and 1164 m a.s.l..

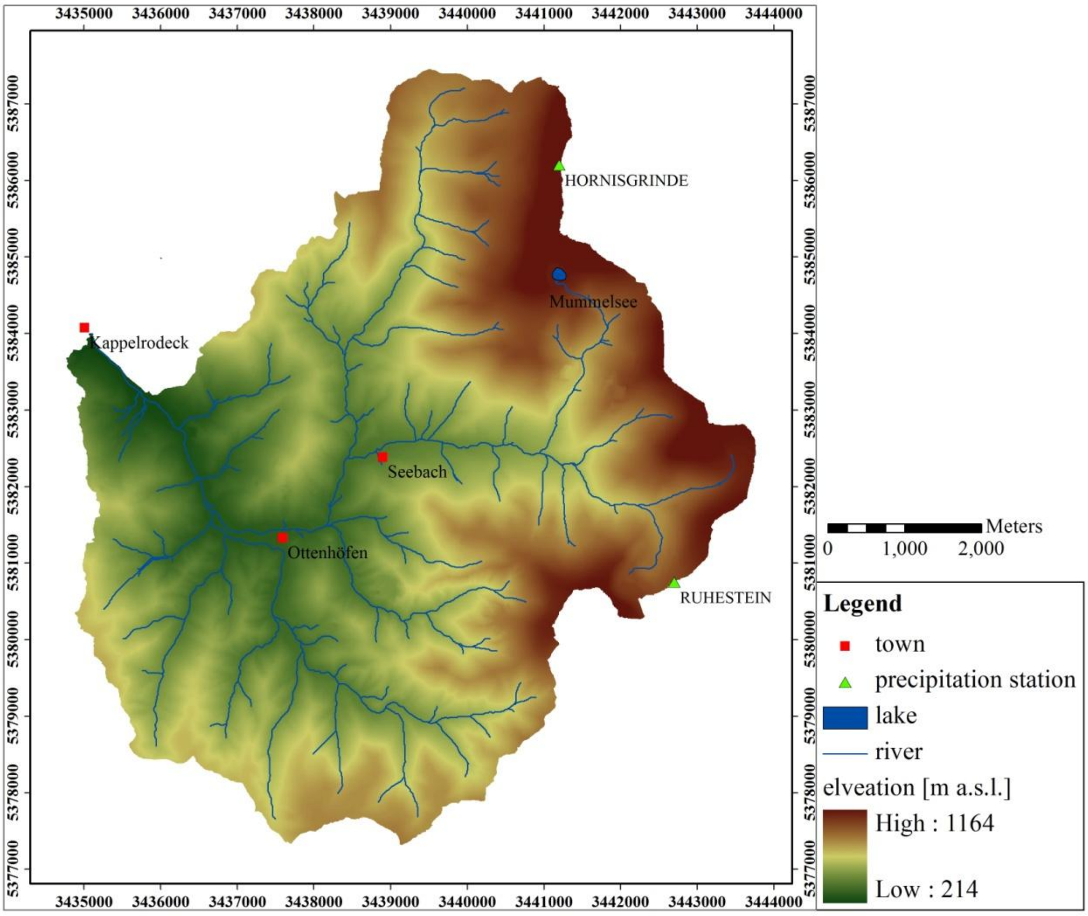

Figure 2: The Acher catchment

In the catchment area there are two precipitation stations, Hornisgrinde and Ruhestein named after the mountain and the pass height on which they are located. They are operated by the German National Meteorological Service (DWD) and the climate data for the time period between 1961 and 1990 is freely available (URL 2). The data for the two stations located in the Acher catchment is given in table 1. With an average annual precipitation of about 2000 mm and annual average air temperature of 4.8 °C these locations are very humid. However, as they are located at the highest elevation of the catchment they probably overestimate the catchment precipitation and underestimate the average air temperature due to orographic effects. Nevertheless, the general function of the precipitation with a maximum in July and December is shown. In July the evapotranspiration can be assumed to be high as the temperature also has its maximum there and it is in the middle of the vegetation period. Therefore the wettest conditions are expected in the catchment during the second precipitation maximum. Regarding the temperatures it is expected that there is a second maximum for wet conditions in the catchment when in early spring time the temperature raises and the precipitation fallen earlier as snow melts.

Table 1: Average climate data for the time period of 1961 to 1990 for the Acher catchment

	mean monthly precipitation [mm]												
	J	F	M	A	M	J	J	A	S	O	N	D	Year
Ruhstein 920 m a.s.l.	184	157	162	153	169	190	168	165	141	161	181	202	2033
Hornisgrinde 1122 m a.s.l.	169	148	156	157	181	202	170	171	144	147	171	183	1999
	mean monthly air temperature [°C]												
Hornisgrinde 1122 m a.s.l.	-2.6	-2.3	-0.3	3	7.4	10.6	12.9	12.5	10.1	6.6	1	-1.6	4.8

As the topography plays a major role for delineating saturated areas a closer look is taken in figure 3, where you can see the slope angle derived from the method of ZEVENBERGEN and THORNE (1987), which is explained later in chapter 3.3.2, for the 1 m grid LIDAR DEM. The slope values range from 0 to 86.5° and the mean slope of the catchment is 20.8°. The very high slopes are mostly manmade and are located in stone quarries, one is located 3.5 km in the west of Ruhestein and two 2.5 km south of the Hornisgrinde. Beside these extremes slopes there is a steep valley between Ruhestein and the one stone quarry near it, where there are cascades, called Edelfrauengrab and a ridge called Karlsruher Grat. Contrary to these steep examples there also quite flat examples that are beside the valley bottoms mainly in the heights in the northeast of the catchment. What in the DEM is shown as a very flat area a little south of the Hornisgrinde is a lake called Mummelsee.

The geology of most of the catchment area is dominated by granite. Only in a few percent in the most elevated parts in the north east the underlying bedrock consists of middle and lower Buntsandstein and a very small area in the north of metamorphic rock. Along the valley in the catchment Late Quaternary alluvial deposits covered with alluvial soils can be found. Beside these alluvial soils most of the bedrock is covered with braunerde (cambisol) that gets more and more podzolic with increasing elevation (WABOA 2007).

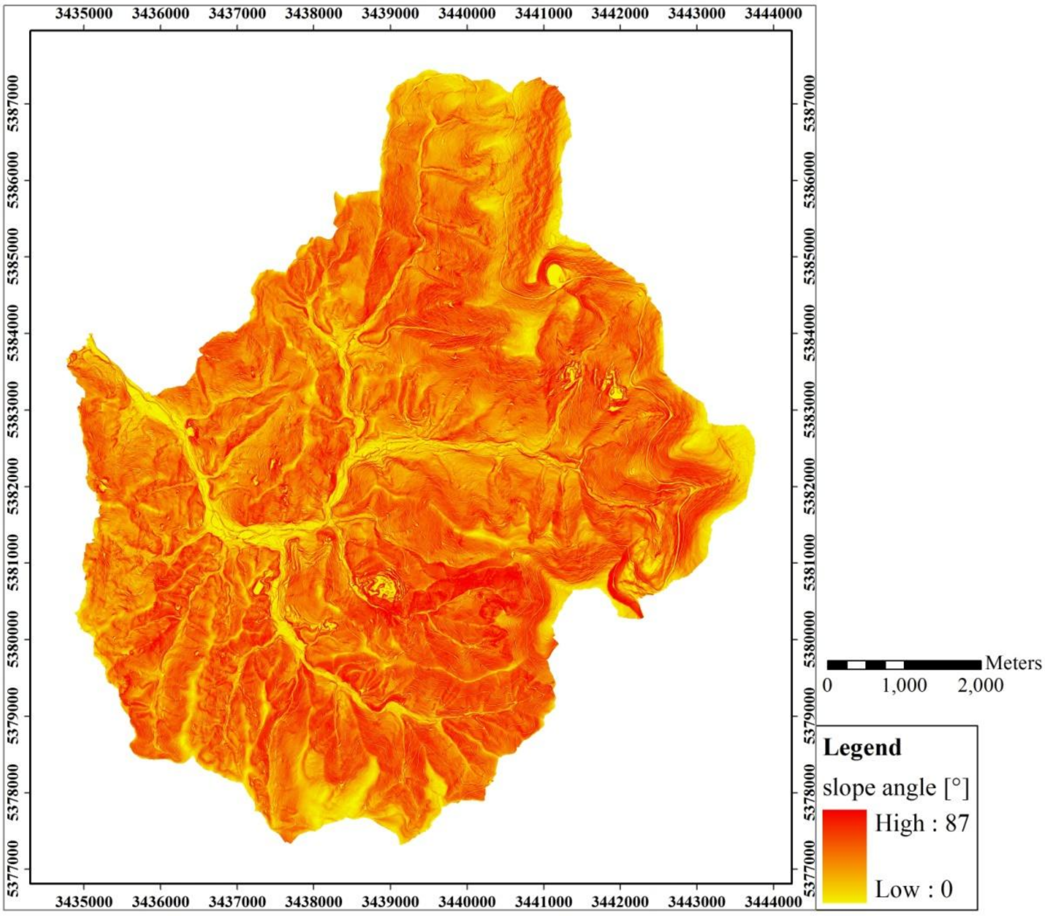

Figure 3: Slope angle after ZEVENBERGEN and THORNE (1987) for the Acher catchment

2.2 Eyach

The Eyach catchment is the medium size catchment with an area of 29.7 km^2 and an elevation range from 482 to 947 m. Within the catchment there is no town and most of the area, according to FVA 98%, is covered with forest and only little grasslands. Around the lake Wildsee located in the south of the catchment there is a highmoor.

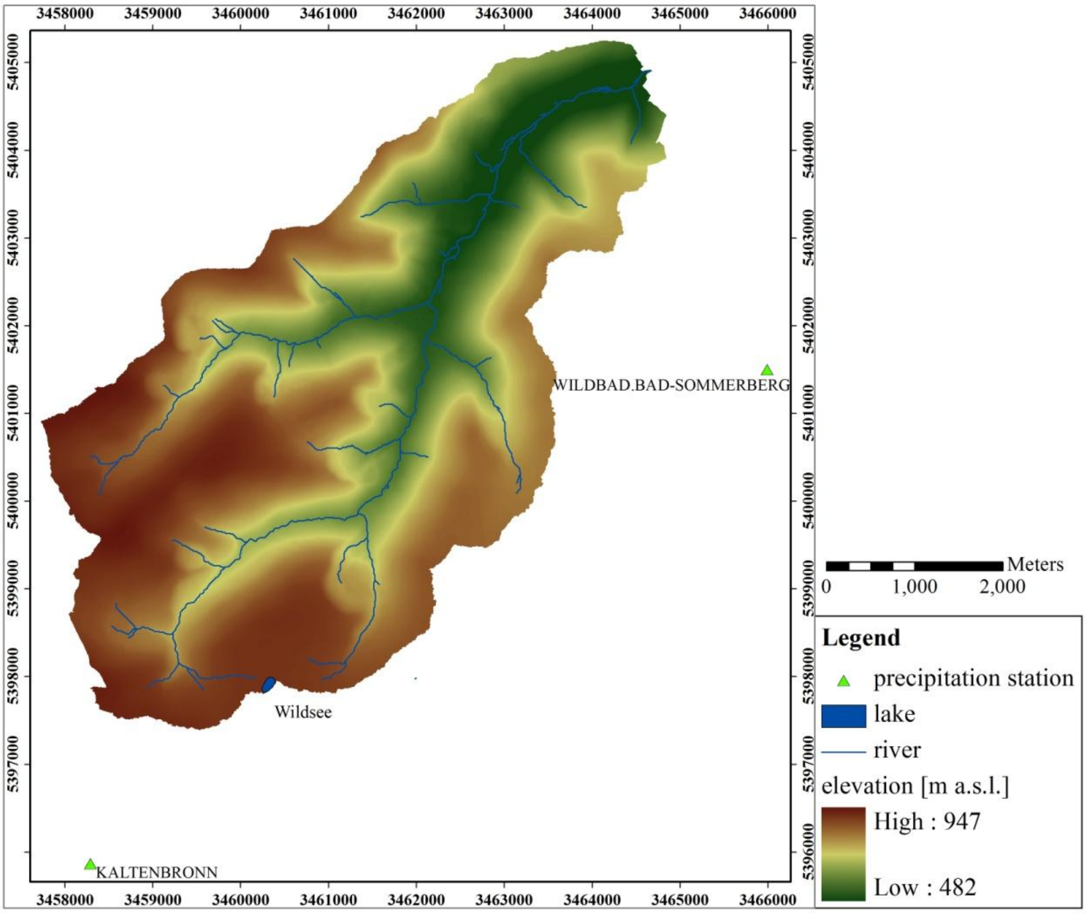

Figure 4: The Eyach catchment

Inside the catchment there is no precipitation station, but in close proximity there are two (figure 4) and the catchment precipitation is assumed to be comparable to them. The climate data is shown in table 2. The annual average precipitation is 1385 and 1601 mm at Bad Wildbad-Sommerberg and Kaltenbronn, respectively. The annual average air temperature at Bad Wildbad-Sommerberg was measured to be of 7.25 °C. The precipitation has two maxima, one in July and one in November and December. Similar to the Acher catchment (chapter 2.1) the wettest time is expected within the second maximum of precipitation and in the melting period.

Table 2: Average climate data for the time period of 1961 to 1990 for the Eyach catchment

	mean monthly precipitation [mm]												
	J	F	M	A	M	J	J	A	S	O	N	D	Year
Kaltenbronn 858 m a.s.l.	139	126	132	140	147	154	122	124	101	111	154	151	1601
Bad Wildbad-Sommerberg 740 m a.s.l.	131	117	119	114	120	123	101	102	83	92	140	143	1385
	mean monthly air temperature [°C]												
Bad Wildbad-Sommerberg 740 m a.s.l.	-0.8	-0.1	2.5	6	10.4	13.5	15.7	15.3	12.6	8.5	3.2	0.2	7.25

A closer look at the topography of the catchments is shown in figure 5. The slope angle ranges between 0 ° and 78 °. There are only few steep parts in the catchment that are located in the middle elevation part. Flat areas are located at the high elevation parts, where you can see a very flat part in the south representing the highmoor. But also in the valley, like in the center of the catchment there are flat areas. The average slope angle so results in a moderate value of 13.7°.

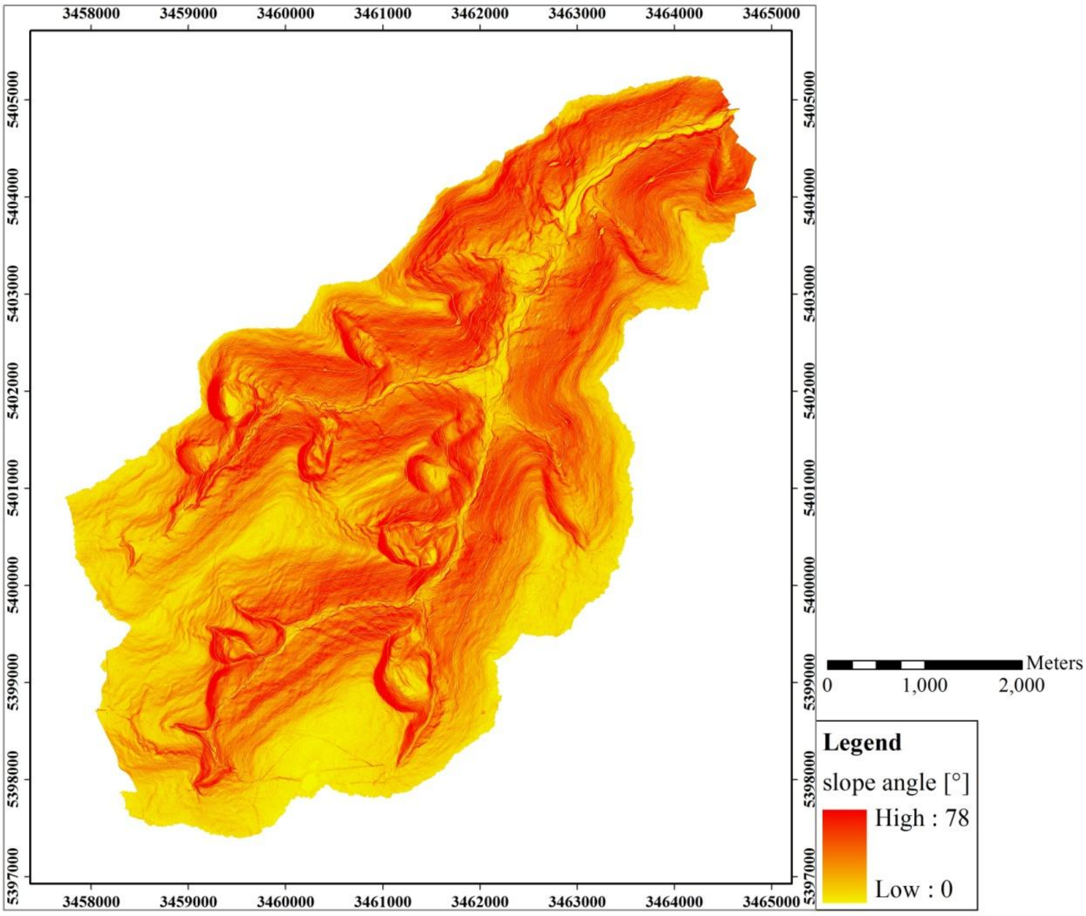

Figure 5: Slope angle after ZEVENBERGEN and THORNE (1987) for the Eyach catchment

The bedrock consists mostly of middle and lower Buntsandstein and in the lower valley part of the flat area described above to near to the outlet of the catchment there are alluvial sediments of the Quaternary. Additionally, in the area of the highmoor Holocene accumulations can be found. In the lower valley parts the bedrock is covered with podzolic braunerde (cambisol) and with higher elevation it becomes podzol. At the highest elevation a mixture of podzols and gleyic soil is found, the latter especially in the area around the highmoor (WABOA 2007).

2.3 Zastlerbach

The Zastlerbach catchment is the smallest of the three catchments with only 18.3 km^2 and an elevation range of 540 m to 1493 m (figure 6). Within the catchment there are a few land settlements, but no towns. The major proportion of the catchment area is covered with forests, according to FVA 83%, and a few grassland areas.

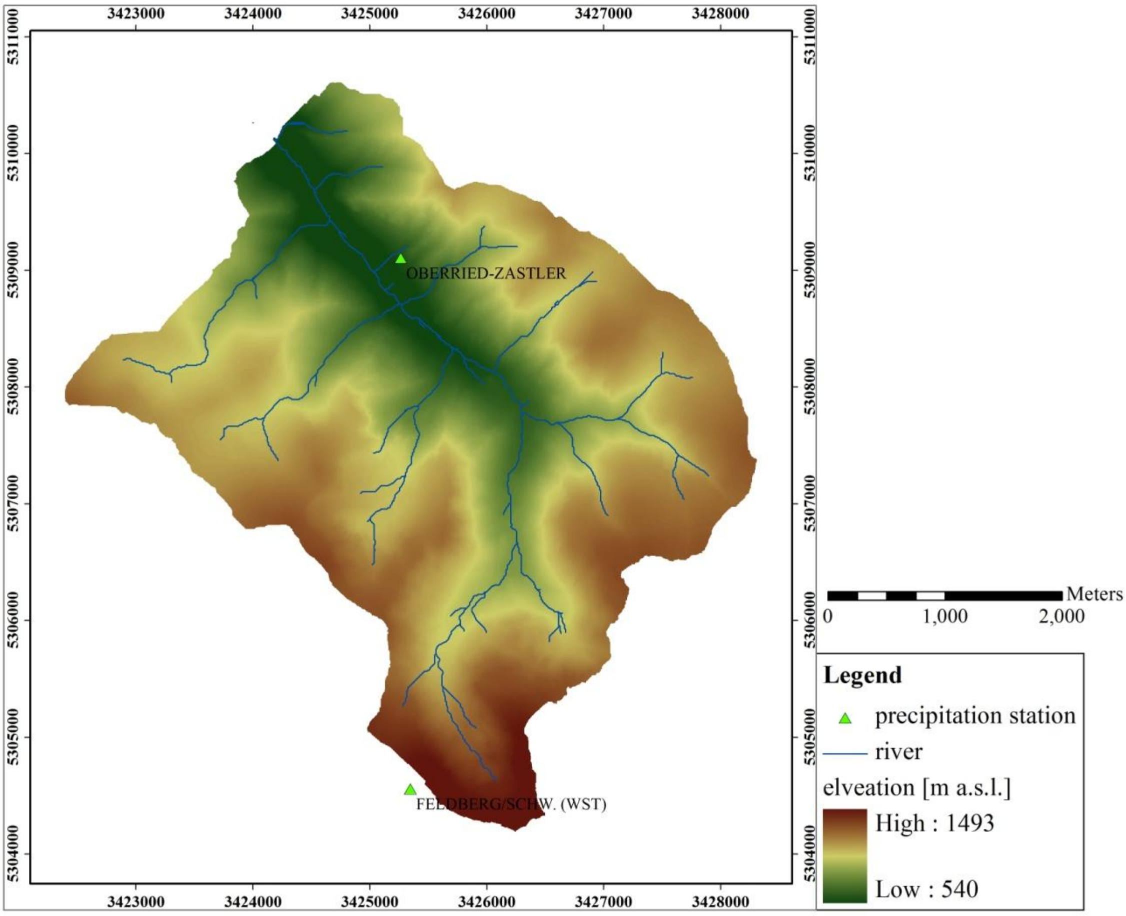

Figure 6: The Zastlerbach catchment

The Oberried-Zastler precipitation station is located within the catchment in the valley and the Feldberg (Schwarzwald) station near the catchment border in the south at nearly 1500 m a.s.l.. Therefore the orographic effect on precipitation is distinctly shown here as the average annual rainfall is 1911 mm at the high elevation and only 1652 mm at the lower elevation (table 3). However, both follow the same function with a maximum precipitation in May/July and a second maximum in November/December. Similar to the other two catchments (chapter 2.1, and 2.2) the wettest time is expected within the second maximum of precipitation and in the melting period.

Table 3: Average climate data for the time period of 1961 to 1990 for the Zastlerbach catchment

	mean monthly precipitation [mm]												
	J	F	M	A	M	J	J	A	S	O	N	D	Year
Oberried-Zastler 625 m a.s.l.	144	120	136	139	155	148	135	141	102	119	159	154	1652
Feldberg/Schwarzwald 1486 m a.s.l.	168	142	148	140	165	173	162	166	126	147	184	190	1911
	mean monthly air temperature [°C]												
Feldberg/Schwarzwald 1486 m a.s.l.	-0.8	-0.1	2.5	6	10.4	13.5	15.7	15.3	12.6	8.5	3.2	0.2	7.25

The catchment is characterized by the highest relief intensities with an average slope angle of 23.7° which is reflected in figure 7. The Zastlerbach catchment can thereby be divided into three parts. These are a relative gently upland area, partly very steep slopes at the valley margins, and an again gentle valley bottom.

The bedrock consists of gneiss, a metamorphic rock, covered by weathering material of Pleistocene origin: debris, drift, and soils of varying depth of 0 to 10 m (GÜNTNER et al. 2004). The major soil type is braunerde (cambisol). From the Oberried-Zastler precipitation station on you find in the valley bottom Late Quaternary alluvial deposits.

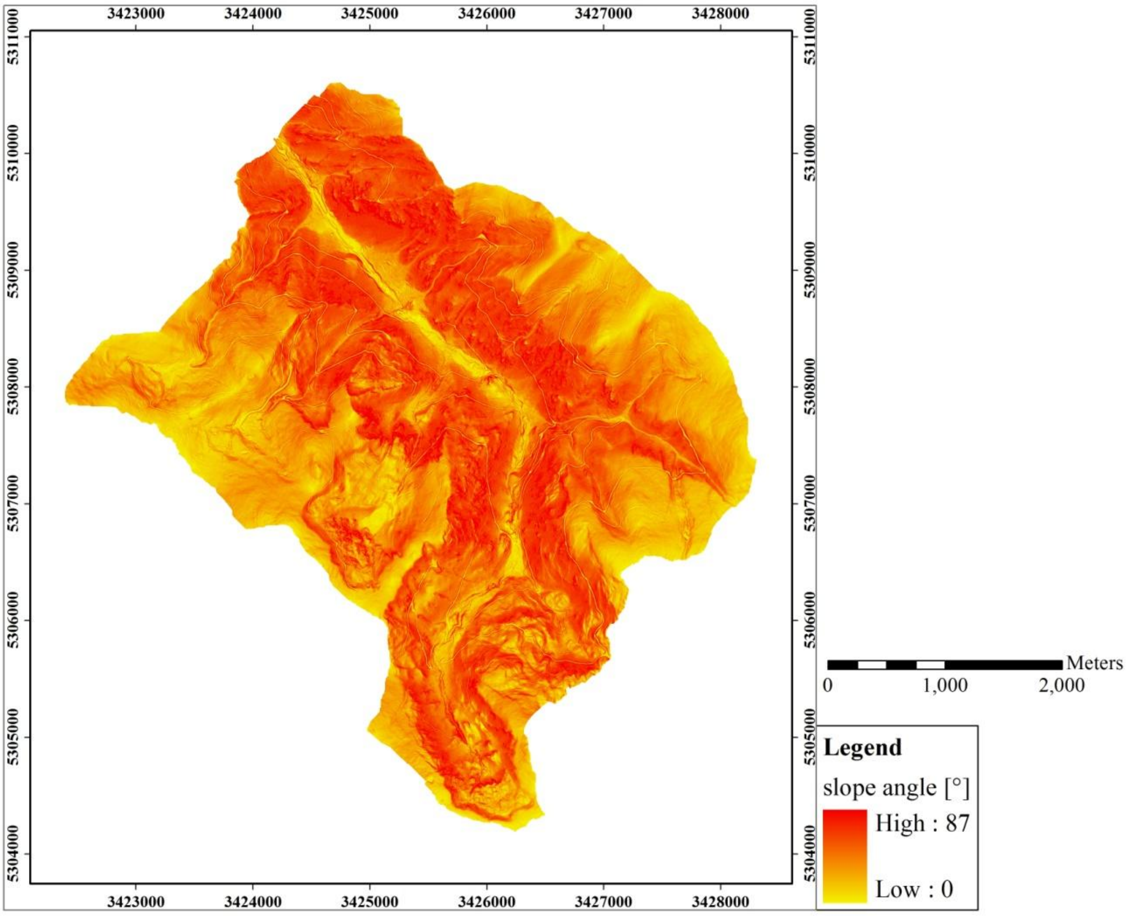

Figure 7: Slope angle after ZEVENBERGEN and THORNE (1987) for the Zastlerbach catchment

2.4 Summary of the catchments

In table 4 a comparison of the three catchments is shown. The climate conditions are comparable, remembering that the climate stations used for the Acher catchment are assumed to overestimate precipitation conditions and underestimate temperature conditions. The main differences between the catchments are in geology and topography. The Zastlerbach catchment is the one with the most relief energy and highest average slope. The Acher catchment is a little gentler with 20.3° mean slope angle and the Eyach catchment is representing the gentlest sloping catchment with an average slope angle of only 13.7°.

Table 4: Comparison of the three catchments

	Acher	Eyach	Zastlerbach
catchment area [km^2]	53.4	29.7	18.3
elevation range [m a.s.l.]	214 - 1164	482 - 947	540 - 1493
average slope [°]	20.8	13.7	23.7
mean anual precipitation [mm] *	2016	1493	1781
mean annual temperature [°C] *	4.8	7.25	7.25
dominant geology	plutonic rock	sandstone	metamorphic rock
dominant soil type	podzolic braunerde	podzol, podzolic braunerde	braunerde

* only rough estimations, see in chapter 2.1, 2.2, 2.3.

3 Methodology

In the first part of this chapter the input data will be explained. Subsequently the TI will be introduced and following the methods to calculate it will be elaborated. Afterwards the vertical distance to potential groundwater table (VDG) will be presented as an additional approach which is also used in this study. Finally, in the last part, the validation data and methods will be described.

3.1 LIDAR DEM

To generate a LIDAR DEM the landscape is scanned with a laser from an airplane or a helicopter, that is why it is also called airborne laser scanning. The basic idea is that a laser impulse is send from the airplane which will be reflected from the ground and then detected from the plane again - this explains the name LIght Detection And Ranging. The distance between airplane and ground can then be calculated by the time the laser needs for its travel. Knowing the location of the airplane and the direction the laser impulse is sent to the position of the point on the ground can be determined. How that is technical managed is sketched in figure 8.

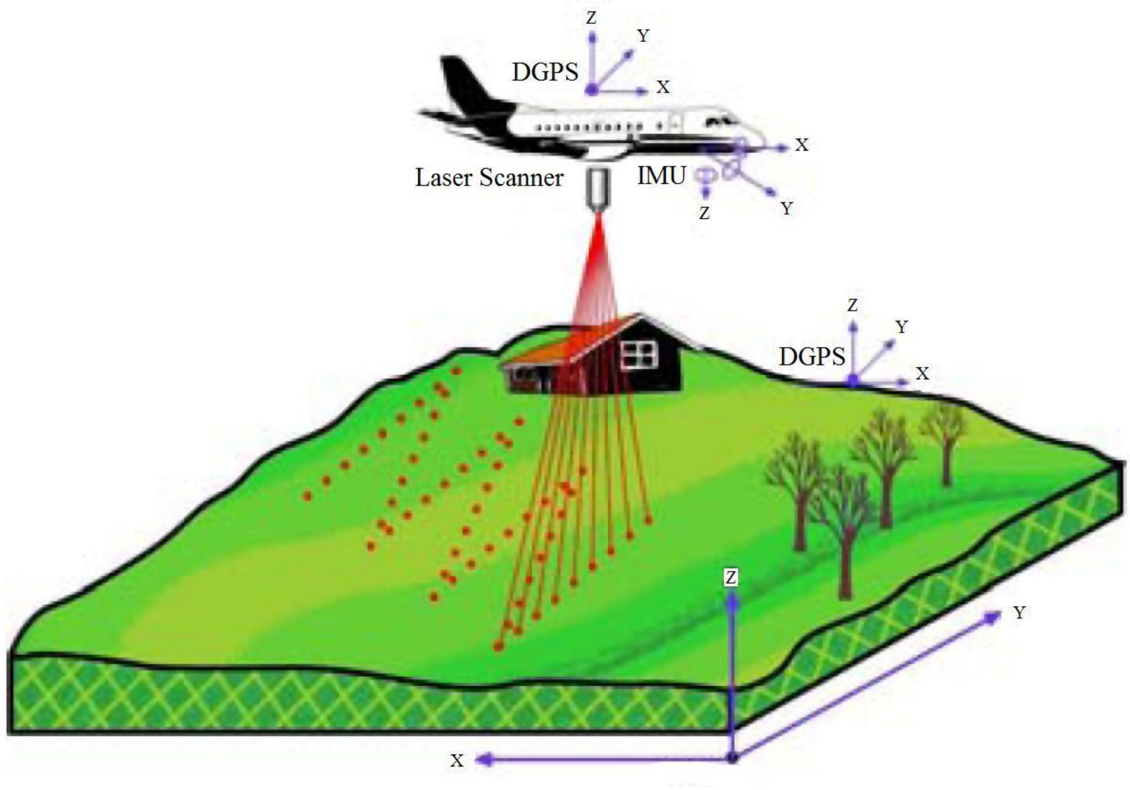

Figure 8: Airborne-LIDAR system principle (ZHAOLIJIAN et al. 2008)

As shown in figure 8 there is, additional to the Global Positioning System (GPS) on the airplane, a reference GPS station located close to the overflown landscape. The so called differential GPS (dGPS) is necessary to get more precise positioning of the airplane. With the dGPS system it is possible to locate the plane every second which leads by an velocity of 170 to 300 km/h to an interval of every 47 to 84 m (GAJSKI 2004). Therefore there is also an inertial navigation system (INS) installed in the airplane which improves the localization intervals to a range of centimeters by measuring the acceleration in the three Cartesian directions. After calibrating the relative position of the laser system to the GPS on the airplane the distance to the ground point can be measured. Therefore a pulse is send from the laser system, reflected by the ground, and then recorded by a receiver in the laser systems which measures the transit time. With the position of the airplane, the angle of the pulse direction, and the transit time of the impulse the exact position of the ground point can be calculated. Doing this for the overflown area results in a big point cloud that will be interpolated to an area.

However, before interpolating to a DEM the point cloud needs some more treatment. Looking again at figure 8 one can notice that where the laser impulse hits the ground you actually get what you want. But when it hits a building or a forest it gets more sophisticated. Points of buildings though can be filtered out relative easy with algorithms that notice the sharp and typical shape of them. But with vegetation the phenomenon of multiple responses occurs which is shown in figure 9:

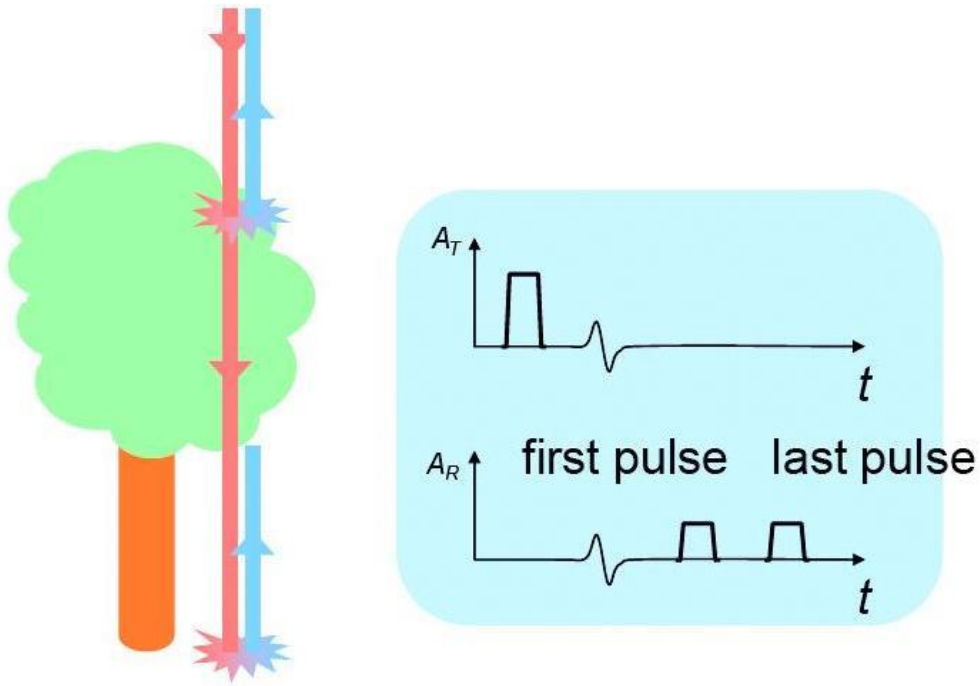

Figure 9: Sketch of the phenomenon of first and last pulse (edited after BRENNER 2006)

When the laser beam hits the surface it has a diameter of about 0.2 to 1 m. That is the reason why it can happen, that a part of the beam will be reflected from the canopy and a part reaches the ground (GAJSKI 2004). This is shown in figure 9, where the sent impulse after some travel time (A_t) gets after reflection split in a first and last impulse (A_r). Hence, the receiver at the airplane gets multiple reflection signals which can be related to vegetation points and ground points. However, this only works when the beam really reaches the ground and the time interval between the pulses is longer than the pulse width. The vegetation for example has to be higher than 75 cm when the impulse width is 5 ns (GAJSKI 2004). As a result from all mapped point a surface cover of the ground can be generatet but to get a DEM you have to filter these points. This is shown in figure 10 where the red line represents the surface cover and the blue line represents the resulting DEM after filtering the ground points.

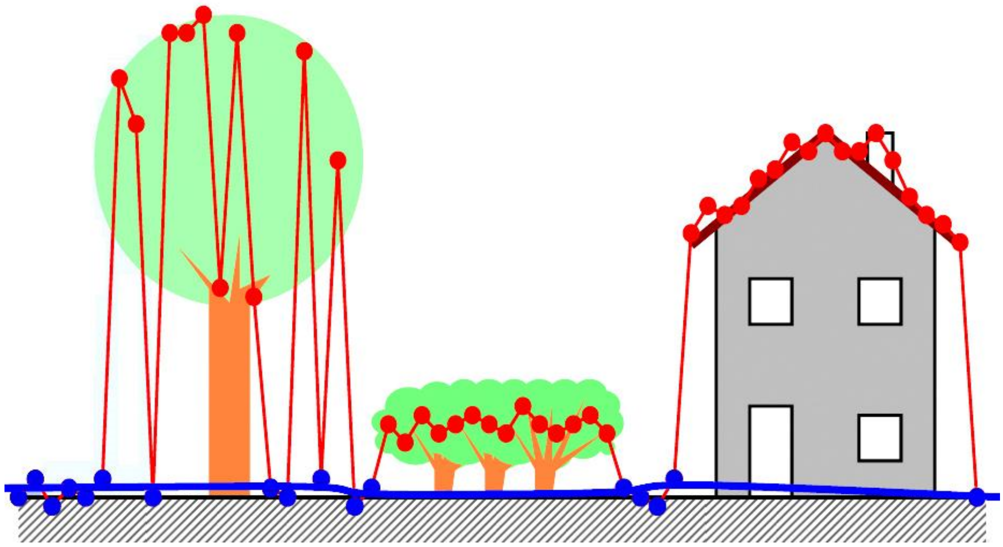

Figure 10: Surface cover (red) and DEM (blue) (edited after BRENNER 2006)

The procedure of filtering involves basically two steps. First, a mathematical algorithm that filters non ground points because of unnatural height differences between the points. However, a misinterpretation of these algorithm does inescapable occur (SCHLEYER 2001). For example the shrub in the middle of figure 10 could be delineated as a little hill in the DEM by the algorithm. Therefore the data has to be reviewed by a person and manually corrected. To get a better impression of the effect of filtering in a real DEM an example of unfiltered and filtered area is shown in figure 11. It shows the big difference and a central interest would be to evaluate the quality of such a filtered DEM like the one on the right side. Therefore, however, many factors have to be considered: The equipment for measuring (dGPS, INS, and the laser system), the characteristic of the overflown landscape, the filtering, and the interpolating. The characteristics of the landscape are important, because it is obvious that for an area covered with forest, like in figure 11, the quality is supposed to be worse than for an area with no vegetation as many points have to be filtered out. Additional the filtering depends on the worker in charge of it and sometimes the landscape is even not exact definable (e.g. for a fresh ploughed field). Hence, there is a random influence on the quality of the DEM, whose error cannot be calculated mathematical (ZOLLINGER 2010). However, for the data used in this study, the LGL applied empirical methods and had test areas where they compared LIDAR data with observed data. They found that their LIDAR DEM with the grid size of 1 m has a accuracy of position of 20 to 30 cm and the standard deviation of the elevation is +/- 15 cm (ZOLLINGER 2010). This is comparable to the accuracy that is promised by the company which was commissioned from the LGL to evaluate the LIDAR DEMS. They state an absolute error of 25 to 50 cm for the position and 10 to 25 cm for the elevation and an relative error from point to point of 6 to 15 cm in position and 3 to 5 cm in elevation (LINDENBERGER 2006).

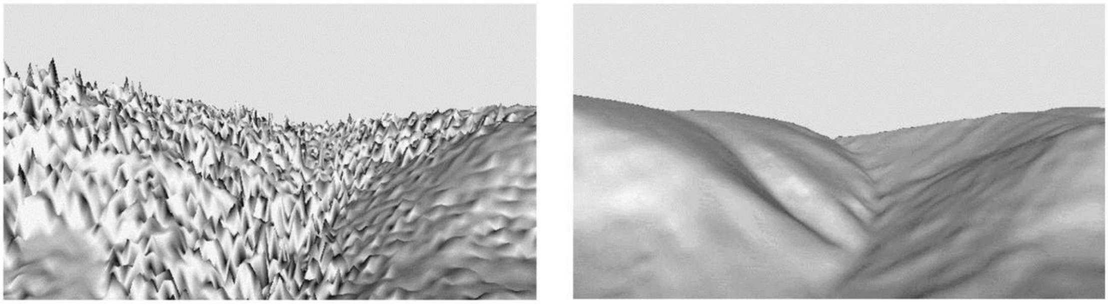

Figure 11: An example of an unfiltered (left) and filtered (right) DEM (KRAUS and PFEIFER 1998)

Additional to the LIDAR DEMs of the study areas, which were scanned between 2002 and 2004, the LGL delivers orthophotos. These are orthoscopic and lifelike pictures of the surface with a resolution of 0.25 m and support the orientation within the DEMs.

3.2 The Topographic Index

According to BEVEN 1997 the TI was first introduced by KIRKBY and WEYMAN 1974. It describes the tendency of a specific point to accumulate water considering the drainage potential of the point. The higher the TI value the more the point tends to get saturated and generate saturation overland flow as the soil cannot transmit all water coming from upslope areas. The TI is so used as an index of hydrological similarity. All points with the same value of the index are assumed to respond in a hydrologically similar way (BEVEN 1997). How the TI is linked to saturated areas is shown within the TOPMODEL, a complete hydrological model which was developed by BEVEN and KIRKBY 1979 . A model though can only be a simplification of the complex reality, whereas it tries to capture the essential functions governing the modeled hydrological system. Under certain assumptions and simplifications a simple relation between the TI and the saturation can be derived. This is summarized here presented following the description in BEVEN et al. 1995: The conceptualization of the original TOPMODEL is premised upon three basic assumptions:

A1: that the dynamics of the saturated zone can be approximated by successive steady state representations;

A2: that the hydraulic gradient of the saturated zone can be approximated by the local surface topographic slope.

A3: that the distribution of downslope transmissivity with depth is an exponential function of storage deficit or depth to water table:

$$T = T_0 e^{-SD/m} \tag{1}$$

Where T_0 is the lateral transmissivity when the soil is just saturated (m^2/h), *SD* is the actual storage deficit (m) and *m* is a model parameter (m) which can be interpreted physically as it controls the effective depth of the catchment soil profile. A higher value of *m*, by a constant T_0, increases the active depth of the soil profile, whereas a small value generates a shallow effective soil. With the equation

$$f_s = \frac{n_{eff}}{m} \tag{2}$$

where *fs* is a scaling parameter [m^{-1}] and n_{eff} is the effective porosity [-] equation (1) can also be formulated in terms of the water table depth

$$T = T_0 e^{-fz} \tag{3}$$

where *z* is the local water depth (m).

Under the assumption A2 and eq (1), according to Darcy's law, at any point *i* on a hillslope the downslope saturated subsurface flow rate q_i per unit contour length [m^2/h] may be described by

$$q_i = T_{oi} \tan\beta_i \, e^{-\frac{SD_i}{m}} \tag{4}$$

where β_i is the local slope [°], T_{0i} the local transmissivity, and SD_i is the local storage deficit [m].

Under the assumption A1 and assuming (A4) a spatially homogeneous recharge rate *r* [m/h] entering the water table, the subsurface downslope flow per unit contour length q_i may also be given by

$$q_i = ra_i \tag{5}$$

where a_i is the area of the hillslope per unit contour length [m] that drains through point i (specific catchment).

By combining (4) and (5) the storage deficit at any point i can be calculated by

$$SD_i = -m \cdot \ln\left(\frac{r \cdot a_i}{T_{oi} \tan \beta_i}\right) = -m \cdot \left(TI_i + \ln\left(\frac{r}{T_{oi}}\right)\right) \quad (6)$$

with TI_i is the Topographic Index at point i:

$$TI_i = \ln\left(\frac{a_i}{\tan \beta_i}\right). \quad (7)$$

If you would include T_{0i} in (7) you would get the so called soil-TI.

The average storage deficit for the catchment can be calculated by integrating (6) over the entire area that contributes to the water table. In case of discrete data this areal averaging can be expressed in terms of a summation over all points within the catchment A [m^2]:

$$\overline{SD} = -\frac{m}{A} \sum_i TI_i + \ln(\mathrm{r}) - \ln(T_{0i}) \quad (8)$$

By using (6) in (8) you can eliminate r and assuming (A5) a spatially homogeneous transmissivity the storage deficit at a point i can be related to the average storage deficit. This has the form:

$$SD_i = \overline{SD} - m \cdot \left(\ln \frac{a_i}{\tan \beta_i} - \lambda\right) \quad (9a)$$

or in terms of water table depth

$$z_i = \bar{z} - \frac{1}{f} \cdot \left(\ln \frac{a_i}{\tan \beta_i} - \lambda\right) \quad (9b)$$

where z_i is the local water table depth at point i and $\bar{z}$ is is the average water table depth in the catchment, and λ is the average of TI of the catchment:

$$\lambda = \frac{1}{A} \sum_i TI \quad (10)$$

The equations (9a,b) express the deviation between the catchment average storage deficit (or water table depth) and the local catchment storage deficit (or water table depth) at any point in terms of the deviation of the local TI from its areal mean (BEVEN et al. 1995). The higher the local TI value is the less is the local storage deficit. Of particular interest is the case when the equations (9a,b) predicts that the local storage deficit or the local water table depth is negative which means nothing else that the local area is saturated. Such areas are where saturated overland flow is predicted to occur, and their spatial distribution constitute the variable source areas which generate the modeled surface runoff response (BEVEN et al. 1995). Therefore there is a threshold for the local TI from which on the local area will be determined as a saturated area or not. Consequently, the TI can be used as predictor for saturated areas.

3.3 Methods for calculating the TI

In early applications of TOPMODEL, the TI was calculated manually using counter data. However, the advent of gridded DEMs has allowed this procedure to be automated (QUINN et al. 1995). In chapter 1.1.2 it was shown that there is yet no one best way to calculate the TI and various different methods exist. The methods used in this study will be presented here in more detail. As the TI exists of two parameters they will be sorted by how to calculate each parameter.

3.3.1 Different methods for specific catchment

By using gridded DEMs the sensitive part for the calculation of the specific catchment is how the flow between cells is routed. Therefore flow algorithms are used to route the accumulated area of upstream cells to downstream cells. An appropriate estimation of it is substantial for the correct calculation of the TI (SEIBERT and MCGLYNN 2007). As there is yet not one best method defined three different flow algorithms will be used and tested in this study: D8, MD, and MDinf.

D8

This single-flow algorithm was introduced by O'CALLAGHAN and MARK 1984 and is the earliest and simplest of the methods used in this study. The flow direction is calculated for each cell within a 9x9 matrix. For the central point it is then computed as the direction to the neighbor which has minimum elevation under adjusting the elevations in diagonal direction by a factor $2^{-0.5}$ to compensate the increased path length. When there is no neighbor with lower elevation the direction is undefined (O'CALLAGHAN and MARK 1984). The direction is though limited to eight directions, the four cardinal and the four diagonal directions which explains the abbreviation D8. The specific catchment of each cell is calculated as its own area plus all upslope cells that drain into the cell of interest. These upslope cells can be identified using a recursive procedure which searches for the particular next upslope neighbor cell until there is no more upslope neighbor.

MD

As D8 allows a cell to contribute to only one neighbor cell and therefore only strong convergent flow occurs QUINN et al. 1991 presented a multi flow algorithm for calculating divergent flow. The principle is the same than in D8, where a central cell within a 9x9 matrix can drain to its eight neighbors but contrary to D8, it is possible to have multi flow directions to all cells with lower elevation than the central cell. The distribution of the upslope contributing areas to each flow direction is weighted according to the respective slopes according to the term

$$F_i = \frac{\tan \beta_i L_i}{\sum \tan \beta_i L_i}, \tag{11}$$

where F_i is the proportion of the area that drains into direction i, $\tan\beta_i$ is the local slope in direction i, $\sum\tan\beta_i L_i$ is the summation of all downward slopes, and L_i is the contour length. The cardinal and diagonal directions are treated different as L_1 is for cardinal direction and is 0.5 times the grid size and L_2 is for diagonal direction and is 0.35 times the grid size. This is a result of geometric calculation regarding that the contour length in diagonal direction is a little smaller than in cardinal direction. An example of how the MD computes the flow proportioning you can see in figure 12.

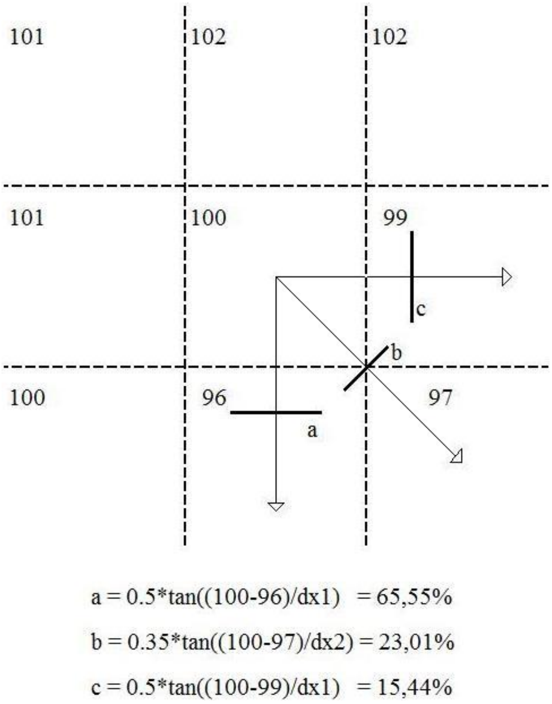

Figure 12: An example of calculating flow proportions with MD. The numbers in the cells are elevations (edited after QUINN et al. 1995)

The resulting proportions of the flow in the directions a, b, and c follows equation (11) and it is shown how all cells with lower height receive their relative proportion by their position and height. The specific catchment can be calculated the same recursive way as in D8, but from each cell only the proportion that drains into the cell of interest is accumulated.

The flow paths calculated with the MD are highly divergent as all downslope cells receive some part of the accumulated area above. Therefore MD predicts flow paths in the upper part of a catchment more accurately while the D8 has higher predictive power in lower parts (QUINN et al. 1991). A method to find a flow algorithm that lies between the divergent MD and convergent D8 is introduced by FREEMAN 1991. He modified the way how the distribution to the downslope cells is calculated to

$$F_i = \frac{S^p}{\sum S^p} \tag{12}$$

where S is the calculated slope, and p is a convergence factor.
A quite similar approach to FREEMAN 1991 was presented by HOLMGREN 1994. He modified the proportioning of flow in nearly the same way but he eliminated also the different treatment of cardinal and diagonal direction by eliminating the contour length in the proportion equation. The reason for that was that the diagonal neighbors consequently received proportionally less runoff and it seemed as if the contour length have been assigned arbitrarily HOLMGREN 1994. The proportion equation can then be formulated as

$$F_i = \frac{(\tan \beta_i)^h}{\sum (\tan \beta_i)^h} \tag{13}$$

where h is a convergence factor.
The influence of these convergence factors on the distribution is shown in figure 13. The flow proportions were calculated for the same 9x9 matrix as in figure 12. A convergence factor of one results thereby in the original MD method when you compare both figures. The higher the convergendce value the more steeper slope paths will be preferred compared to lower slope paths. This results in a more convergent flow. In FREEMAN 1991 the convergence factor was suggested to be 1.1 which approximated to a circular contour length shape (QUINN et al. 1995). The higher the value of the convergence factor the narrower and more converging the flow pattern will become. Values in excess of 10 tend to give more of a single flow direction approximation. A value of around 100 is equivalent to the single flow direction algorithm (QUINN et al. 1995).

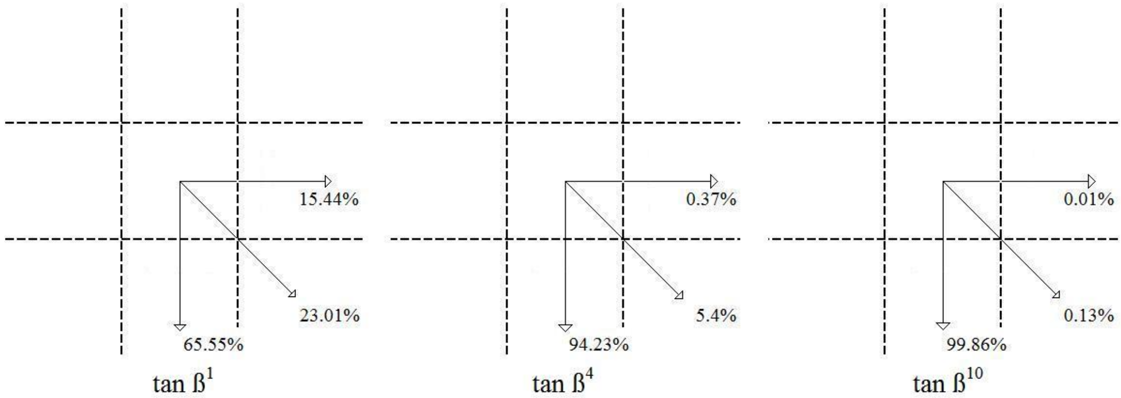

Figure 13: The effect of the convergence factor h on MD. The cells have the same elevation than in figure 12. (edited after QUINN et al. 1995)

Dinf

Although there is with the D8 and the MD combined with a convergence factor the whole spectrum of convergent and divergent flow covered they are both limited to the fact that flow only can occur in 8 different directions. Therefore TARBOTON 1997 proposed a new flow algorithm that allows a cell to drain in infinite directions. In figure 14 a 9x9 matrix is shown with eight triangular facets that are created around the cell of interest in the middle. The steepest downslope of each triangular facet is calculated and the steepest of these eight is determined as the flow direction for the cell of interest. The direction is then given as a counter-clockwise angle from east. If the angle falls along a cardinal or diagonal direction all flow from the cell drains to the according neighbor cell. If the angle, however, falls between those directions the flow is proportioned between these two neighbor pixels according to how close the flow direction angle is to the cardinal or diagonal direction, as shown in figure 14. The calculation of the specific catchment follows then the same routine as in MD.

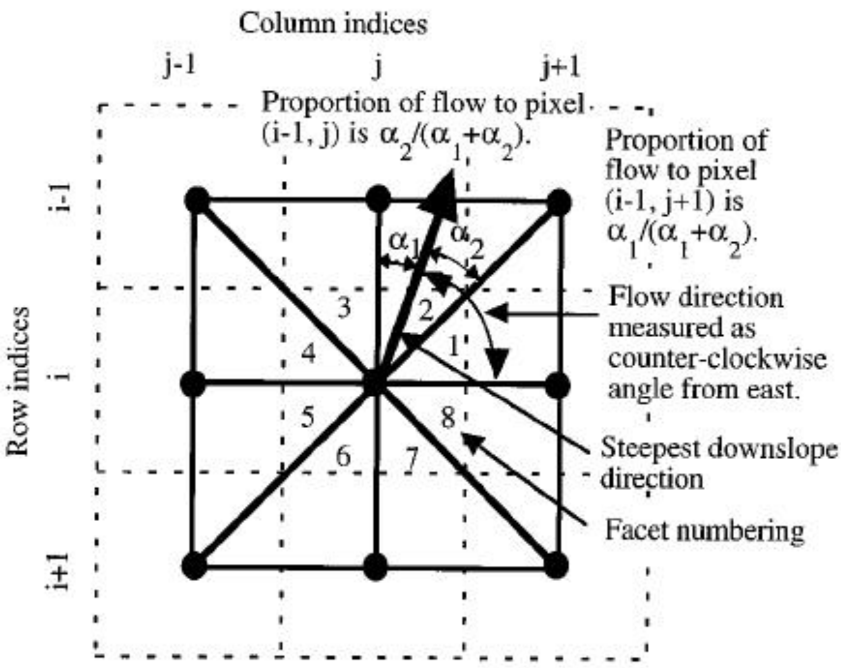

Figure 14: The triangular facets of Dinf (TARBOTON 1997)

MDinf

SEIBERT and MCGLYNN 2007 introduced a new flow algorithm MDinf which combines the advantage of Dinf with infinite possible direction with the advantage of MD where multi flow directions are possible. After computing the steepest direction for all eight triangular facets, those directions that have a steeper gradient than both of their adjacent facets are identified. These directions are interpreted as local outflows and the outflow of the cell of interest was distributed among these directions. This distribution follows the same form than in MD, where the weighting of the different directions occurs according to their respective slope. To vary the flow characteristic from convergent to divergent also the same convergence factors can be used like for the MD. The specific catchment can be calculated the same way than in Dinf or MD.

Summary of the different flow direction algorithms

To get an idea what different effects the four methods on the calculation of flow directions have, SEIBERT and MCGLYNN 2007 compared them on demonstrative artificial DEMs which is shown in figure 15. The general difference between the single and the multi flow algorithms can be seen, whereas the D8 represents the most convergent and the MD the most divergent flow system. Both, the Dinf and the MDinf are located between those borders. Another remarkable matter is that the more divergent the DEM is the bigger the differences between the flow algorithms get. Whereas the MD drains in seven cells for the divergent hillslope and three for the convergent hillslope the D8 is draining for both per definition in only one cell. Regarding the Dinf and MDinf it can be seen that they behave the same like the D8 for the convergent hillslope and only for divergent hillslopes they distinguish from each other. Comparing

Dinf and MDinf you can see that for the convergent and planar hillslope they are the same, but for the divergent hillslope and the saddle the limitation of only one flow direction in Dinf is noticeable.

convergent hillslope	planar hillslope	divergent hillslope	saddle

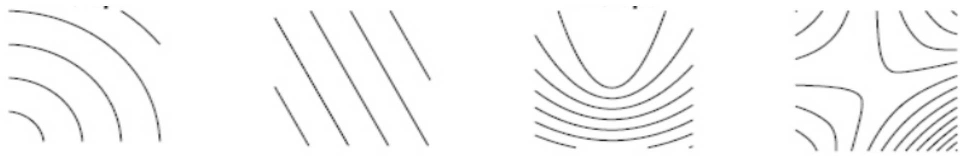

Elevation

convergent hillslope			planar hillslope			divergent hillslope			saddle		
283.2	290	297	159	161	163	119.3	120	119.3	99.6	100	100.4
295.9	282.8	290	158	160	162	118.6	120	118.6	100	100	99.8
286.7	275.9	283.2	157	159	161	117.3	118	117.3	100.4	99.8	98.8

Single-direction, D8

convergent hillslope			planar hillslope			divergent hillslope			saddle		
0	0	0	0	0	0	0	0	0	0	0	0
0	1	0	0	1	0	0	1	0	0	1	0
1	0	0	1	0	0	0	1	0	0	0	1

Multiple-Direction, MD

convergent hillslope			planar hillslope			divergent hillslope			saddle		
0	0	0	0.12	0	0	0.04	0	0.04	0.19	0	0
0.29	1	0	0.34	1	0	0.12	1	0.12	0	1	0.13
0.42	0.29	0	0.37	0.17	0	0.21	0.26	0.21	0	0.13	0.55

Triangular single-direction, Dinf

convergent hillslope			planar hillslope			divergent hillslope			saddle		
0	0	0	0	0	0	0	0	0	0	0	0
0	1	0	0.4	1	0	0	1	0	0	1	0
1	0	0	0.6	0	0	0.26	0.74	0	0	0	1

Triangular multiple-direction, MDinf

convergent hillslope			planar hillslope			divergent hillslope			saddle		
0	0	0	0	0	0	0	0	0	0.25	0	0
0	1	0	0.4	1	0	0	1	0	0	1	0
1	0	0	0.6	0	0	0.13	0.74	0.13	0	0	0.75

Figure 15: Comparison of the different flow algorithms (SEIBERT and MCGLYNN 2007)

The question for this study is which of those flow algorithms performs best for calculating the specific catchment for the TI. To evaluate that question the different flow direction algorithms will be compared for the different grid sizes. Therefore the D8, the MD and the MDinf with different convergence factors will be used. The Dinf will be represented by MDinf with a high convergence factor.

3.3.2 Different methods for tan β

The tan β term in the TI represents the hydraulic gradient. Based on the second assumption (A2) described in chapter 3.2 the local surface slope is assumed to approximate the hydraulic gradient of the saturated zone. To calculate the slope there are in general two different approaches, the local slope and the global slope. A sketch of these two different ideas can see in figure 16. The local slope will be very sensitive to fine features in the near neighborhood, whereas the global slope will be smoother as it integrates fine features over a bigger area.

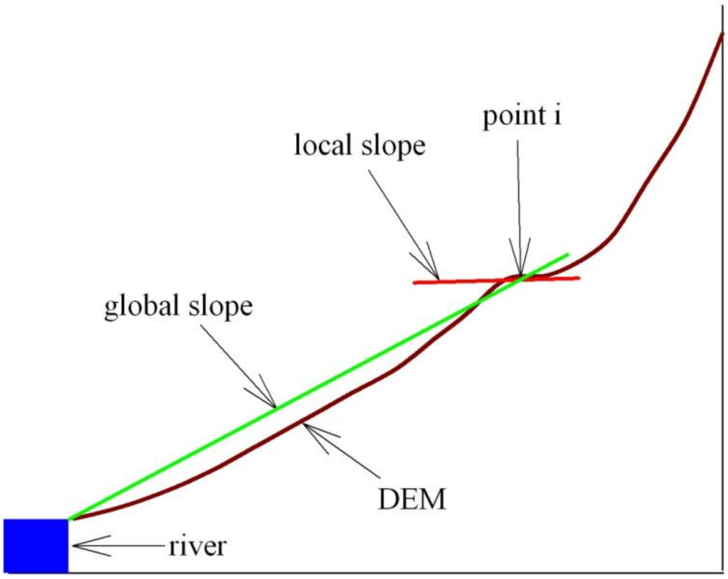

Figure 16: Comparison of local and global slope

The local slope in this study will be calculated in two ways. A steepest downward slope will be calculated after the method of TARBOTON 1997. This steepest slope is the same than used for the delineating the flow direction with Dinf. A second local slope is calculated according to ZEVENBERGEN and THORNE 1987. There a plane is fitted in a 9x9 matrix so that all 9 center points of the cells are located on the plane. The resulting downward slope of the plane gives an averaged slope for the point in the middle. Therefore this approach does not only consider downward slopes but also upward slopes and average them.

It is, however, questionable if such a local slope, especially for the fine resolution of 1 m grid size DEM used in this study, is representative for the hydraulic gradient as the water table configuration may be smoother than the land surface topography (WOLOCK and PRICE 1994). Therefore a more global gradient that integrates larger areas may represent the groundwater table better. As in GÜNTNER et al. 2004 it was shown that there was no improvement with the slope method of HJERDT et al. 2004 in this study the used gradient of each point is related to the next downward river cell (compare figure 16). This gradient can be derived by calculating the overland flow path distance needed form the cell of interest to the next downward river cell. After portioning this in its horizontal and vertical component the slope is calculated as the quotient of the vertical distance by the horizontal distance.

3.3.3 Rivers and the topographic index

Already when QUINN et al. (1991) introduced the MD he noticed that while on a hillslope the MD is performing better than the D8, in the permanent draining system water tends to move in its given river network and is therefore strongly convergent which would be good represented using the D8. Additional the water movement in a river does not fulfill the basic assumptions (chapter 3.2) of TI and is exported from a catchment without contributing to the development of saturated areas in downhill cells. Therefore QUINN et al. (1995) introduced a method, based on MORRIS and HEERDEGEN (1988), called channel initiation threshold (CIT) to distinguish river cells from hillslope cells. Thereby a cell is marked as a river cell as soon as the specific catchment exceeds a specific threshold. The river cells can then be treated in a special way.

In this study the CIT it is standardized handled the following: As soon as the flow accumulation reached the CIT the flow direction algorithm is changed to D8 and all downslope cells in the direction of steepest gradient are then regarded as river cells. All the multiple flow algorithms are modified in a way that they are overlaid with a permanent drainage system so that once hillslope flows reach a channel they remain there whilst being routed out of the catchment (QUINN et al. 1991). The most probable CIT was chosen in a trial and error method so that the resulting stream network is most similar to the stream network shown in the topographic map with scale 1:250000. Nevertheless also higher and lower values of CIT were evaluated.

3.4 Vertical distance to channel network

The study of MURPHY et al. (2009), presented in chapter 1.1.2, proposed better results than all the studies which used the TI. Therefore in this study a quite similar approach is realized and compared with the results derived from the different TI methods. Their depth-to-water index approximates the elevation difference between the cell in the landscape and the nearest downslope surface water body. It is then assumed that the smaller this value is the more probably saturation is. The index calculated in this study is quite similar but a little different in its logic. The idea is to evaluate the vertical distance between the surface and the groundwater table and the smaller this distance is the more probable is saturation. Contrary to the depth-to-water index of MURPHY et al. (2009) it is not searched for the next downward surface body, but a potential groundwater table is created on the basis of the stream network. This can be approximated on a regional scale by an imaginary surface which is interpolated from the altitude of existent watercourses and bottom lines (ETZRODT et al. 2002). An example of such a potential groundwater table is shown in the left side of figure 17. After subtracting the potential groundwater table from the surface DEM the vertical distance to the potential groundwater table (VDG) is obtained which is shown on the right side of figure 17. Cells with a small value can be expected to have water at or near the surface and can therefore be used as an indicator for saturated areas. In this process, all streams are assumed to have a VDG of zero, while the values tend to increase away from it into the landscape more rapidly in steeper terrain and more slowly in gentle terrain. The goal is to find then a threshold value for VDG, whish distinguish saturated areas from non saturated areas.

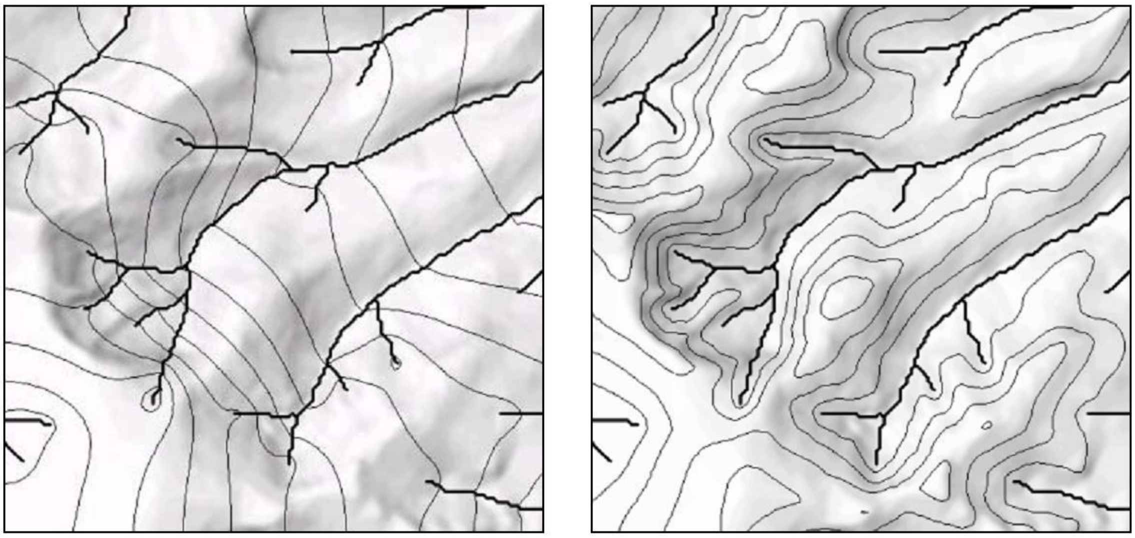

Figure 17: Left: potential groundwater table, right: VDG (CONRAD 2007)

The stream network needed for VDG will be generated in this study from the DEM itself. For this purpose the D8 method is used to compute flow accumulation and the CIT explained earlier is used to delineate the stream network.

3.5 Summary of the applied methods

Figure 18 shows an overview of all applied combinations of methods that are planned in this study to obtain. The arrows that meet in one point for then getting split again mean that for each variations above the point all variations beneath are obtained. The variations of the convergence factor are results of previous studies. The convergence factor of 1.1 was selected since it is the recommendation of FREEMAN (1991), the convergence factor of 8 since this performed best in GÜNTNER et al. (2004) and the convergence factor of 4 as a medium value. The different CIT were selected since 25,000 m² showed good agreement with the real river systems and the higher values since in GÜNTNER et al. (2004) values of 60,000 m² and 100,000 m² performed best. However, it already can be mentioned that not for all grid sizes and all catchment all variations were evaluated since the first results showed a trend towards specific variations.

The calculation of all methods was done with the software SAGA version 2.0.4 which is freely available in URL (1).

Because of the amount of up to 76 different modeled saturated areas they should be evaluated in an objective way. This will be presented in chapter 3.6.3. The software used for the spatial comparison is IDL Student Edition 6.2.

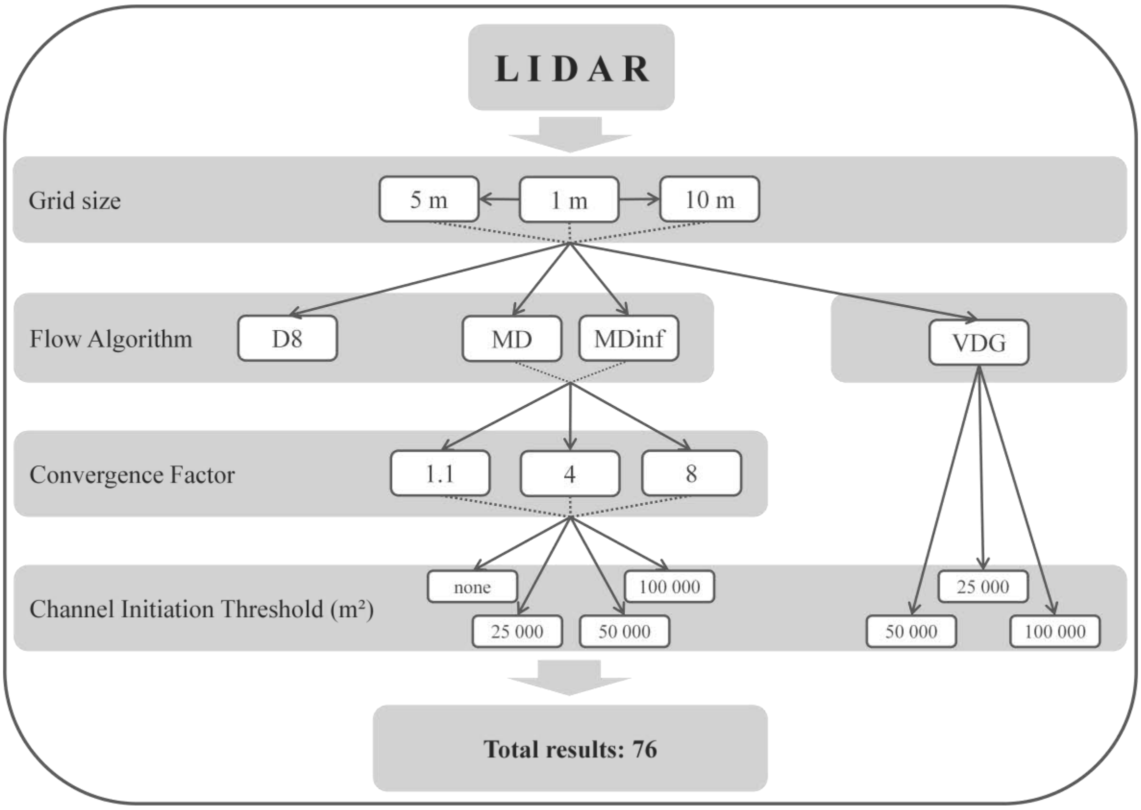

Figure 18: Overview over all applied methods in this study

3.6 Validation

To evaluate the modeled saturated areas they have to be compared with observations, the validation data. The central validation data for this purpose is a forest habitat map derived from the FVA. Additional field surveys where executed for mapping saturated areas in data gaps, but also to benchmark the FVA data. These field surveys could only be control samples, because a field survey of the whole three catchments was not possible within the time budget for this study.

3.6.1 Forest habitat map from the FVA

The forest habitat map results from an ecological method of multi factor site classification. The habitats do not have to be identical, but should be that similar that they offer same qualities or difficulties for forestry and the main tree species should grow with same performance (SEEMANN 2007). One of the ecological characteristics that is relevant and divides habitats from each other is the water supply. In particular, it is important for the ecology of trees and forests to include the borderline between waterlogged (saturated) soils and non waterlogged (non saturated) soils (SEEMANN 2007). This fact makes the forest habitat map so valuable for this study. The classification for the map is done by field survey during the vegetation period from April to November, where in an average distance of 50 to 60 m soil profiles are taken. The major roles in identifying waterlogged areas are hydromorphic characteristics in these soil profiles. Therefore, the classification of waterlogged soils represents a time integrated method. The FHM not only distinguish between waterlogged and non waterlogged areas but they classify various different wetness degrees by the magnitude of hydromorphic characteristics within these soil profiles (MICHIELS 2010). The classified wetness degrees of the FHM are thereby non waterlogged, non or a little waterlogged, more or less waterlogged, waterlogged, highly waterlogged, and groundwater influenced soils. The goal is a final accuracy of the THM of 20 to 25 m (MICHIELS 2010). According to its name the forest habitat map covers only forest areas of the landscape and additional private forests are normally not included.

In figure 19 the parts of the three catchments that are covered by the forest habitat map are shown and also the different wetness classifications of it. For the Acher catchment only the areas of higher elevation are covered by the FHM and wet areas are mainly located in the little valleys or gentle upland areas. The Eyach catchment is nearly completely covered by the FHM except some little grassland areas in the valley bottom. The groundwater influenced areas are located in the gentle uplands, whereas the valleys are more covered with the lower wetness degree. The Zastlerbach catchment is also mostly covered by the FHM and saturated soils are mostly scattered over the little valleys in the hillslopes.

As figure 19 gives a good spatial overview about the location and distribution of the waterlogged soils table 5 gives a quantitative analyze about the proportions of the forest habitat map and the different levels of waterlogged soils. The FHM covers 98.4 % of the Eyach catchment, 83.1 % of the Zastlerbach catchment, and 42.3% of the Acher catchment. The highest proportion of waterlogged areas can be found in the Eyach catchment with 24.33 %. There is also the most variability of the different wetness degrees and they all occur. The Acher catchment follows with and proportion of 9.44 % of waterlogged areas and also all wetness degrees occur even though the groundwater influenced areas play a major role compared to the Eyach catchment. The least proportion of waterlogged areas has the Zastlerbach catchment with 5.64 % and almost all of them are groundwater influenced while the other wetness degrees play only a minor role.

Table 5: Proportions of the forest habit maps for the three catchments

	Acher		**Eyach**		**Zastlerbach**	
	absolute [km2]	relative [%]	absolute [km2]	relative [%]	absolute [km2]	relative [%]
catchment area	53.4	100.0	29.7	100.0	18.3	100.0
area covered with forst habitat map	22.6	42.3	29.2	98.4	15.2	83.1

proportions of the forest habitat map	absolute [km2]	relative [%]	absolute [km2]	relative [%]	absolute [km2]	relative [%]
non waterlogged area	20.44	90.56	22.11	75.67	14.36	94.36
waterlogged areas cumulated	2.13	9.44	7.11	24.33	0.86	5.64
- non or a little waterlogged	0.65	2.88	2.34	8.02	0.01	0.04
- more or less waterlogged	0.11	0.48	1.96	6.71	0.00	0.00
- waterlogged	0.08	0.34	0.57	1.94	0.00	0.00
- highly waterlogged	0.28	1.26	0.90	3.08	0.03	0.22
- groundwater influence	1.01	4.49	1.34	4.58	0.82	5.38

3.6.2 Field survey

The field survey was done between the 27th of November 2009 and 6th of January 2010. Regarding the climate and vegetation situation this time period offers optimal circumstances for evaluating saturated areas in the field (compare chapter 2).

Therefore it was possible to apply a relative simple approach to evaluate saturated areas with the benefit of an efficient procedure. The methodology was to dig holes in soil and see from which depth on the soil is saturated. The soil was declared as saturated when the water drains out of the soil with a depth less than 10 cm. It is thereby important to get most exact position possible of the location of the sample point. This was done by using a combination of a Global Positioning System (GPS) receiver and laser distance measurement. First fix points at every observation area were chosen and the position was derived from the GPS-receiver. These fix point were chosen so that later they could be additional identified in the DEM with orthophotos or the hillshade function to improve the accuracy. That was necessary as the GPS-receiver had an inaccuracy in forest up to +/- 15 m according to its own information. The position of the sample points were than related to the fix points using the laser distance measurement. To get from the point information to saturated areas various helping tools were used. These were photos and notes taken while the field survey, orthophotos, hillshade and slope function (ArcGis) for the DEM. The accuracy of these observed saturated areas is therefore difficult to define. Subjectively estimated it is within 5 to 10 m.

Even though the method was not that sophisticated and time consuming it was not possible to examine the entire three catchments but only samples. These were chosen in three ways. First, before going in the field a modeled map with values of a TI for each catchment was studied and the areas with the highest values were then marked as objectives for the field survey. Second, areas mapped by the FHM as saturated areas were preselected. And third, while being in the field, I have looked out for suspicious areas, where saturated areas seemed to be possible. A good example of that is shown on the cover picture. Here the little amount of snow covered non saturated areas but on the saturated area it was melted.

Additional some plants (juncus acutifloris, juncus effuses, scirpus sylvaticus) could still be used as wetness indicators even though the vegetation period was mostly over. The distribution of all taken samples is shown in figure 19. It can be seen that some interesting areas, for example the area near the Hornisgrinde in the Acher catchment or the highest elevations in the Eyach catchment, were not part of the field survey. This was mainly because of the weather conditions, where the high areas of the mountains were already that much covered with snow that I could not reach them anymore and also the used method under a big snow cover may be questionable. This was also the reason why I stopped my field surveys after the 6th of January as there was the big onset of winter.

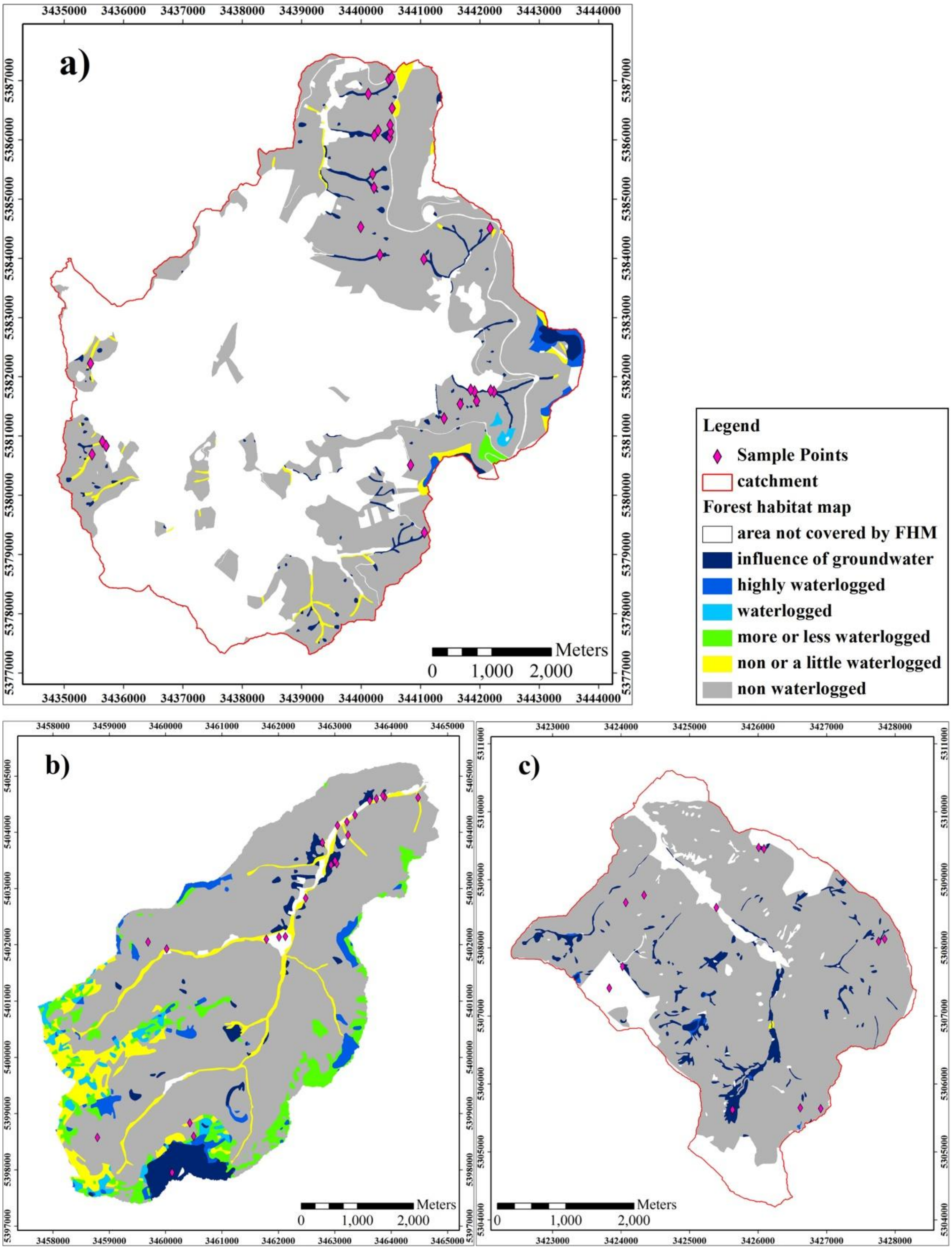

Figure 19: Waterlogged soils derived by the forest habitat map and sample points of the field survey. A) Acher b) Eyach c) Zastlerbach

3.6.3 Validation of modeled saturated areas with FHM

The first step of validation was visual comparison which leaded to the adjustment of the used methods and the sample plots chosen in field. Afterwards an objective validation between modeled saturated areas and those of the FHM was obtained and the field survey is mainly used to interpret the results of this objective validation. The methodology of the used objective validation is described in this chapter.

All the modeled topographic indexes will have an according value range for each catchment, but will not yet show saturated areas. Therefore thresholds are needed that distinguish saturated from non saturated areas. That this threshold is not arbitrarily, validation data is used to define it. Afterwards the distribution of saturated areas between modeled and validation data can then be compared and the agreement evaluated.

The steps to get to that point of comparing were the following. First, all the methods (compare chapter 3.5) were calculated for the catchment including their near neighborhood. This was done because using different flow algorithm might result in slightly different catchment areas. Then the catchment borders calculated by the D8 method were used to clip that part of all grids so all have the exact same size. The six wetness classes of the FHM were grouped to three. This was done as it was not known a priori how the classes classified from a forestry point of view fit to classification of the hydrologic point of view and where the borderline between non saturated areas and saturated areas is defined. Thereby the non waterlogged areas are the non saturated areas. The non or a little waterlogged and the more or less waterlogged areas are regarded as an transitional state group and are therefore called transitional areas. The waterlogged, highly waterlogged, and groundwater influenced are are grouped to saturated areas. As the FHM original data was in form of polygons the grouped FHM were transferred into grids of the corresponding sizes of 1 m, 5 m, and 10 m, considering the same catchment borderlines than the modeled areas. For the further validation only the cells of the modeled grids are included where also validation data by the FHM exists. The proportions of the transitional and saturated area of the FHM where then used to define the thresholds of the modeled grids so that the cumulated area of all TI values between the first and the second threshold equals the area of the transitional areas of the FHM and the cumulated area of all TI values larger than the bigger thresholds equals the saturated area of the FHM.

The spatial validation is then executed by a cell to cell comparison which leads to a matrix of agreement or disagreement as you can see in table 6. The summated portions m_ns, m_t, and m_s have the same amounts then summated portions of the validation grid of the FHM.

Table 6: Validation matrix. nn, tt, and ss shows the agreement between the grids, whereas the rest shows disagreement. Each column is summated in the lowest row

		modeled grid		
		non saturated	transitional	saturated
	non saturated	nn	nt	ns
FHM	transitional	tn	tt	ts
	saturated	sn	st	ss
	summation	m_ns	m_t	m_s

The following performance criteria are then calculated for each method on the basis of the according validation matrix:

- Proportion of agreement for all the three classes:

$$k_a = \frac{nn + tt + ss}{m\_ns + m\_t + m\_s}$$

- Proportion of agreement only for the saturated area:

$$k_s = \frac{ss}{m\_s}$$

- Proportion of agreement only for transitional area:

$$k_t = \frac{tt}{m\_t}$$

- Proportion of agreement of transitional area and saturated area:

$$k_{s+t} = \frac{tt + ss}{m\_t + m\_s}$$

- Proportion of agreement of the aggregated saturated area:

$$k_{a\_s} = \frac{tt + ts + st + ss}{m\_t + m\_s}$$

Additional to the cell to cell comparison also a cell to neighborhood comparison will be done. The reason is to attend slight spatial inaccuracies of the used methods and the validation data. Therefore the grouped FHM polygons were increased by a buffer of 10 m and then transferred into the different grid sizes. The modeled grids, however kept the same threshold from the original FHM and so the same areas of modeled grids were compared with the buffered FHM. Only k_s, k_t, and k_{st} will be regarded and called kb_s, kb_t, and kb_{st}. The amount of the improvement of the proportion of agreement gives then information if the disagreement between the original FHM and the modeled grids is due to inaccuracies or due to conceptual errors. However, it has to be mentioned that the improvement has a random component as a spatial random increase in validation area would probably also lead to an increase of the regarded proportion of agreement. Nevertheless this random component is for all methods and all grid sizes the same as always the same buffer is used and so relative conclusions can be made.

4 Results

First results showed that before the different TIs and VDGs could be calculated the input data had to be adjusted for the use in this study. This is shown in the next chapter and afterwards the results will be presented.

4.1 Adjustment of the LIDAR DEMs

As a result of a first visual comparison of the calculated stream network with a topographic map of the scale 1:25000 several mistakes were obvious. This is because of bridges or culverts are not implemented as flow paths in the DEM, but only the surface of them. Hence, when there is a bridge the height of the DEM corresponds to the surface of the bridge and not to the river flow path that might be under it. When you calculate then a stream network the bridge behave like a impermeable wall and so non realistic stream networks develop. Therefore, where it was definitely identifiable, rivers were "burned" into the DEM by reducing the height of a small part of a barrier manually. To prove the clearness about the hydrologic error it was compared to the orthophotos and the hillshade function of ESRI® ArcGis 9.3 (ArcGis). A representative example for that procedure you can see in figure 20, located in the Eyach catchment. The red line is the stream calculated for the original DEM and the green is the stream after correction.

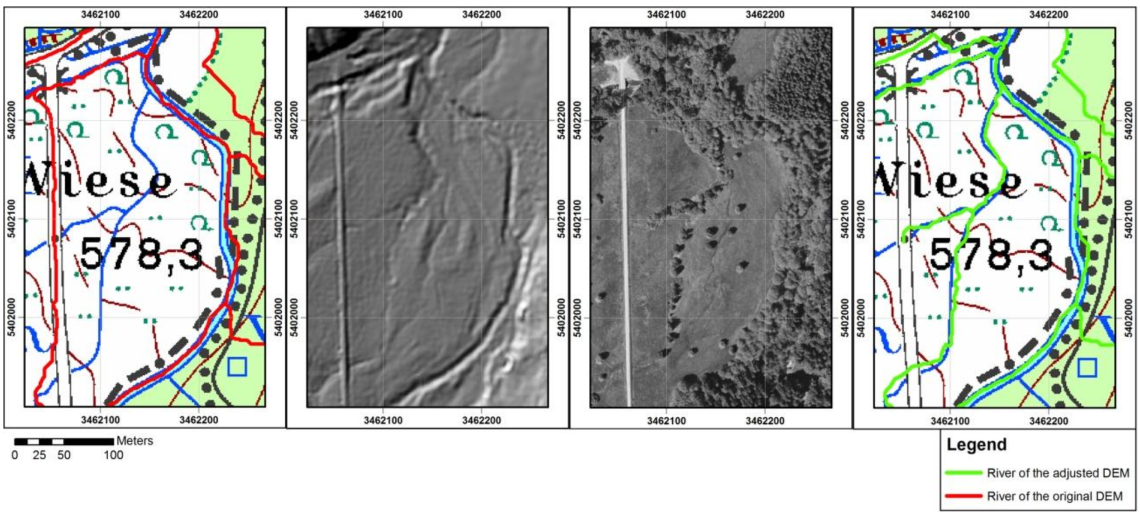

Figure 20: Adjusting a river. From left to right: river of original DEM, hillshade, Orthophoto; river of adjusted DEM

Another problem are little sinks in the DEMs. The occurrence of those is not specific for LIDAR DEMS. They occur within virtually every digital elevation model, regardless of their origin and they are negligible for most applications of a DEM but not for a hydrologic terrain analysis (ETZRODT et al. 2002). Therefore the sinks in the DEMs were filled so that the calculation of flow pathways was possible after the method of PLANCHON and DARBOUX (2002). However, the sinks were not only filled with this method, but also a downward slope along a flow path was created by accomplishing a minimum slope gradient between cells. This was needed for calculating the specific catchment area but had additional the positive side effect that there are no flat areas with a slope of zero for which value the TI is not defined. The minimum slope angle was set to the value of 0.01 °.

To generate the DEMs with coarser resolution the function aggregate in ArcGis was used. The value of the coarser grid cell was determined by calculating the arithmetic mean of the enclosed 1 m grid cells. The method of averaging the method seemed to express best the smoothing character of the water table surface compared to the surface of the landscape. DEMs with the grid size of 5 m and 10 m were generated for this study.

4.2 Validation of the different TIs with FHM

The methods that are presented in the following tables (table 7 - table 20) will have a code of AA_BB_CCC_DD. The AA stands for the used flow algorithm, the BB for the convergence factor, the CCC for the CIT, and the DD for the slope method. The CIT has thereby the unit 1000 m^2. As an example the listed method MDinf_h4_C25_Sz is the abbreviation for the TI with the combination of the MDinf flow algorithm with a convergence factor of 4, a CIT of 25000 m^2, and the slope calculated using the method of ZEVENBERGEN and THORNE (1987). The following two columns are the TI thresholds from which on all higher values are regarded as transitional cells or accordingly saturated cells. And the rest of the columns are the different performance criteria.

For the first shown catchment a broader assortment of all calculated results will be presented and they will be analyzed in more detail than for the others. Therefore, the Eyach catchment was selected, because it is the catchment, where most of the area is covered by the FHM. For this purpose the grid size of 10 m was selected because the results show that the TI performs best for this grid size. Subsequently, the results for the other catchments and other grid resolutions are presented. Thereby only a little assortment of the results will be presented. This can be done as there is a general agreement between the catchment and grid sizes which methods perform best.

4.2.1 Eyach catchment; grid size 10 m

Different performance criteria

A first general overview over all applied methods shows, that only for k_a and k_{as}, and bk_{as} an agreement close to 50 % or more occurs. The k_a, which includes non saturated cells in its calculation, has always the highest value up to 69.03%. This is followed by k_{as} and bk_{as}, which aggregate the transitional and saturated area to one big saturated area, with a maximum of 53.44%. The performance criteria k_s, k_t, $k_{s+t,}$ bk_s, bk_t, and bk_{s+t}, however, which only regard the direct agreement between the transitional or the saturated cells result in an agreement of only 30.16% as a maximum. These latter low values indicate that a prediction of the different wetness degrees of the FHM for this catchment is nearly impossible, whereas the prediction of the aggregated saturated area performs about twice as good. The values of the buffered performance criteria are in average 3.34 percentage points higher than the non buffered performance criteria (k_a is excluded from this calculation) which implies an improvement of 12.46%. Thereby the performance criterion with the highest improvement is bk_s with an average value improvement of 15.33 % followed by bk_{s+t} with 12.47 %, bk_{as} with 11.88 %, and bk_t with 10.41%. The best TI for the performance criterion k_a, k_{as} and bk_{as} is MD_h1_C0_Sz, for k_s and bk_s MD_h1_C25_Sz, for k_t, k_{s+t}, bk_t, and for bk_{s+t} MD_h1_C100_Sz.

Table 7 shows that for all performance criteria some variation of the MD method performs best. Thereby, the ones with the lowest convergence factor perform in general better than the ones with higher convergence factor. The MDinf performance with a convergence factor of 1.1 can be in its performance located somewhere between the MD variations with a convergence factor of 4 and those with 8. Therefore the performance of all MDinf is in general worse than those of MD with a convergence factor of 1.1. The performance criteria for D8 have in general the lowest values. The differences between different CITs are smaller. Whereas the values of k_a, k_{as}, and bk_{as} decrease with the initiation of CITs the values of the performance criteria, which consider the different wetness degrees, can increase.

Table 7: Assortment of validation results for Eyach, 10 m grid.

method	TI - thresholds		k_a	k_s	k_t	k_{s+t}	k_{as}	bk_s	bk_t	bk_{s+t}	bk_{as}
	t	s	[%]	[%]	[%]	[%]	[%]	[%]	[%]	[%]	[%]
MD_h1_C0_St	10.22	11.18	68.70	24.43	23.70	23.98	47.53	27.97	25.64	26.55	52.90
MD_h1_C0_Sz	10.22	11.16	69.00	25.19	24.00	24.46	48.28	28.64	25.87	26.95	53.44
MD_h1_C0_Sg	10.05	10.85	66.49	22.46	17.28	19.33	38.73	26.07	19.90	22.35	44.20
MD_h1_C25_St	10.14	10.94	68.38	25.68	23.14	24.13	46.06	29.31	25.28	26.85	51.06
MD_h1_C25_Sz	10.14	10.92	68.72	26.56	23.55	24.72	46.86	30.16	25.70	27.44	51.71
MD_h1_C25_Sg	9.98	10.66	65.99	23.43	17.44	19.82	37.70	26.92	19.87	22.67	42.73
MD_h1_C50_St	10.16	10.99	68.42	25.57	23.35	24.21	46.16	29.19	25.54	26.96	51.19
MD_h1_C50_Sz	10.16	10.96	68.75	26.54	23.76	24.85	46.85	30.15	25.92	27.57	51.73
MD_h1_C50_Sg	10.00	10.70	66.08	23.44	17.61	19.93	37.94	26.98	20.14	22.86	43.03
MD_h1_C100_St	10.16	11.02	68.49	25.54	23.70	24.42	46.25	29.11	25.89	27.15	51.30
MD_h1_C100_Sz	10.16	10.99	68.81	26.47	24.13	25.04	46.92	29.95	26.26	27.70	51.81
MD_h1_C100_Sg	10.01	10.73	66.15	23.54	17.86	20.11	38.05	27.08	20.44	23.08	43.16
MD_h4_C0_St	10.03	10.97	68.08	24.03	23.10	23.46	45.51	27.67	25.13	26.12	50.71
MD_h4_C0_Sz	10.03	10.93	68.32	24.47	23.39	23.81	46.16	28.09	25.39	26.44	51.20
MD_h4_C0_Sg	9.86	10.63	66.00	21.98	17.16	19.07	36.93	25.55	19.50	21.90	42.13
MD_h8_C0_St	9.95	10.89	67.60	23.33	22.53	22.84	44.17	27.06	24.64	25.58	49.24
MD_h8_C0_Sz	9.94	10.86	67.73	23.60	22.64	23.01	44.52	27.24	24.79	25.75	49.49
MD_h8_C0_Sg	9.78	10.55	65.53	21.21	16.79	18.54	35.52	24.75	19.01	21.29	40.58
MDinf_h1_C0_St	9.95	10.88	67.75	23.78	22.74	23.14	44.48	27.48	24.87	25.89	49.53
MDinf_h1_C0_Sz	9.95	10.85	67.95	24.16	22.96	23.43	45.00	27.87	25.22	26.26	49.96
MDinf_h1_C0_Sg	9.78	10.54	65.67	21.73	17.02	18.89	35.77	25.23	19.23	21.61	40.78
D8_St	9.66	10.80	65.28	19.73	19.13	19.36	38.10	23.12	21.04	21.85	42.57
D8_Sz	9.66	10.77	65.39	19.70	19.27	19.44	38.47	23.09	21.23	21.96	42.83
D8_Sg	9.43	10.36	62.28	17.08	13.52	14.90	28.41	19.97	15.47	17.23	32.44

Comparison of the different flow algorithms and its components

A visual overview about the different TIs and their influence on the performance criterion bk_{as} is shown in figure 21. Thereby also the results listed in annex A1 are included. Each flow algorithm is grouped in the three different slope methods so that differences between the different calculations for the specific catchment can be examined. When the flow algorithms will be described in the following they are always compared to the corresponding slope method of the other flow algorithms.

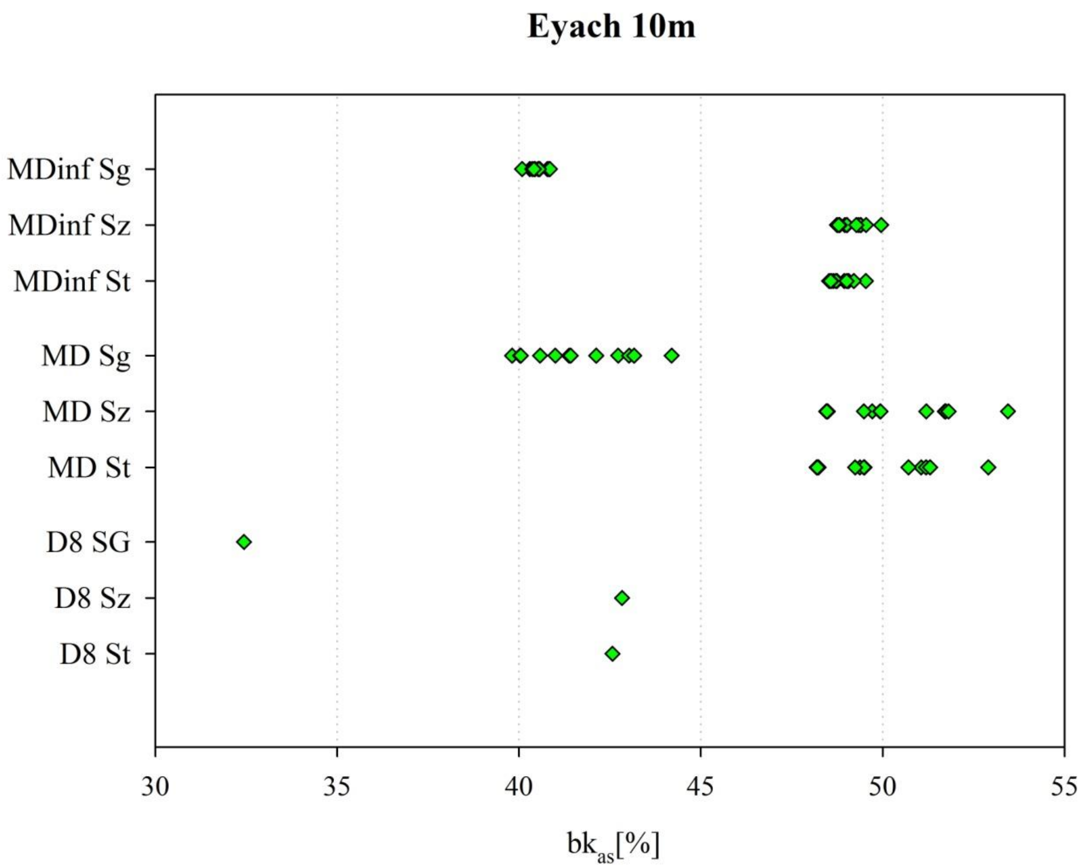

Figure 21: Performance of TIs with different combinations of flow algorithm and slope for bk_{as}; Eyach catchment 10 m

The D8 method performs in general worse than the other flow algorithms.

Comparing the two flow algorithms there is a different behavior of them for the different calculating factors noticeable. The MD is thereby more sensitive to the applied variations for the TI. The values of bk_{as} are scattered in a range of about 5 %, whereas the range for the MDinf is only about 1 %. To distinguish this range in the influence of the convergence factor and CIT the average was calculated for each of the different methods, whose results are shown in table 8. Both show a better performance of the TI the more divergent the flow algorithm is applied. The lower the convergence factor the higher the average value of bk_{as}. The fewer cells are forced to drain to only one downward cell the higher the average performance regarding bk_{as}. Thereby the TI is more sensitive to different convergence factors than different CITs. Finally, the points that have highest values of bk_{as} are for each slope-flow algorithm combination the ones with no CIT and a convergence factor of 1.1.

Table 8: Influence of the convergence factor and CIT. The values show the arithmetic mean of bk_{as} for all TI based on the corresponding variation.

arithmetic mean of	all	convergence factor = 1.1	convergence factor = 4	convergence factor = 8	
MD	47.31	49.02	47.15	45.77	
Mdinf	46.19	46.47	46.14	45.96	
arithmetic mean of	all	no CIT	CIT = 25000 m²	CIT = 50000 m²	CIT = 100000 m²
MD	47.31	48.21	46.89	47.06	47.09
Mdinf	46.19	46.45	46.01	46.15	46.15

As it is the most divergent flow algorithm of all that performs best there was the question if an even lower convergence factor could improve the performance. The evaluation of the question is shown in table 9. The lowest convergence factor used in the study as a standard value was 1.1 as it was the recommendation of FREEMAN (1991) and in all other tables and figures the abbreviation of it is h1 but here it is h1.1. For the average value of all performance criteria the two TIs with a convergence factor of 1.1 keep on having the highest value with 35.96 %. The lowest average value is for the convergence factor of 1.0 with 35.59 % and the lower convergence value average performance criteria range between 35.89 % and to 35.92 %. However, the convergence factor of 0.1 improves in average several performance criteria, the k_t, k_{s+t}, bk_t, bk_{s+t}, and bk_{as}. Finally, for the bk_{as} there is a new maximum of 53.56 % for the method MD_h0.1_C0_Sz which is 0.66 percentage points higher and therewith an improvement of 1.2 %, compared the maximum of the standardized applied methods, the MD_h1_C0_Sz.

Table 9: Lower convergence factors

method	TI - tresholds t	TI - tresholds s	k_a [%]	k_s [%]	k_t [%]	k_{s+t} [%]	k_{as} [%]	bk_s [%]	bk_t [%]	bk_{s+t} [%]	bk_{as} [%]
MD_h1.1_C0_St	10.22	11.18	68.70	24.43	23.70	23.98	47.53	27.97	25.64	26.55	52.90
MD_h1.1_C0_Sz	10.22	11.16	69.00	25.19	24.00	24.46	48.28	28.64	25.87	26.95	53.44
MD_h1.0_C0_St	10.21	11.16	68.44	24.12	23.38	23.67	46.78	27.65	25.36	26.25	52.17
MD_h1.0_C0_Sz	10.22	11.14	68.77	24.89	23.78	24.21	47.57	28.32	25.70	26.72	52.78
MD_h0.1_C0_St	10.40	11.37	68.67	24.08	23.94	24.00	47.40	27.58	25.87	26.54	52.89
MD_h0.1_C0_Sz	10.41	11.36	68.99	24.72	24.32	24.47	48.21	28.09	26.28	26.99	53.56
MD_h0.01_C0_St	10.43	11.40	68.66	24.06	23.90	23.96	47.37	27.57	25.86	26.52	52.88
MD_h0.01_C0_Sz	10.44	11.39	68.96	24.69	24.24	24.42	48.16	28.08	26.25	26.96	53.54
MD_h0.001_C0_St	10.44	11.41	68.65	24.05	23.88	23.95	47.36	27.56	25.84	26.51	52.87
MD_h0.001_C0_Sz	10.44	11.40	68.95	24.67	24.23	24.40	48.14	28.06	26.23	26.94	53.52

Results of trying to apply only the specific catchment calculated by the different flow algorithms as predictor for saturated areas are shown in table 10. However, this does not only lead to confirming results as here the MD_h1_CO performs worse for k_s, k_t, and k_{s+t} than MDinf_h1_C0 and thereby k_t, and k_{s+t}. Only for the aggregated saturated area MD_h1_C0 performs best.

Table 10: Specific catchment as predictor for saturated areas

method	area thresholds		k_a	k_s	k_t	k_{s+t}	k_{as}	bk_s	bk_t	bk_{s+t}	bk_{as}
	t [km²]	s [km²]	[%]	[%]	[%]	[%]	[%]	[%]	[%]	[%]	[%]
D8	0.31	0.77	57.90	8.99	9.52	9.32	19.22	10.96	11.19	11.10	22.76
MD_h1_C0	0.49	0.87	58.54	9.82	7.87	8.63	21.16	12.17	10.25	11.00	25.76
MDinf_h1_C0	0.39	0.70	58.32	10.13	8.34	9.04	19.85	12.33	10.44	11.18	23.95

Comparison of the different methods for the slope calculation

The differences in performance of the different methods for calculating the slope are outstanding between the global method on the one side and the local methods on the other side. The differences between the local methods are thereby comparable little and as shown later for the other catchments it is also not always Sz that performs best. However, the difference between the global and the local ones could occur because of the special calculating method of Sg. As it is calculated with dividing by the horizontal distance to the stream network all stream cells are not defined and are therefore excluded from the validation with the FHM. To get a better comparison with the other slope methods and maybe also better results for the TIs using SG there are two possibilities. Also exclude the river cells from the other slope methods or add the river cells as a high value to the TI using Sg. As an additional problem to the conceptual differences between the slope methods a problem with calculating Sg occurred and some cells at the border of each catchment were not calculated and so a little less modeled area was compared with FHM. Both problems were evaluated and results for the best method MD_h1_C0 you can see in table 11. The abbreviation “all” represents that the missing cells at the border of the catchment were added, “r” that river cells were added to the TI grid as high values and so regarded as saturated cells, and “nr” that the river cells were excluded from the TI grids.

The complement of the missing cells does only have minor influence on the performance of the Sg method and the average of performance criteria decreases by only 0.07 %. However, it resulted in a slight higher value for k_s and k_{s+t}, whereas all other performance criteria have decreasing values. Comparing MD_h1_C0_all with the local slope methods with excluded river cells shows that the difference between them got smaller as performance criteria decreased for the local slope methods. However, the local methods have still in all performance criteria in an average of 5.68 % higher values. Adding the river cells as saturated cells to the Sg method resulted in an increasing of an average amount of 0.23 % for all performance criteria, whereas for k_s, bk_s, and bk_{s+t} a decreasing occurs. But the increasing of the performance criteria was also not enough to compete with the local slope methods, whereby the conclusion is that the global methods used in this study does not improve the results, but downgrade them.

Table 11: Evaluation of the Sg method

method	TI - tresholds		k_a	k_s	k_t	k_{s+t}	k_{as}	bk_s	bk_t	bk_{s+t}	bk_{as}
	t	s	[%]	[%]	[%]	[%]	[%]	[%]	[%]	[%]	[%]
MD_h1_C0_Sg	10.05	10.85	66.49	22.46	17.28	19.33	38.73	26.07	19.90	22.35	44.20
MD_h1_C0_Sg_all	10.02	10.84	65.67	22.74	17.19	19.36	38.72	26.32	19.69	22.27	44.05
MD_h1_C0_Sg_all_r	10.12	11.13	65.92	20.21	18.84	19.37	40.71	23.43	21.25	22.10	46.23
MD_h1_C0_St_nr	10.17	11.00	69.28	24.49	26.21	23.35	46.60	27.14	29.85	25.35	51.93
MD_h1_C0_Sz_nr	10.17	10.98	69.65	25.17	27.09	23.91	47.49	27.73	30.65	25.80	52.61

CIT and the impact of rivers

The standard method how rivers are concerned in this study is that all river cells are routed with the D8 as soon as the specific catchment is higher than the CIT. Thus all water is kept in the river until the outlet and now water is added to the surrounding area. Consequential the specific catchment for all river cells is very high and they are automatically calculated as saturated areas within the validation. However, in the FHM not all rivers are mapped as saturated areas. To evaluate that bias a closer examination was done regarding the river cells, whose results are shown in table 12. Thereby river cells calculated by different CITs (25000 m², 50000 m², and 100000 m²) were excluded from the TI grids.

The average value for all performance criteria is highest for the excluded river grids with the CIT of 10000 m² with 34.35 %, followed by the CIT of 25000 m² with 34.34 %, and the lowest value for the CIT of 50000 m² with 34.28 %: This shows that differences between them are not big. Comparing the performance criteria, however, to the non excluded TIs changes can be seen. Whereas the performance criteria of the aggregated saturated areas decreases with excluding river cells, the criteria k_s and bk_s show higher values. The average value of bk_{as} of all methods using the local slopes decreases from 51.479 % for the corresponding non excluded river TI grids to 50.36 % for the TIs with rivers excluded.

Table 12: Influence of rivers on the performance of different TIs

method	TI - thresholds		k_a	k_s	k_t	k_{s+t}	k_{as}	bk_s	bk_t	bk_{s+t}	bk_{as}
	t	s	[%]	[%]	[%]	[%]	[%]	[%]	[%]	[%]	[%]
river cells with CIT = 25000 m² excluded											
MD_h1_C25_St	10.09	10.80	68.96	27.31	22.96	24.69	45.08	31.16	25.00	27.45	50.02
MD_h1_C25_Sz	10.09	10.78	69.36	28.48	23.43	25.44	46.00	32.13	25.46	28.11	50.78
MD_h1_C25_Sg	9.98	10.66	65.99	23.43	17.44	19.82	37.70	26.92	19.87	22.67	42.73
river cells with CIT = 50000 m² excluded											
MD_h1_C50_St	10.13	10.88	68.87	26.89	22.99	24.54	44.94	30.66	25.16	27.35	49.97
MD_h1_C50_Sz	10.14	10.86	69.22	27.93	23.40	25.20	45.77	31.65	25.65	28.04	50.66
MD_h1_C50_Sg	10.00	10.70	65.90	23.26	17.54	19.81	37.69	26.78	20.09	22.75	42.77
river cells with CIT = 100000 m² excluded											
MD_h1_C100_St	10.15	10.94	68.87	26.88	23.30	24.72	44.99	30.57	25.52	27.53	50.05
MD_h1_C100_Sz	10.15	10.91	69.20	27.76	23.72	25.33	45.74	31.44	25.95	28.13	50.65
MD_h1_C100_Sg	10.00	10.72	65.86	23.30	17.69	19.92	37.70	26.80	20.25	22.86	42.80

Thresholds of the TI

The thresholds for the TI, which distinguish transitional and saturated areas, vary with the convergence degree of the used flow algorithm. Thereby the threshold generally increases with increasing divergence. The thresholds for the Sg slope method is due to its calculation method always lower than for the other two slope methods. The average values of the two thresholds are for the D8 methods 9.58 and 10.65, for all MDinf methods they are 9.87 and 10.70, and for all MD methods 9.97 and 10.79. The average values for the best three methods according to bk_{as} are 10.20 and 11.11.

4.2.2 Eyach catchment; grid size 5 m

From now on only the three best results, considering bk_{as}, for each catchment and grid size are presented in and table and the rest of the results are listed in the annex (A2 – A8) in the corresponding chapter. Thereby not for all catchments the same amount of results was calculated, as especially for the high resolution grids the TIs with a high convergence degree resulted in very poor agreement. Additional, an overview for the performance criterion bk_{as}, like figure 21, which is based on the data in the annex, will be presented.

The arrangement of the scatterplot in figure 22 has a quite similar shape than for the 10 m grid, when comparing it with figure 21. The D8 performs worse than the other flow algorithms. The range of the MD methods is higher than for the MDinf methods. Thereby there is an intersection at the low agreement end of the MD methods with all MDinf methods, while the most proportion of MD performs better than MDinf. The slope characteristic is also similar as the global method results in worse performance than the comparable local slope methods. However, there is one big and deciding difference and that is the magnitude of the agreement. Whereas the scale range for figure 21 is from 30 % to 55 % here it is from 25 % to only 50 % and there is a shift for the values of about 5 percentage points towards worse results. As the best value for bk_{as} for the 10 m grid is 53.44 % for the 5 m grid it is only 47.06 %.

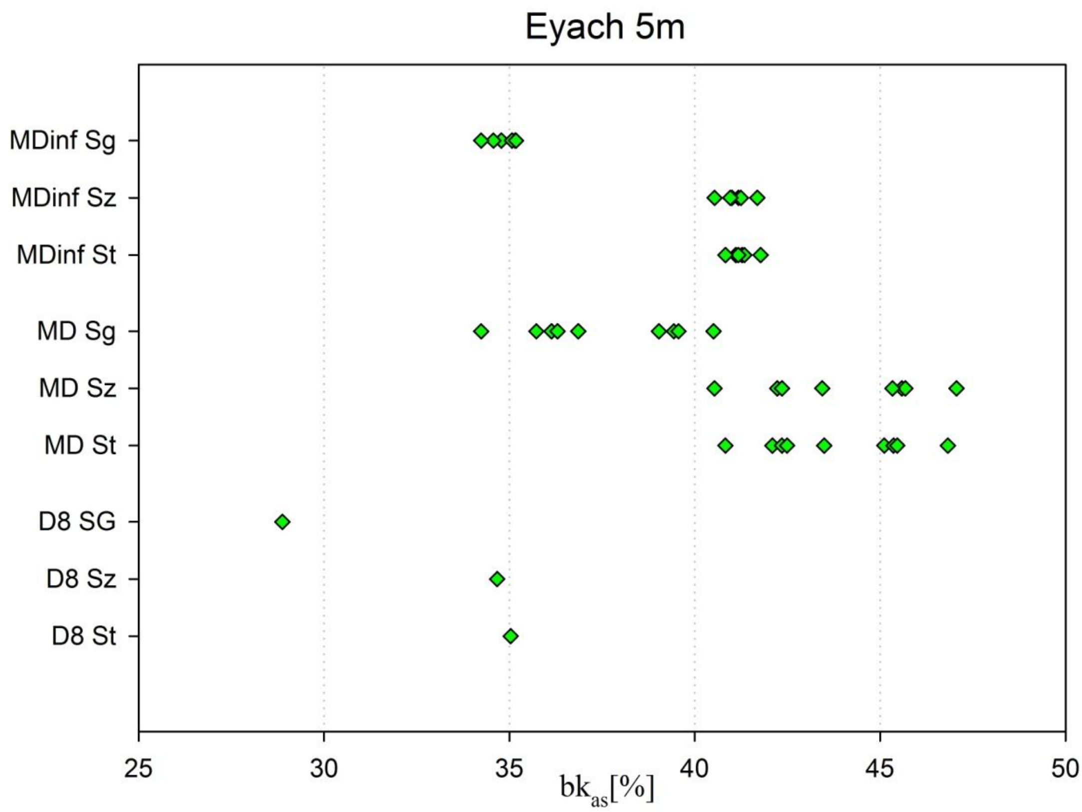

Figure 22: Performance of TIs with different combinations of flow algorithm and slope for bk_{as}; Eyach catchment 5 m

In table 13 it is shown that the shift towards worse agreement does not only occur for the performance criterion bk_{as} but for all performance criteria. The average value for all performance criteria for the methods in table 13 is 32.51 %, whereas the corresponding value for the results of the 10 m grid is 36.09 %.

The thresholds, which were used to classify the TI grids, are in general lower for the 5 m grids than for the 10 m grids. For the methods in table 12 the average value for the threshold for transitional areas is 9.41 and for the saturated areas 10.32, whereas it is 10.20 for transitional areas and 11.11 for saturated areas for the 10 m grid.

Table 13: Best three TIs according to bk_{as}; Eyach catchment 5 m

method	TI - thresholds		k_a	k_s	k_t	k_{s+t}	k_{as}	bk_s	bk_t	bk_{s+t}	bk_{as}
	t	s	[%]	[%]	[%]	[%]	[%]	[%]	[%]	[%]	[%]
MD_h1_C0_St	9.43	10.39	66.65	21.60	21.63	21.62	41.61	25.19	23.87	24.39	46.83
MD_h1_C0_Sz	9.42	10.34	66.74	21.31	21.96	21.71	41.90	24.86	24.14	24.42	47.06
MD_h1_C100_Sz	9.37	10.22	66.39	21.40	21.60	21.52	40.68	24.91	23.83	24.25	45.68

4.2.3 Eyach catchment; grid size 1 m

Here the results for the 1 m grid are presented. However, results calculated for the highest resolution and so most detailed DEM do not result in highest agreement between modeled and validation data. Actually, the contrary occurs and results calculated for the 1 m grid are worse than for the 5 m and 10 m grid. This is shown in figure 23 where the maximum value of the scale range of bk_{as} is only 36 %. The maximum of bk_{as} is thereby 34.26 % and contrary to the 5 and 10 m grid it is not MD_h1_C0_SZ but MD_h1_C25_St (table 14). The arrangement of the values still follows the rule that the more divergent the flow algorithm is the better the agreement concerning bk_{as} and the shape of the scatterplot is still comparable. However, the initialization of a CIT improved for the 1 m grid the results as the best three methods all have one. Another difference to the coarser resolutions is a different behavior for the slope methods. For the 10 m grid it is the Sz method which performs best with all flow algorithms. For the 5 m grid the St method already resulted in better performance with the D8 and MDinf methods and in the 1 m it is, finally, St which performs best with all flow algorithms.

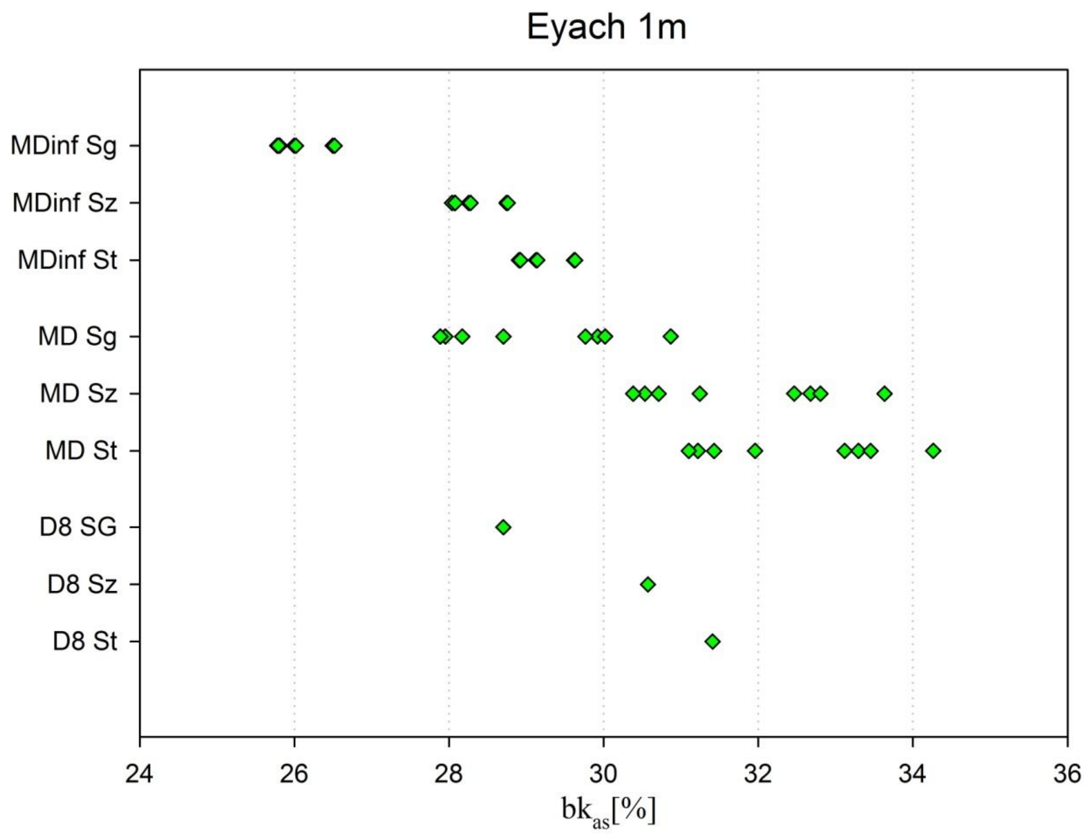

Figure 23: Performance of TIs with different combinations of flow algorithm and slope for bk_{as}; Eyach catchment 1 m

In table 14 is shown that there is not only an improvement of the best method of bk_{as} but for performance criteria, compared to the best method without a CIT, MD_h1_C0_St. However, all values are lower than for the coarser resolutions. The threshold are again lower and 7.11 for the transitional area and 8.26 for the saturated areas as an average for the three best methods according to bk_{as}.

Table 14: Best three TIs according to bk_{as}; Eyach catchment 1 m

method	TI - thresholds		k_a	k_s	k_t	k_{s+t}	k_{as}	bk_s	bk_t	bk_{s+t}	bk_{as}
	t	s	[%]	[%]	[%]	[%]	[%]	[%]	[%]	[%]	[%]
MD_h1_C25_St	7.07	8.23	62.43	17.27	14.57	15.64	29.93	20.29	16.58	18.04	34.26
MD_h1_C25_Sz	7.05	8.17	62.18	16.20	14.57	15.21	29.33	19.14	16.55	17.57	33.63
MD_h1_C50_St	7.20	8.40	62.16	16.85	14.38	15.35	29.13	19.82	16.38	17.74	33.45
for comparison:											
MD_h1_C0_St	7.36	8.65	62.02	16.02	14.45	15.07	28.83	18.86	16.57	17.47	33.30

4.2.4 Zastlerbach catchment; grid size 10 m

The next catchment presented is the Zastlerbach catchment as it has the second most percentage of covered FHM. For the Zastlerbach catchment the arrangement of the scatterplot in figure 24 is comparable to the Eyach catchment (figure 21), whereas the maximum value of bk_{as} is with 52.39 % a little lower than for the Eyach catchment with 53.44 %. Thereby, contrary to the Eyach catchment in the Zastlerbach catchment MD_h1_C0_St performs a little better than MD_h1_C0_Sz.

While the D8 method is performing the worst, there is an intersection between the MDinf methods and the MD methods, and the best performances occur again for the MD methods. However, the variability of the performances is a little higher compared to the Eyach catchment as there is a range of more than 10 percentage points for the MD methods and more than 5 for the MDinf. Thereby the outstanding position of the most divergent flow algorithm is more noticeable. This is shown in table 15, where the two best methods are more than 3.5 % higher in the value of bk_{as} than the next best and also for all other performance criteria these two most divergent flow algorithms perform better.

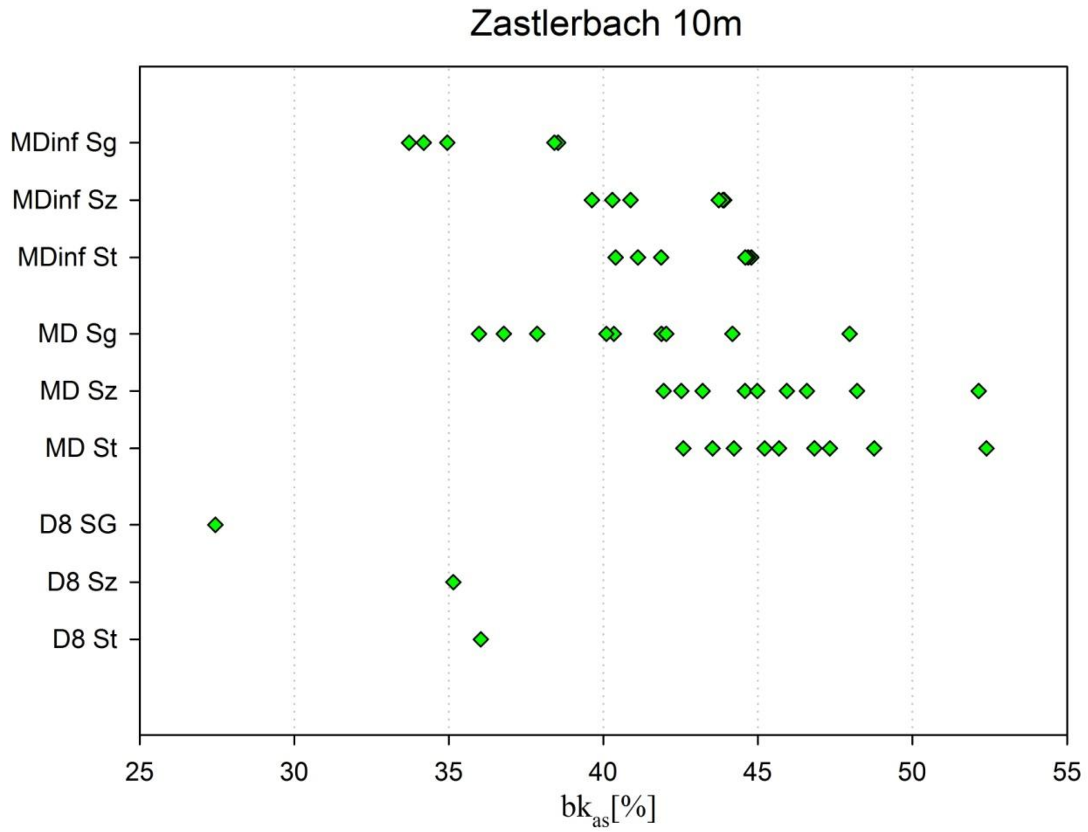

Figure 24: Performance of TIs with different combinations of flow algorithm and slope for bk_{as}; Zastlerbach catchment 10 m

In table 15 there are several new things to see compared to the Eyach catchment. The performance criterion, which includes non saturated cells in its calculation, is very high with a value up to 93.13 %. Contrary, for the transitional area there is totally no agreement which results in a value of 0 % for k_t and bk_t. But as the transitional area is only very small for the catchment the performance criteria k_{s+t} and bk_{s+t}, which considers the transitional and saturated areas separately, are close to k_s and bk_s, which consider only the saturated areas. Also k_{as} and bk_{as}, which are calculated for the aggregated saturated area, are only little higher than k_s and bk_s.

Interesting is that the third best variation of the TI is the one with no extra treatment for river cells but the one with a higher convergence factor.

The thresholds are with an average of 10.68 and 10.69 in the same magnitude than for the best two methods for the Eyach catchment with the same grid size which are 10.20 and 11.11.

Table 15: Best three TIs according to bk_{as}; Zastlerbach catchment 10 m

method	TI - thresholds		k_a	k_s	k_t	k_{s+t}	k_{as}	bk_s	bk_t	bk_{s+t}	bk_{as}
	t	s	[%]	[%]	[%]	[%]	[%]	[%]	[%]	[%]	[%]
MD_h1_C0_St	10.71	10.72	93.13	39.09	0.00	38.84	39.24	52.31	0.00	51.97	52.39
MD_h1_C0_Sz	10.65	10.66	93.13	39.06	0.00	38.80	39.22	52.04	0.00	51.70	52.15
MD_h4_C0_St	10.41	10.42	92.84	36.47	0.00	36.23	36.62	48.73	0.00	48.41	48.76

4.2.5 Zastlerbach catchment, grid size 5 m

The biggest difference between the 5 m grid (figure 25) and the 10 m grid (figure 24) for the Zastlerbach is, like for the Eyach catchment, the different scale range of bk_{as}. Whereas the arrangement of the scatterplot is comparable there is a shift towards worse performance from the 10 m grid to the 5 m grid of an average of 6.72%. Nevertheless, there are slight changes as that the outstanding position of the most divergent flow algorithm becomes even more pronounced and the difference between the Sg method and the two local slopes methods decreases. Therefore there is another third best TI the MD_h1_C0_Sg, whereas the best two stay the same (table 16).

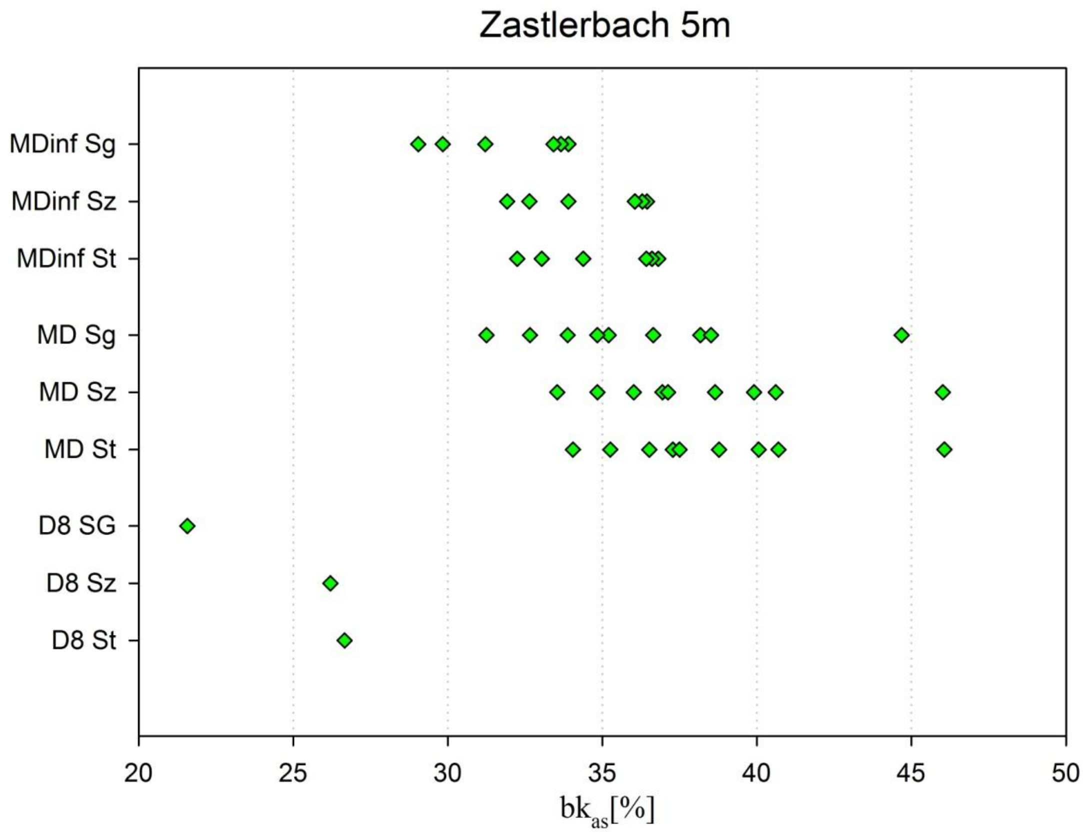

Figure 25: Performance of TIs with different combinations of flow algorithm and slope for bk_{as}; Zastlerbach catchment 5 m

The maximum value of 46.06 % for bk_{as} is 6.33 % lower than the maximum of the 10 m grid. Also all the maxima of the other performance criteria are worse than for the coarser grid, except the special values for k_t and bk_{ts}.

The thresholds are, like in the Eyach catchment, lower for the 5 m grid than for the 10 m grid. Thereby they are with average values for of 9.78 and 9.79 for the two best methods 0.905 lower compared to 10 m grid thresholds.

Table 16: Best three TIs according to bk_{as}; Zastlerbach catchment 5 m

method	TI - thresholds		k_a	k_s	k_t	k_{s+t}	k_{as}	bk_s	bk_t	bk_{s+t}	bk_{as}
	t	s	[%]	[%]	[%]	[%]	[%]	[%]	[%]	[%]	[%]
MD_h1_C0_St	9.80	9.81	92.63	34.75	0.00	34.51	34.87	45.97	0.00	45.66	46.06
MD_h1_C0_Sz	9.75	9.76	92.63	34.79	0.00	34.55	34.94	45.92	0.00	45.61	46.02
MD_h1_C0_Sg	9.68	9.69	92.90	33.61	0.00	33.39	33.66	44.64	0.00	44.35	44.68

4.2.6 Zastlerbach catchment, grid size 1 m

As there was already a shift to worse performance from the 10 m grid to the 5 m grid there is a further shift from the 5 m grid to the 1 m grid, as shown in figure 26. The range of the values of bk_{as} goes from 13.62 % to only 30.89 %. The agreement for the best method for the 1 m grid is therefore 21.5 % lower than for 10 m grid. However, it is noticeable that for the high resolution DEM the global slope method performs best and it is again the most divergent flow algorithm which performs best.

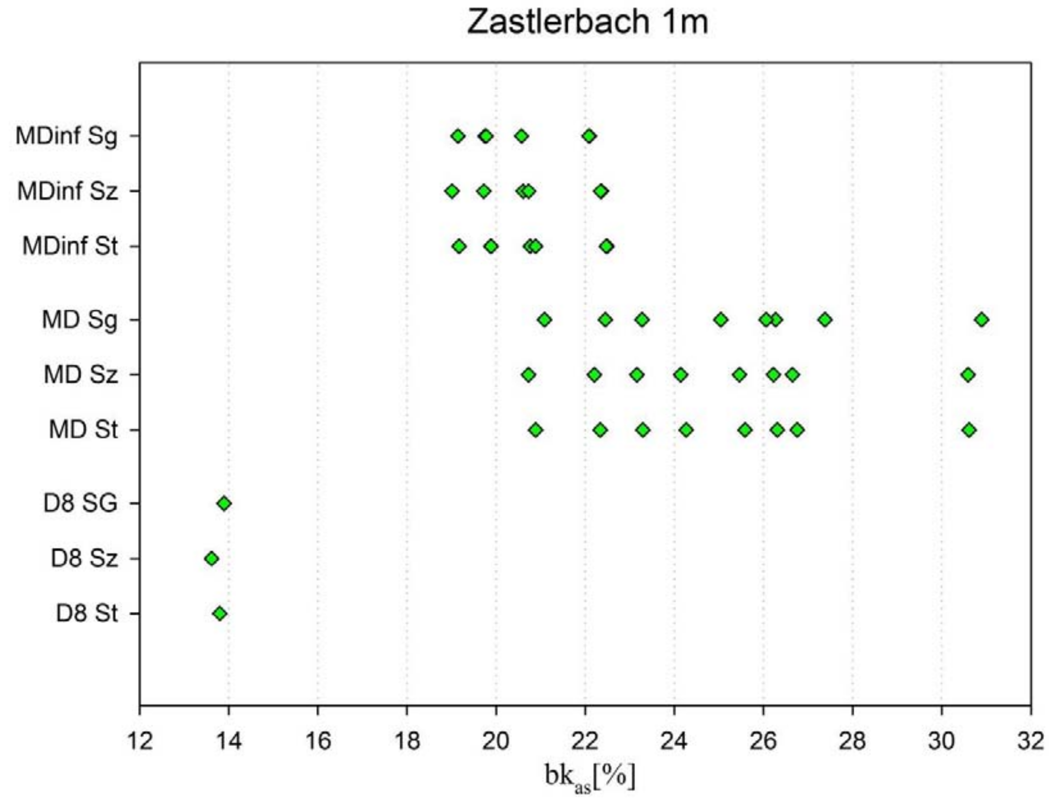

Figure 26: Performance of TIs with different combinations of flow algorithm and slope for bk_{as}; Zastlerbach catchment 1 m

In table 17 it is shown that all performance criteria, except the special case of k_t and bk_t, are worse than for the coarser grids.

The thresholds are like the 1 m grid for the Eyach catchment lower than for the coarser grids.

Table 17: Best three TIs according to bk_{as}; Zastlerbach catchment 1 m

method	TI - thresholds		k_a	k_s	k_t	k_{s+t}	k_{as}	bk_s	bk_t	bk_{s+t}	bk_{as}
	t	s	[%]	[%]	[%]	[%]	[%]	[%]	[%]	[%]	[%]
MD_h1_C0_Sg	8.01	8.02	91.32	21.92	0.00	21.78	22.00	30.85	0.00	30.65	30.89
MD_h1_C0_St	8.03	8.04	91.18	21.77	0.05	21.63	21.88	30.55	0.07	30.35	30.61
MD_h1_C0_Sz	8.01	8.02	91.17	21.74	0.00	21.59	21.85	30.53	0.05	30.33	30.59

4.2.7 Acher catchment, grid size 10 m

The distribution of the performance of the methods is for the Acher catchment also comparable with those of the other two (figure 27). Beside the fact, that the D8 methods perform worst it are again the MDinf methods and MD methods that have for the more convergent variations of MD an intersection. The more divergent the Variations of MD get the better the performance till there is again the outstanding position of the most divergent flow algorithm. For the Acher catchment it is, like for the Zastlerbach catchment, the combination with the St method that gives best performance. However, with an agreement of only 47.66 % it has the worst maximum value of the three catchments.

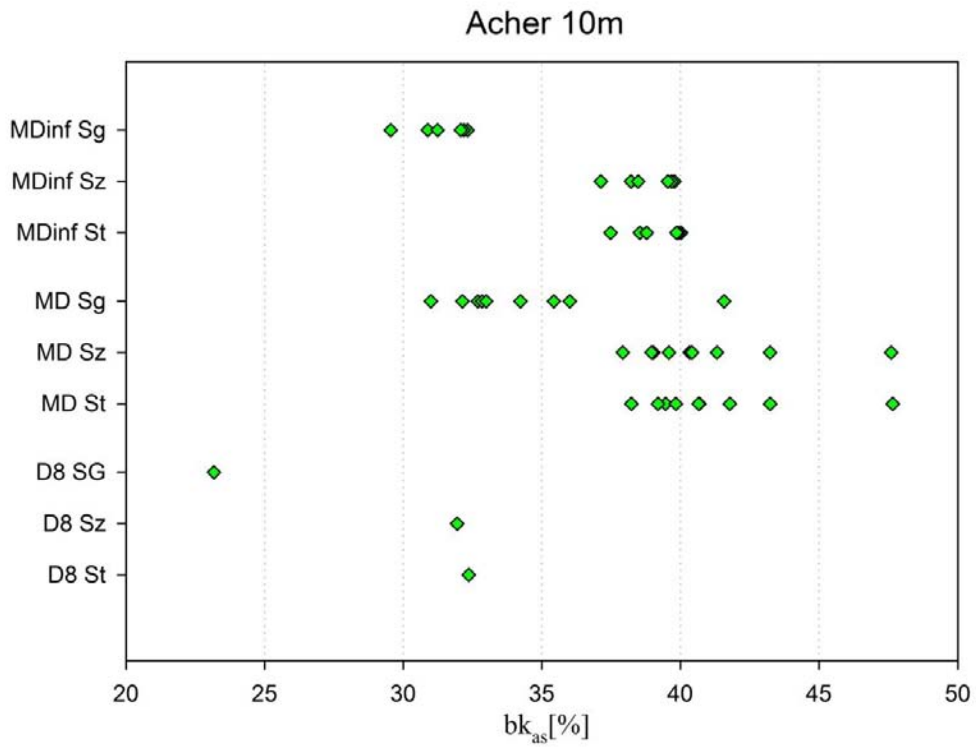

Figure 27: Performance of TIs with different combinations of flow algorithm and slope for bk_{as}; Acher catchment 10 m

In table 18 is shown that the k_a values for the Acher catchment are up to 87.47 % which represents an agreement between the other two catchments. The k_s value gives an agreement of up to 33.19 %, whereas the maximum of the k_t value is only 8.37 % and the corresponding buffered values are 39.81 % and 9.73 %. So also for the Acher catchment there is a poor prediction of the different saturation classes, whereas the agreement of the saturated areas is relative better than for the Eyach catchment and the agreement of the transitional areas is worse. The maximum of the aggregated saturation performance criteria are with values of 40.37 % for k_{as} and 47.66 % for bk_{as} less than for the Eyach catchment.

The thresholds are with 10.04 and 10.48 for the two best methods the lowest of the three catchments, as for the Eyach catchment they are 10.20 and 11.11 and for the Zastlerbach catchment 10.68 and 10.69.

Table 18: Best three TIs according to bk_{as}; Acher catchment 10 m

method	TI - thresholds		k_a	k_s	k_t	k_{s+t}	k_{as}	bk_s	bk_t	bk_{s+t}	bk_{as}
	t	s	[%]	[%]	[%]	[%]	[%]	[%]	[%]	[%]	[%]
MD_h1_C0_St	10.05	10.50	87.45	32.92	8.12	24.35	40.37	39.63	9.51	29.22	47.66
MD_h1_C0_Sz	10.03	10.46	87.47	33.19	8.37	24.62	40.31	39.81	9.73	29.42	47.60
MD_h4_C0_St	9.84	10.28	86.90	30.16	7.14	22.20	36.67	35.92	8.50	26.44	43.24

4.2.8 Acher catchment, grid size 5 m

For the 5 m grid the same shift towards worse values is noticeable than for the other two catchments, as shown in figure 28. The maximum value of bk_{as} is thereby 6.9 % lower than for the 10 m grid. As for the 10 m the best TI is grid MD_h1_C0_St it changes for the 5 m and MD_h1_C0_Sz is here the best.

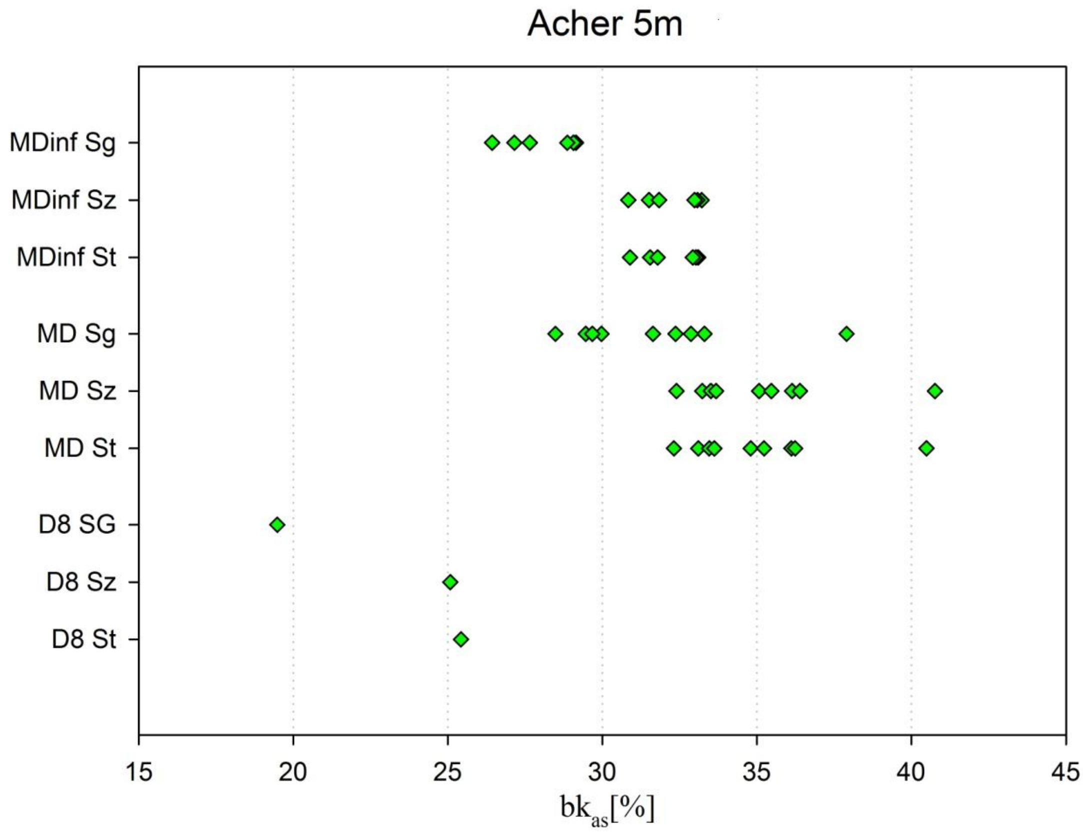

Figure 28: Performance of TIs with different combinations of flow algorithm and slope for bk_{as}; Acher catchment 5 m

In table 19 is shown that this shift towards worse performance does also like for the other catchments occur for all the performance criteria. The thresholds are also lower than for the 10 m grid.

Table 19: Best three TIs according to bk_{as}; Acher catchment 5 m

method	TI - thresholds		k_a	k_s	k_t	k_{s+t}	k_{as}	bk_s	bk_t	bk_{s+t}	bk_{as}
	t	s	[%]	[%]	[%]	[%]	[%]	[%]	[%]	[%]	[%]
MD_h1_C0_Sz	9.24	9.65	86.42	28.40	6.81	20.83	34.35	34.25	7.94	25.02	40.76
MD_h1_C0_St	9.27	9.70	86.37	28.13	6.68	20.60	34.07	33.94	7.86	24.79	40.49
MD_h1_C0_Sg	9.23	9.59	86.56	24.71	7.40	18.61	31.38	30.39	8.69	22.73	37.90

4.2.9 Acher catchment; grid size 1 m

As the Acher catchment is the largest of the three catchments there were several problems in handling the coming up data volume for the 1 m grid. A grid which covers the Acher catchment exists thereby of about 9000 columns and 10000 rows which result in a total cell number of 90,000,000. This was too much for the software used for validation (IDL) even on a 64bit system computer with 8GB RAM. So there would have been only the possibility to make the whole validation with other very time consuming methods. However, it is questionable to invest much time to get results for which already many indicators exist that they will not improve already existing results and will also not provide much additional information. For both other catchments the results show that for the 1 m grid the methods perform definite the worst and for the Acher catchment the shift from the 10 m grid to the 5 m grid towards worse performance indicate that it will be for the Acher catchment probably the same. Therefore for the Acher catchment only the most divergent flow algorithm was evaluated and the results are shown in table 20. This results show just the same trend as for the other two catchments, whereas all performance criteria decrease and no improvement at all is noticeable. Therefore it was assumed that the validation of the other variations would not improve the information content in an acceptable relation to the time effort needed for it.

Table 20: The three most divergent TIs as representatives; Acher catchment 1 m

method	TI - thresholds		k_a	k_s	k_t	k_{s+t}	k_{as}	bk_s	bk_t	bk_{s+t}	bk_{as}
	t	s	[%]	[%]	[%]	[%]	[%]	[%]	[%]	[%]	[%]
MD_h1_C0_St	7.35	7.89	84.52	17.91	5.26	13.41	22.59	22.42	6.22	16.66	27.69
MD_h1_C0_Sz	7.33	7.85	84.51	17.90	5.25	13.41	22.54	22.44	6.21	16.67	27.66
MD_h1_C0_Sg	7.45	7.94	84.42	17.28	5.10	12.95	22.04	21.86	6.24	16.31	27.40

4.3 Validation of VDG with FHM

Here the results of the validation of the modeled saturated areas with the VDG method are presented. As for this method there were only three variations used for each catchment and grid size the results of the different grid sizes for each catchment can be grouped together. In the tables the variations of VDG will have the code VDG_CIT_AA, whereas AA in 1000 m² gives the applied CIT to delineate the needed stream network. The thresholds give here the vertical distance to the potential groundwater table from which on all lower values are regarded as transitional or corresponding saturated cells.

4.3.1 Eyach catchment

For the VDG method it is also the calculation for the 10 m grid which results in best performance according to bk_{as}, as shown in table 21. Thereby, the variation with the lowest CIT performs best for k_a, k_t, k_{s+t}, bk_t, bk_{s+t}, and bk_{as} and for the performance criteria k_s and bk_s the calculation for the stream network with CIT 50000 m² performs best. The modeled saturated areas for the 5 m grid result in the worst performance and consequently results for the 1 m grid have medium performance. However, for the performance criteria k_t, k_{s+t}, bk_t, and bk_{s+t} the modeled saturated areas for the 5 m result in best performance. However, none of the best performance criteria for the VDG method improves the results of the best TI method. The average value of 23.92% for all performance criteria for the best method of VDG according to bk_{as} is 12.28 lower than the corresponding value for the best TI method.

The VDG is less sensitive to the change of grid size than the TI methods. Whereas for the 10 m grid the VDG performs worse than the TI for the grid size of 1 m it performs better at least for the performance criterion bk_{as}.

The threshold follow the rule, that as finer the stream network get the lower the thresholds are. Thereby the values are the highest for the 5 m grid, followed by the 10 m grid and lowest for the 1 m grid.

Table 21: Validation results for VDG; Eyach catchment

method	thresholds		k_a	k_s	k_t	k_{s+t}	k_{as}	bk_s	bk_t	bk_{s+t}	bk_{as}
	t [m]	s [m]	[%]	[%]	[%]	[%]	[%]	[%]	[%]	[%]	[%]
10m grid											
VDG_CIT_100	21.73	5.57	60.69	13.86	4.66	8.25	30.37	16.98	6.40	10.52	37.57
VDG_CIT_50	13.46	2.54	61.95	16.88	6.28	10.41	33.40	19.77	9.50	13.51	40.59
VDG_CIT_25	5.78	0.63	62.25	12.14	10.47	11.12	33.93	15.12	14.68	14.85	40.76
5m grid											
VDG_CIT_100	28.14	8.66	58.13	10.03	18.00	14.90	27.64	12.25	19.94	16.95	31.55
VDG_CIT_50	18.46	4.03	58.26	11.31	17.48	15.08	27.89	13.50	19.29	17.04	31.81
VDG_CIT_25	8.40	1.18	58.00	10.40	17.14	14.52	27.62	12.72	19.02	16.57	31.59
1m grid											
VDG_CIT_100	12.33	2.46	59.73	8.00	6.10	6.85	27.64	10.48	9.30	9.76	34.48
VDG_CIT_50	4.23	0.80	60.82	8.78	11.86	10.64	28.32	11.33	15.60	13.91	34.31
VDG_CIT_25	1.33	0.30	60.25	7.99	14.99	12.23	24.40	10.21	17.57	14.67	29.20

4.3.2 Zastlerbach catchment

For the Zastlerbach the less sensitivity to the change of grid size is remarkable. Here there are only slight differences between the grid sizes, whereby still the results of the 10 m grid perform in average better than for the finer DEMs (table 22). However, also for the Zastlerbach catchment none of the performance criteria, except k_t and bk_t, show an improvement to the best method of TI. The differences are thereby a little less than for the Eyach catchment as the average value for all performance criteria for the best method according to bk_{as} is only 2.41 % less than the corresponding value for the best TI.

The thresholds are also here correlated with the CIT as the higher the CIT gets the higher the thresholds gets. However, the maximum threshold value with 2.37 m for the Zastlerbach catchment is much lower than the maximum threshold value for the Eyach catchment which is 28.14 m.

Table 22: Validation results for VDG; Zastlerbach catchment

method	thresholds		k_a	k_s	k_t	k_{s+t}	k_{as}	bk_s	bk_t	bk_{s+t}	bk_{as}
	t [m]	s [m]	[%]	[%]	[%]	[%]	[%]	[%]	[%]	[%]	[%]
10m grid											
VDG_CIT_100	2.02	1.99	92.81	36.28	0.00	36.05	36.35	48.09	0.00	47.77	48.02
VDG_CIT_50	0.68	0.66	92.56	34.02	0.00	33.80	34.24	45.39	0.00	45.09	45.54
VDG_CIT_25	0.00	0.00	91.83	27.72	-	27.72	27.91	39.19	-	39.19	39.32
5m grid											
VDG_CIT_100	2.37	2.34	92.77	36.05	0.00	35.81	36.12	47.50	0.00	47.18	47.44
VDG_CIT_50	1.08	1.07	92.63	34.71	0.43	34.48	34.89	45.94	0.43	45.63	46.07
VDG_CIT_25	0.39	0.38	91.96	28.78	0.00	28.59	28.94	39.68	0.00	39.41	39.80
1m grid											
VDG_CIT_100	2.16	2.13	92.67	35.02	0.30	34.79	35.24	46.48	0.27	46.17	46.64
VDG_CIT_50	0.99	0.98	92.41	32.70	0.16	32.49	32.87	44.58	0.18	44.29	44.71
VDG_CIT_25	0.42	0.41	91.83	27.58	0.12	27.40	27.71	38.86	0.16	38.61	38.95

4.3.3 Acher catchment

The Acher catchment is the only catchment, where results of the VDG method perform better than the best TI method. Thereby, as shown in table 23, it are again the results of the 10 m grid that perform best and finally the VDG method with a CIT of 50000 m² provide a new best performance according to the bk_{as}. However, the difference between the two maxima for bk_{as} is only 2.04% and for k_a, k_s, and k_{as} it is still the best TI according to bk_{as} that performs better.

The thresholds are like for the other catchments bigger as the CIT increases and the absolute values are between the thresholds for the other to catchments.

Table 23: Validation results for VDG; Acher catchment

method	thresholds t [m]	thresholds s [m]	k_a [%]	k_s [%]	k_t [%]	k_{s+t} [%]	k_{as} [%]	bk_s [%]	bk_t [%]	bk_{s+t} [%]	bk_{as} [%]
10m grid											
VDG_CIT_100	12.09	7.16	86.94	34.17	4.16	23.80	35.43	46.55	8.38	33.36	49.54
VDG_CIT_50	6.05	2.92	87.24	32.45	9.85	24.64	37.80	41.63	13.97	32.07	49.70
VDG_CIT_25	2.14	0.76	86.48	26.32	9.71	20.58	33.69	33.54	11.59	25.96	42.24
5m grid											
VDG_CIT_100	11.35	6.53	86.61	32.13	5.22	22.68	34.54	43.40	9.53	31.51	47.89
VDG_CIT_50	4.36	2.04	86.63	28.92	11.73	22.89	34.62	36.78	14.23	28.86	43.92
VDG_CIT_25	1.65	0.72	86.05	24.73	10.36	19.69	31.58	31.63	11.44	24.55	38.94
1m grid											
VDG_CIT_100	2.65	1.29	85.51	22.24	8.98	17.52	28.98	28.15	9.95	21.68	35.77
VDG_CIT_50	1.27	0.65	85.07	19.25	8.13	15.30	26.51	24.60	9.28	19.16	32.67
VDG_CIT_25	0.63	0.33	84.61	16.75	7.57	13.49	23.46	21.76	8.52	17.06	29.07

4.4 Summary of the validation with FHM

In figure 29 the overview of the performance of the best methods for each catchment at every grid size related to the performance criterion bk_{as} is shown. Regarding the best TIs it is obvious that they all follow the rule that the best TI occurs for the 10 m grids, while the worst of the best TIs is occurring for the 1 m grids. The best VDGs do not follow that strict rule as the results for the 1 m and 5 m grids change their positions but also for the VDGs it are always the 10 m grids that deliver best performance.

Whereas for the Acher catchment the best VDG method is a slight improvement to the best TI method for the other two catchments, especially for the Eyach catchment, the best TI performs much better.

The best VDG for the Eyach catchment is the one with a CIT of 25,000 m², for the Zastlerbach catchment the one with a CIT of 100,000 m² and for the Acher catchment the one with a CIT of 50,000 m², respectively.

The best TI for all the three catchments exists of the most divergent flow algorithm method, the MD with a convergence factor 1.1 and no applied CIT. Only the combination with the slope method differs which is the method of ZEVENBERGEN and THORNE (1987) for the Eyach catchment and is the method of TARBOTON (1997) for the Zastlerbach and Acher catchment.

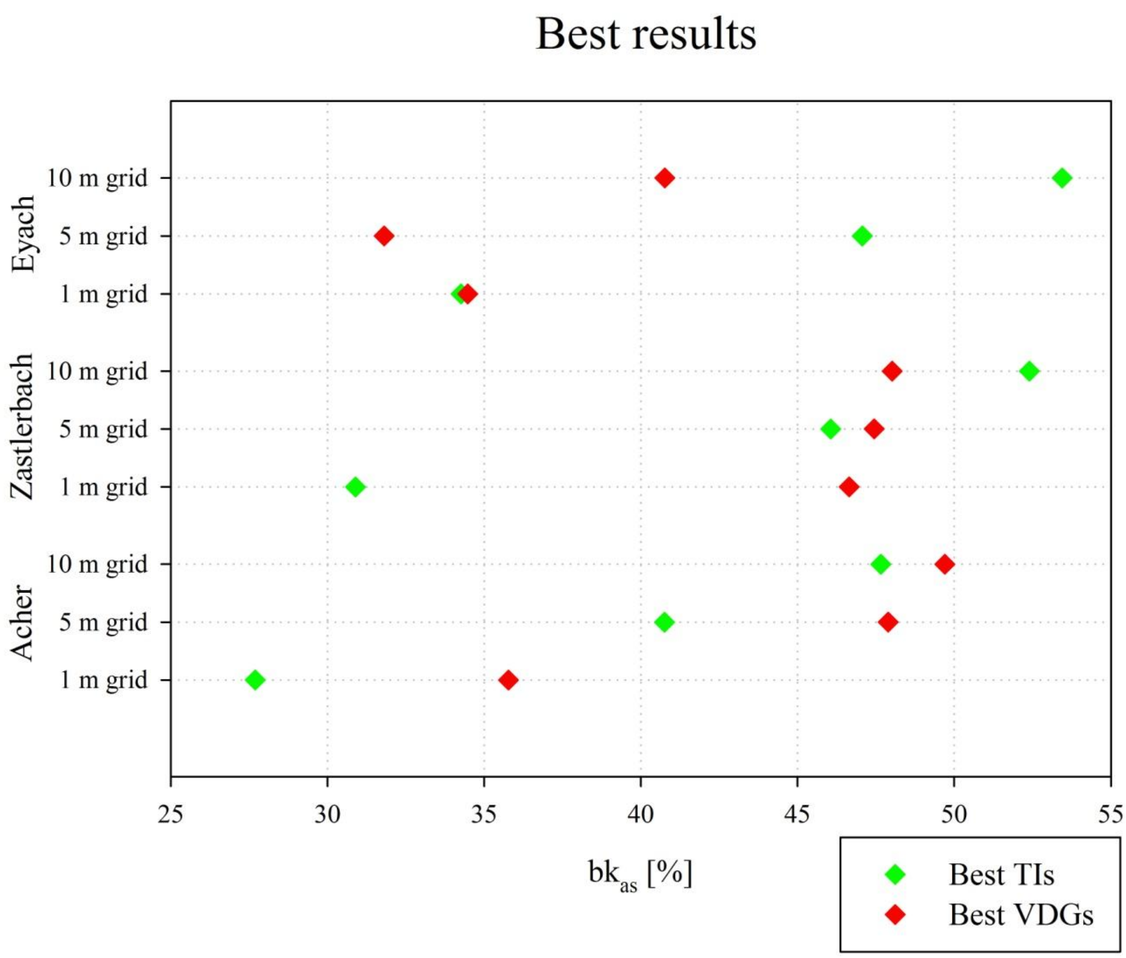

Figure 29: Best results of the validation with FHM according to bk_{as}

4.5 Visual comparison between modeled and validation saturation areas

To get an idea not only of the quantity of the agreement between modeled saturated areas and those mapped by FHM, but also where agreement and where disagreement occurs in this chapter the spatial distribution is presented. Thereby the aggregated saturation areas are chosen for a better overview in visualization and also because the results show best results for them. It is shown the agreement between the best method of TI and VDG with the non buffered FHM.

4.5.1 Eyach catchment

In figure 30 is shown that the gentle area around the highmoor in the south of the catchment is quite good predicted. Also the gentle high area in the east of the catchment shows a good agreement, whereas in the west a big area of the FHM is not modeled as a saturated and also the opposite way around. Also some areas, which are located at the catchment border, are mapped by the FHM as saturated areas but not modeled. Another big mismatch can be assigned to the side valleys and hillslopes along the main stream network, where many modeled saturation areas occur, but only seldom mapped by the FHM. Along the main valleys, however, mostly an agreement occurs.

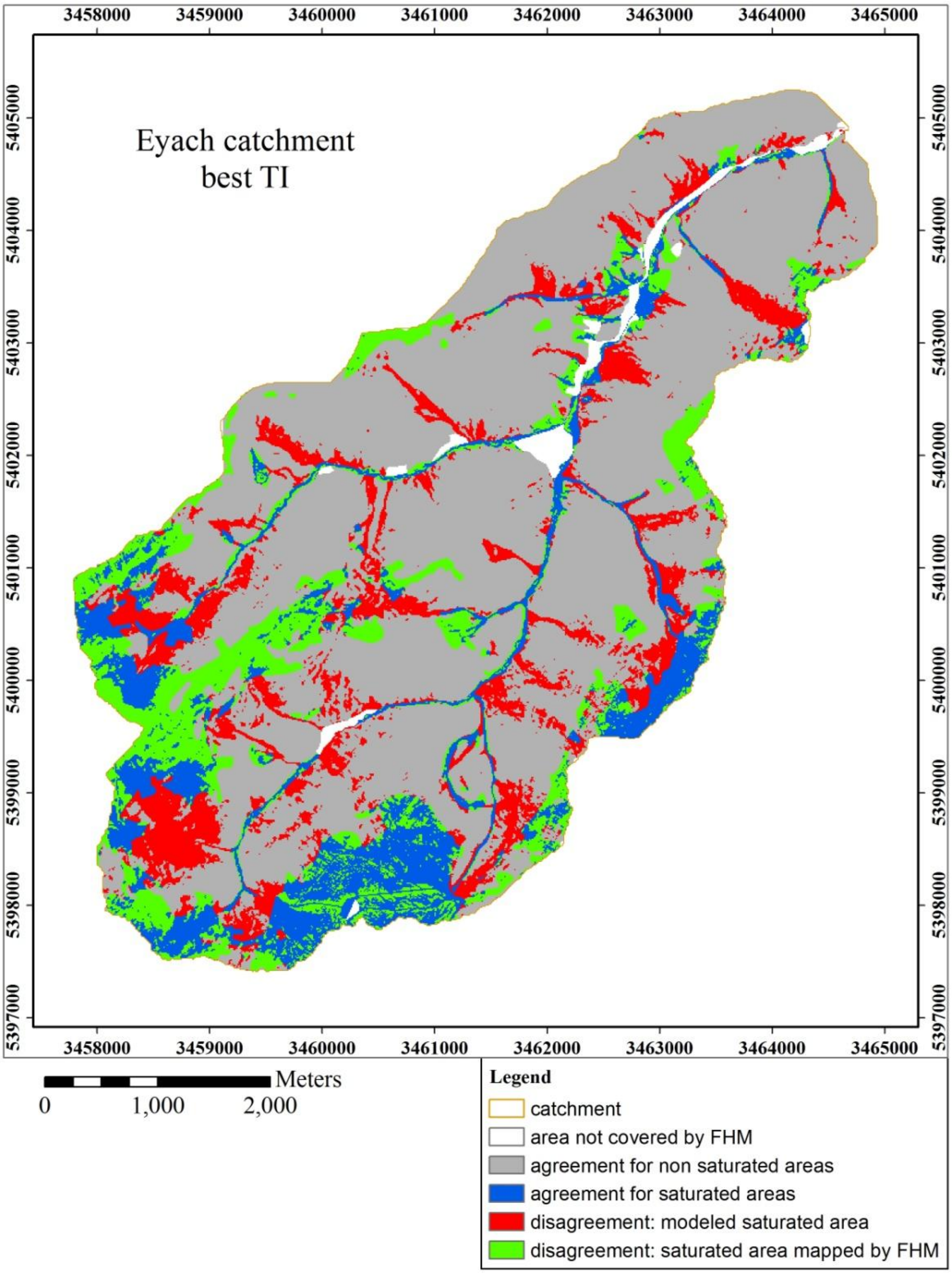

Figure 30: Visual comparison of the validation of the best TI and FHM; Eyach catchment 10 m

In figure 31 the mismatch for the side valleys and hillslopes along the main stream network did grow compared to figure 30. Additional, the gentle high areas along the catchment border and specially the large area in the east, which are mapped by the FHM as saturated areas, are not modeled by the VDG.

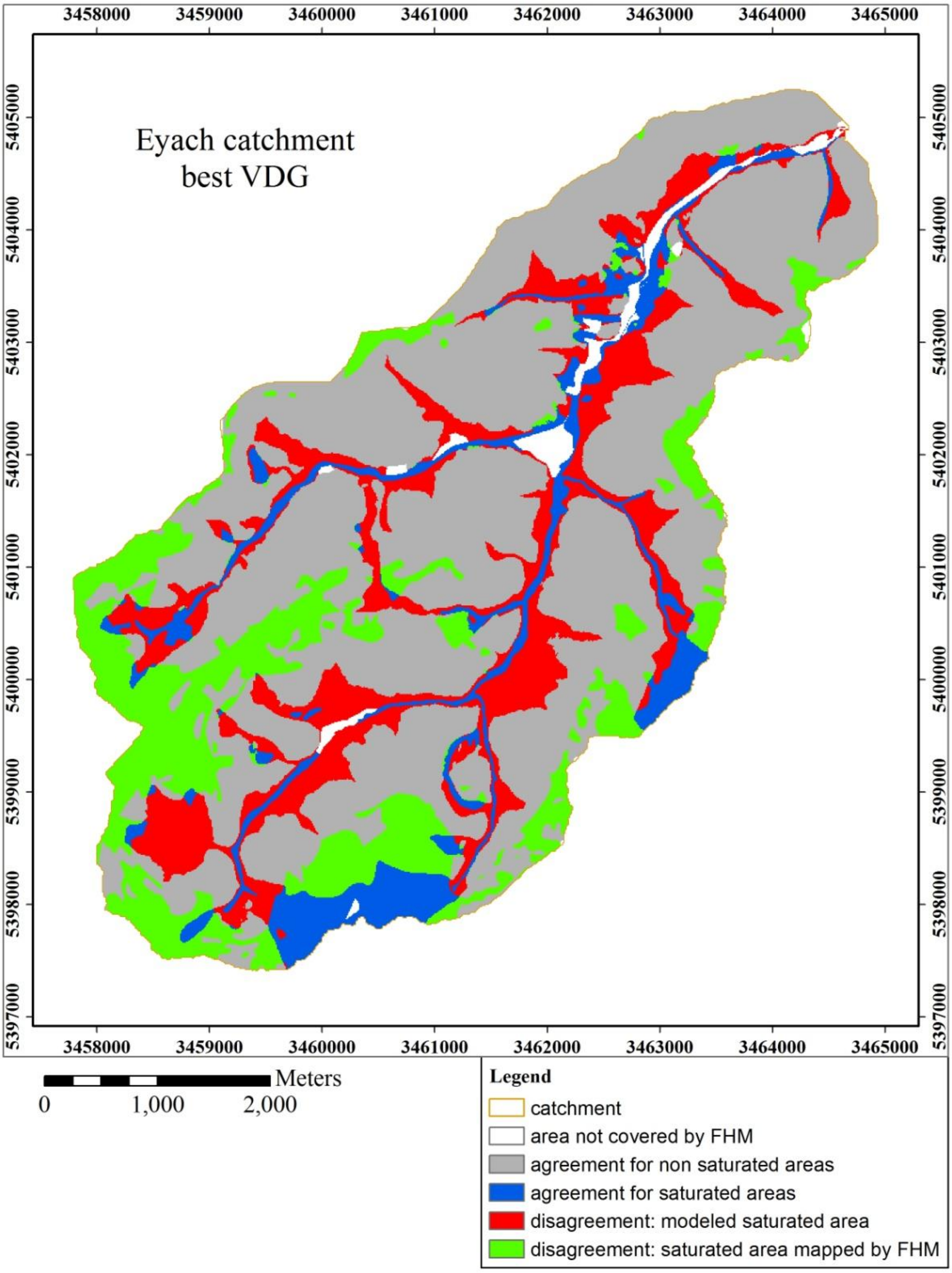

Figure 31: Visual comparison of the validation of the best VDG and FHM; Eyach catchment 10 m

4.5.2 Zastlerbach catchment

In figure 32 is shown that the saturated areas mapped by the FHM that are scattered in the catchment have no agreement with the modeled ones. The rest of the mapped saturated areas are located along the valleys and many of them have a good agreement with the modeled ones. However, the modeled saturated areas are uniform along all valley bottoms, whereas those of the FHM are distributed to only some parts of certain valleys.

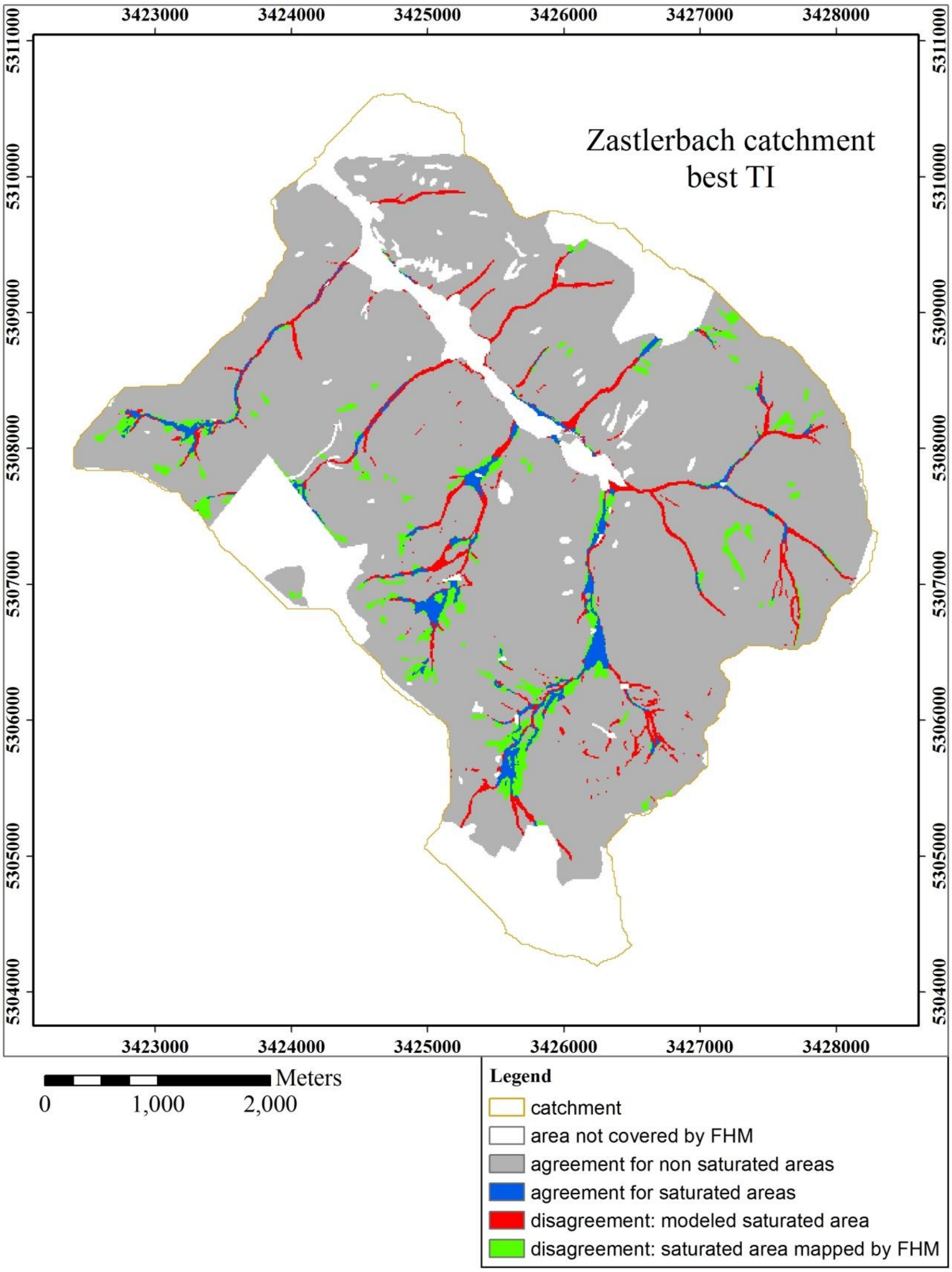

Figure 32: Visual comparison of the validation of the best TI and FHM; Zastlerbach catchment 10 m

The VDG method has also no agreement with the sprinkled saturation areas mapped by the FHM. The modeled saturation areas are strongly related to the stream network and in the main valley much area is modeled as saturated area which is not mapped as such by the FHM. Contrary, in higher elevation there are many mapped saturated areas that are not modeled by the VDG (figure 33).

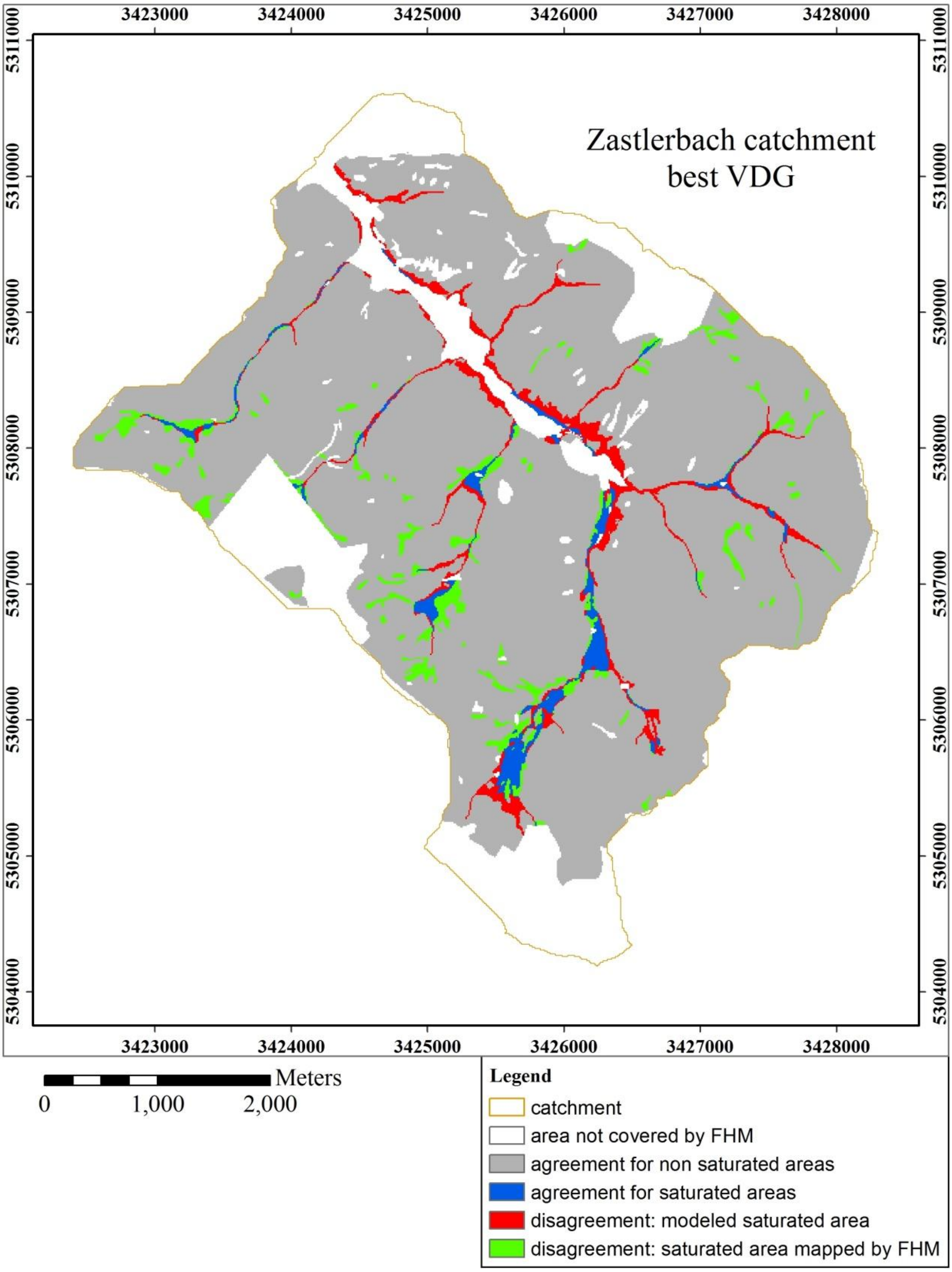

Figure 33: Visual comparison of the validation of the best VDG and FHM; Zastlerbach catchment 10 m

4.5.3 Acher catchment

For the Acher catchment there are two major areas, where disagreement between the TI and FHM saturation areas occurs. Whereas in the north there is much more saturated area modeled by the TI than mapped by the FHM, in the east at the highest elevation there is more mapped saturated area than modeled and at the catchment border near the precipitation station Ruhestein is a mapped saturated area where nearly no agreement occurs (figure 34).

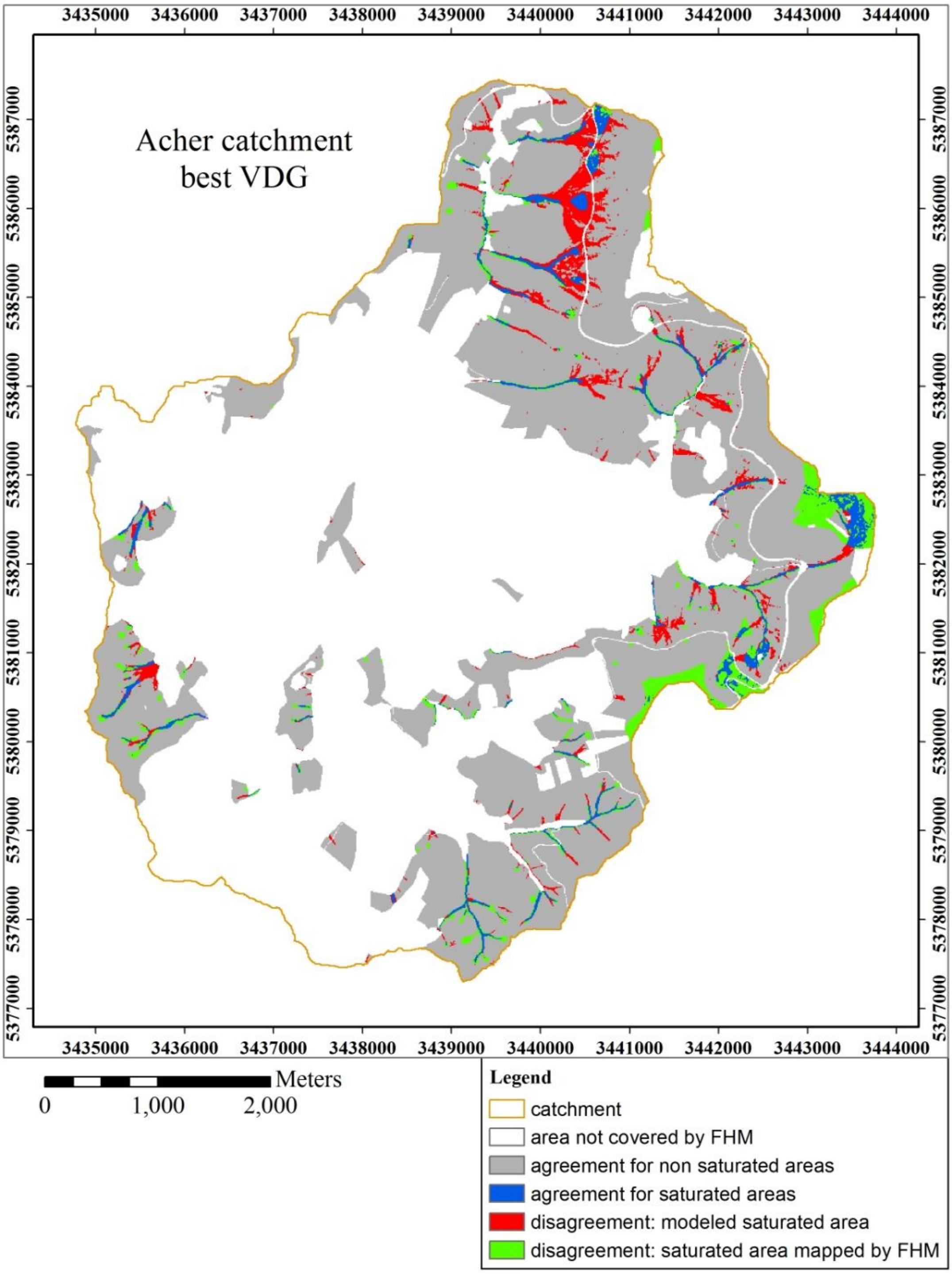

Figure 34: Visual comparison of the validation of the best TI and FHM; Acher catchment 10 m

In figure 35 is shown that the two major disagreement areas of the TI are also for the VDG method areas where disagreement occurs. Thereby for the high elevation areas in the east is even less agreement noticeable.

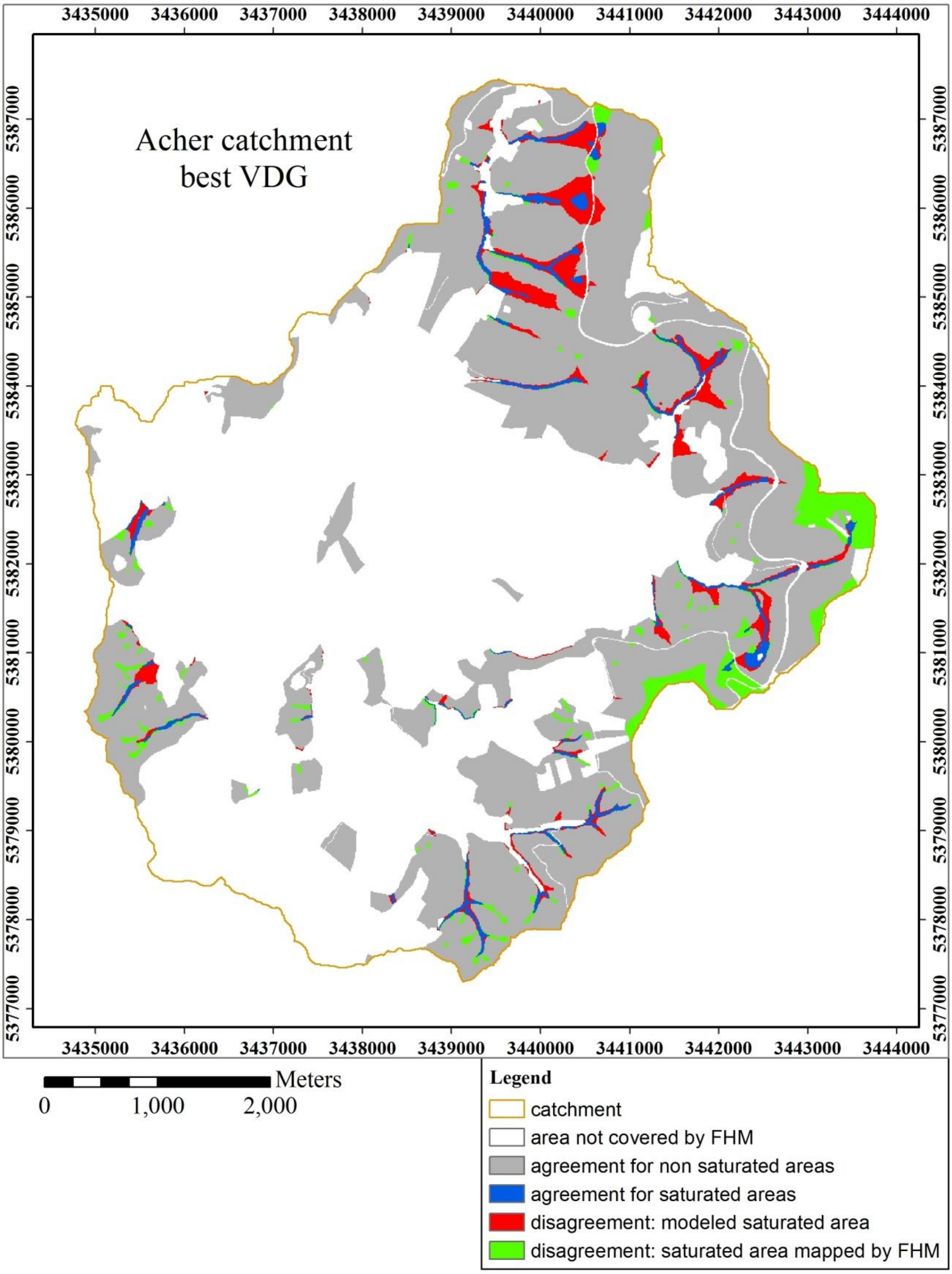

Figure 35: Visual comparison of the validation of the best VDG and FHM; Acher catchment 10 m

4.5.4 Example of a 1 m grid

To show the characteristic of the modeled saturation areas applied on 1 m grids an extract of the Acher catchment is presented in figure 36. The extract is located in the north of the Acher catchment but could have been in any catchment at most locations as the TI shows everywhere same characteristic. This is that the TI calculated for the 1 m is strongly influenced by little changes in topography and the lines or curves that are modeled as saturation areas are streets or forest tracks. From these streets or forest tracks at some given points downslope area is modeled as saturated area. Most of these do not agree with the mapped saturation areas by the FHM.

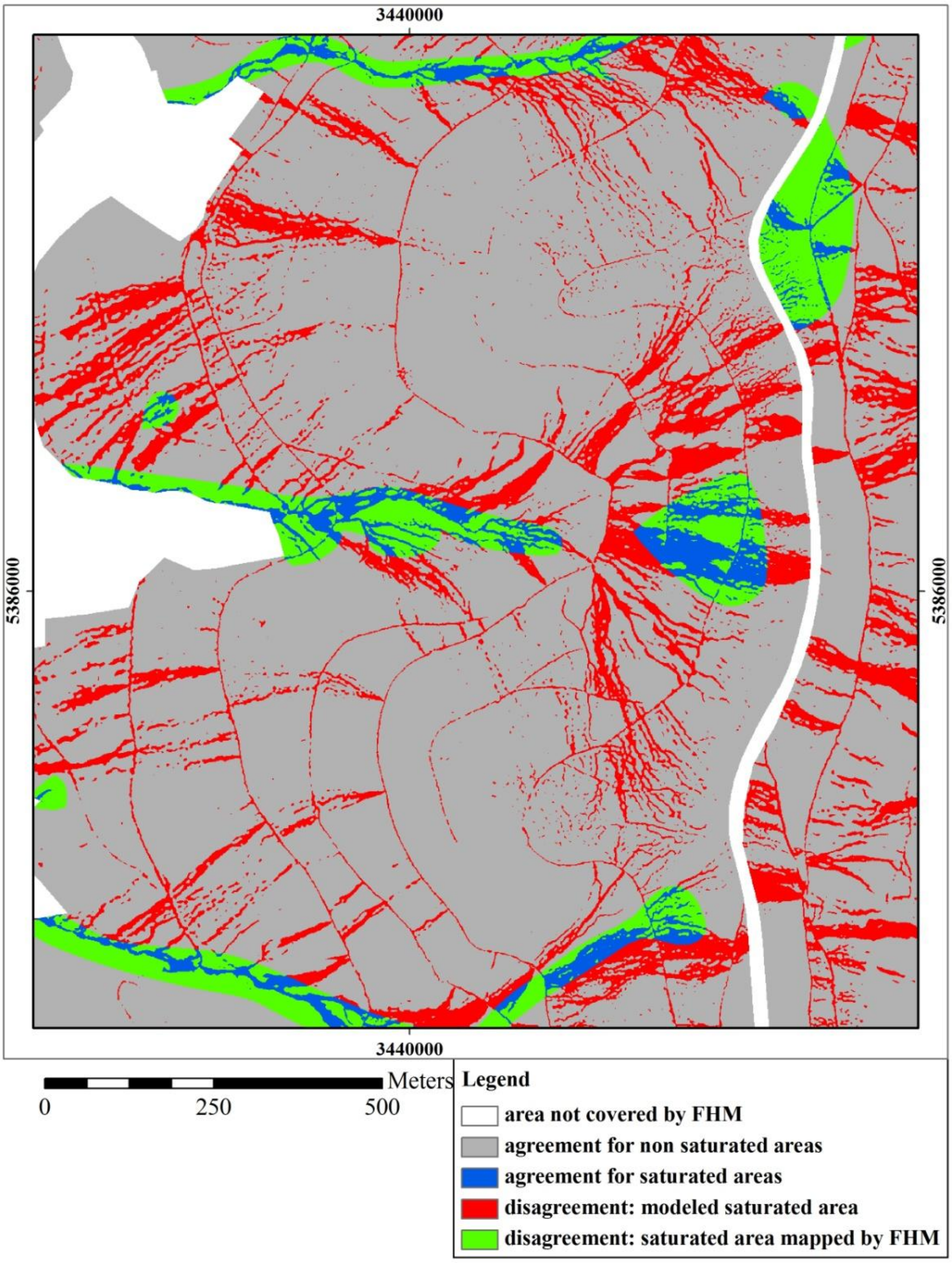

Figure 36: Example of the validation for a TI calculated for a 1 m grid in the Acher catchment

4.6 Field survey

The listed results of the field survey in table 24 only exist of well defined saturated areas in field and uncertain cases where excluded. The results of the Field survey were compared to the mapped saturated areas by the FHM and the modeled saturated areas by the best method of TI and VDG for each catchment. Where the saturated area mapped by the field survey was totally covered by the corresponding object of comparison the agreement or disagreement was counted with one. When only proportions of the saturated area mapped by the field survey have an agreement the agreement count was 0.5. The shape of table 24 has the same form than in the previous chapters, where ns/ns means an agreement for non saturated areas, s/s an agreement for saturated areas, and the other two values mean a disagreement for each object of comparison and catchment. The k_a value is also calculated the same way. The fewer amounts of values for comparison with the FHM is because some sample points were outside the area covered by the it.

The results show that for all catchments the major part of the comparison results in an agreement, however, for every catchment there is also a disagreement. The highest correlation is for the Zastlerbach catchment where an agreement of 94.4 % occurs for the FHM, and the TI and VDG follow with an agreement of 81.8 %.For the Eyach and Acher catchment the agreement is lower, whereas for the Acher catchment the TI has the highest correlation with 70.0% and for the Eyach catchment the FHM with 68.2 %.

Table 24: Agreement of the field survey with modeled and validation saturated areas. ns = not saturated, s = saturated, k_a = agreement between the different saturated area maps

Eyach		FHM		TI		VDG	
		ns	s	ns	s	ns	s
Field survey	ns	2	3	0	5	0	5
	s	0.5	5.5	0.5	10.5	1	10
	k_a	68.2%		65.6%		62.5%	
Zastlerbach		FHM		TI		VDG	
		ns	s	ns	s	ns	s
Field survey	ns	5	0	4	2	6	0
	s	0.5	3.5	0	5	2	3
	k_a	94.4%		81.8%		81.8%	
Acher		FHM		TI		VDG	
		ns	s	ns	s	ns	s
Field survey	ns	1	3	1	3	2	2
	s	3	8	1.5	9.5	3.5	7.5
	k_a	60.0%		70.0%		63.3%	

In figure 37 an example of the comparison of a saturated area mapped in field with the validation between FHM and the best TI method for the Zastlerbach catchment is shown. Thereby the upstream area from the saturation area was examined, whereas the downstream was not further regarded than the mapped saturation area. A typical characteristic is the much finer shape of the field mapped saturated area and specially the smaller area covered by it compared to the saturated areas mapped by FHM and TI. Here, half of the field mapped saturated area is also mapped as such by the FHM, whereas the other half is mapped as a non saturated area, while the whole field mapped saturated area is also modeled as such by the TI.

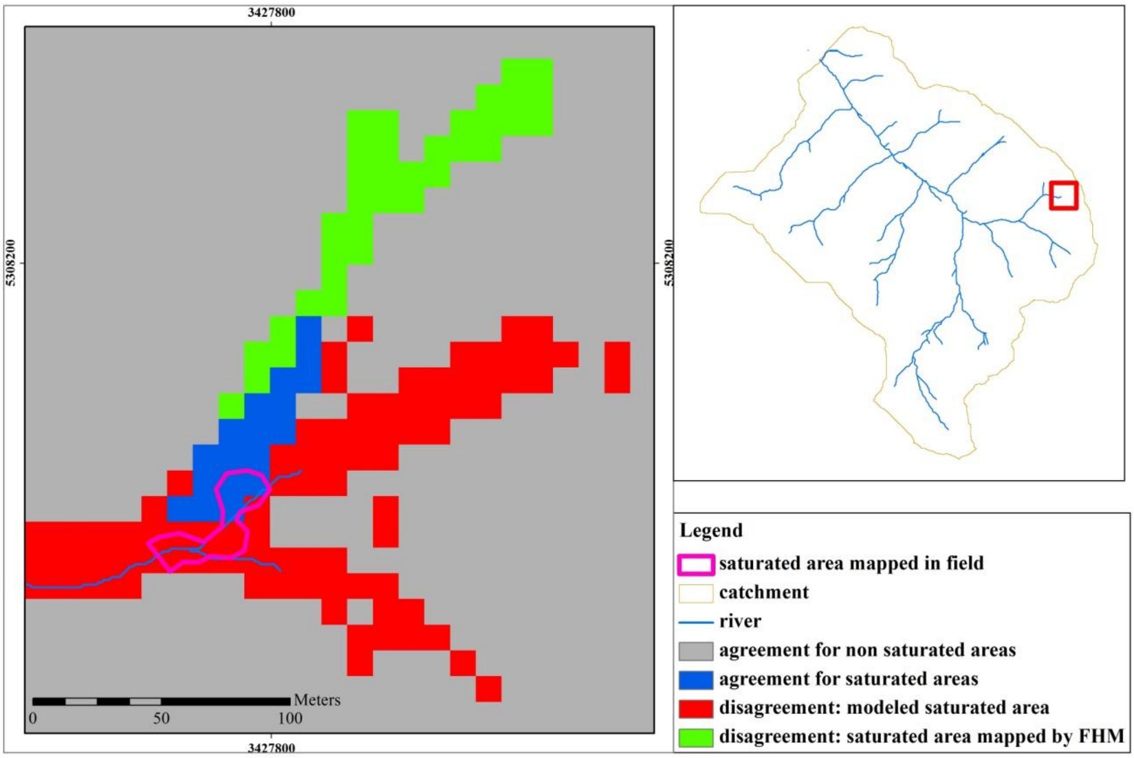

Figure 37: An example of a saturated area mapped in field compared to the validation results of the FHM with the best TI; Zastlerbach catchment grid size 10 m

Figure 38 shows an example of saturated area mapped in field outside the area covered by the FHM, and one at the border of the area covered by FHM. The modeled saturated area outside the area covered by FHM which was delineated applying the same threshold for the TI as for the FHM area fits thereby perfectly with the field mapped one. Also the other larger saturated area is well predicted by TI and also mapped as a saturated area by the FHM.

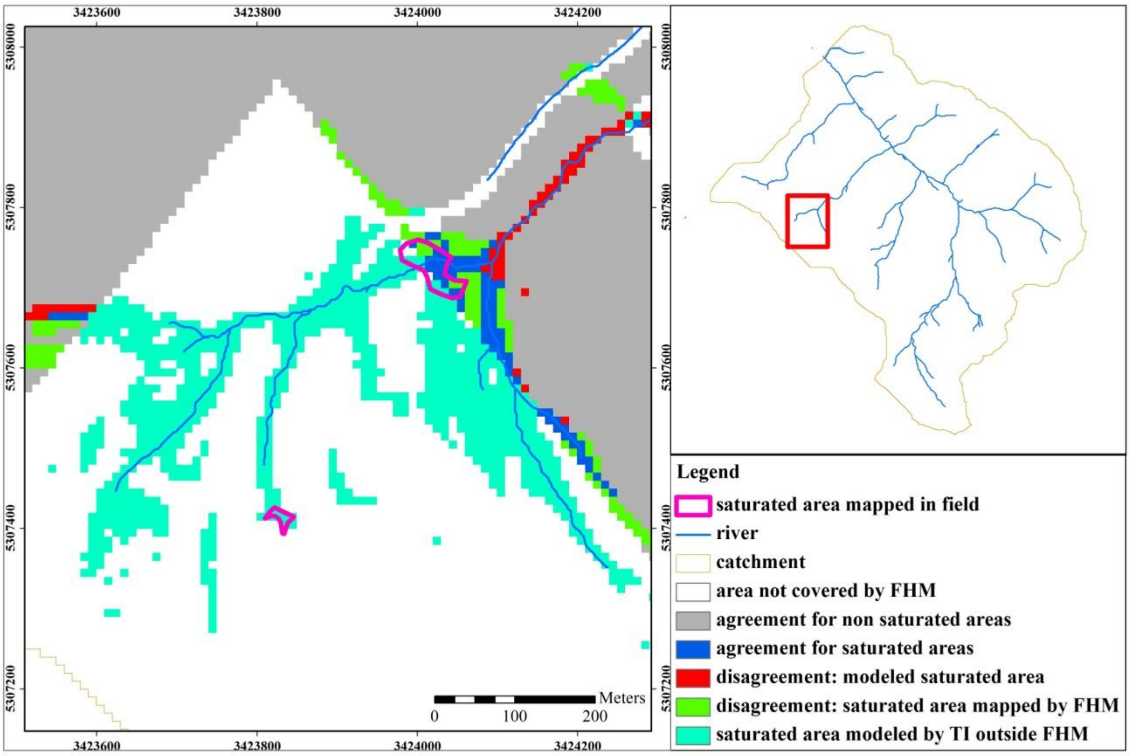

Figure 38: Example of a saturated area mapped in field which is not covered by the FHM; Zastlerbach catchment grid size 10 m

5 Discussion

The results presented in the previous chapter show that there is an agreement between modeled and mapped saturated areas of about 50% for the buffered FHM. This performance provides a slight improvement compared to the previous study by GÜNTNER et al. (2004) performed in the Zastlerbach catchment. They also modeled saturated areas applying variations of the TI using the FHM as validation data. Thereby, they found for a comparable cell-to-cell validation a TI with an agreement of 37.9 %, while in this study the best TI is resulting in a cell-to-cell agreement of 39.2 %. For a cell-to-neighborhood approach, where they considered an area of 50 m around the cell of concern with decreasing weighting for longer distances between modeled and mapped saturated areas they had an agreement up to 52.2 %. In this study the approach of the buffered FHM with a tolerance of only 10 m resulted in an agreement up to 52.4 %.

The aim of this study was to analyze, if the high resolution LIDAR DEM allows for a better evaluation of the spatial pattern of saturated areas. However, with such a slight improvement compared to the study of GÜNTNER et al. (2004) where they applied their methods on a 50 m grid, one has to confess that the new quality level of input data does not result in a significant improvement of performance. Possible reasons for that may be the quality of the input and validation data or conceptual errors in the applied methods. These problems will be discussed in the following chapter.

5.1 Resolution of the input data

The LIDAR DEM is presented as a new quality level of input data and it sure is, but the high resolution results in new problems compared to coarser DEMs. With a grid size of only 1 m and vertical resolution of centimeters the LIDAR DEM is able to map smallest changes in landscape which includes anthropogenic influences like streets, bridges, up to very narrow forest tracks. For hydrologic applications this fact results in enormous problems for calculating flow directions based on the surface elevation. The sharp shapes of streets and bridges build a network of drainage systems or insuperable barriers. Whereas this problem can be solved manually for rivers, as it was done in this study (compare chapter 4.1), it is nearly impossible to do that for hillslopes. For example, this can be seen in figure 36, where high values of the TI and therewith the accumulated area is routed along the forest tracks and at some specific points they cross the tracks and are routed concentrated downwards. The routing does not have to be wrong as streets or forest tracks can indeed behave like a drainage system of upslope area, but when they do, there are mostly culverts along the streets and forest maps that are not recorded or mapped by the LIDAR DEM. Therefore the routing along these forest tracks seems to be somehow arbitrarily.

The influence of these anthropogenic manipulations on the calculated flow directions has a bipolar effect for calculating saturated areas. During the field survey there were some small saturated areas noticeable that were strongly influenced by these anthropogenic influences. An example for that is shown in the cover picture of this thesis. Here the water of upslope area is collected in a rill next to the street and drained to a culvert, which leads to the saturated area. However, only a proportion of the upslope area is drained by the rill. There are also other examples, where the major proportion of the water movement underflows the street and the flow routing along the streets leads to large bias (e.g see figure 36).

To solve these problems a consequent adjustment of the LIDAR DEM to hydrological issues would be a possible solution. Here the most important feature would be to map all culverts and bridges and implement them in the DEM. This would result in an enormous effort, but it would also be of great value for many applications.

Another possible way to improve the results of calculating specific catchments would be to split flow routing as soon as forest tracks occur in a hillslope. A proportion of the flow could be routed along the track according to the draining potential and the other proportion would be routed straight over the track as it would be assumed that there is a subsurface flow beneath the track.

Finally, a third method, performed in this study, is to aggregate the fine 1 m grid to a coarser grid size to smooth the surface and thus eliminate the sharp shapes of streets and forest tracks. This makes additionally sense for calculating saturated area as the water table configuration may be smoother than the land surface topography and may be related more accurately to a coarse resolution DEM (WOLOCK and PRICE 1994). Thereby, the optimal resolution should represent the important topographic features for a certain variable of interest; using a finer resolution might actually weaken rather than improve the calculation of topographic indices (SØRENSEN and SEIBERT 2007). These two statements can be confirmed by the results of this study, as for the 1 m grid the performance especially of the TI is worst and improves along the 5 m grid up to the 10 m grid. However; further increase of the grid size can decrease the performance, again as shown by the study of GÜNTNER et al. (2004). The optimal resolution should therefore be located between 5 m and 50 m; the 10 m grid seems to be an appropriate choice. Nevertheless, this smoothing of finer DEMs also includes some bias as, especially in steep slopes, forest tracks might cut meters of a hillslope and hence behave as a drainage system for the upslope area. This was confirmed in areas beneath such forest tracks where the models for coarser grids predict saturated areas, whereas by the FHM and the field survey no saturated area occurs.

5.2 Quality of the validation data

FHM

The quality of the central validation data, the FHM, is comparable to the quality of the LIDAR data. While the quality of the FHM itself is beyond dispute as it offers many valuable characteristics about the area of interest, its applicability for hydrological question might be problematic in some cases. The central idea of the FHM is to classify the landscape in areas which offer the same environment for forestry. The soil samples were taken up to a depth between 80 and 120 cm for mapping the areas (MICHIELS 2010). When from time to time a soil is saturated by ground water table raise till the most of 30 cm below surface the lower part of the soil sample might have hydromorphic characteristics. Therefore it will be probably delineated as some saturation degree in the FHM as for a tree with deep roots like the fir tree this causes problems. However, from the hydrologic point of view the same soil might never get saturated till the surface and thus saturation overland might never occur.

This possible disagreement between the sciences is also indicated by the field work carried out during this study. The mapped saturated areas were in many cases significantly smaller than in the FHM as shown in figure 37. However, it might then be assumed that the higher saturation degrees of the FHM, which coincidence with higher hydromorphic characteristics in the soil samples (MICHIELS 2010), should have a higher agreement with the corresponding modeled saturated areas than the aggregated saturated areas of the FHM, but the contrary occurs. For the two catchments Acher and Eyach, where there is a broad range of different wetness degrees given by the FHM, the value of the performance criterion k_s, which only regards “wetter” saturated areas, is always less than k_{as}, which is calculated for the aggregated saturated areas.

A reason for that is shown in figure 19, where the spatial pattern of the different wetness degrees is presented. In the Eyach catchment for example the lower wetness degrees are located in the valley bottom whereas the high wetness degrees are in some cases located upwards in the hillslopes. This constellation, however, is not predictable with the applied methods in this study. For the VDG method this is quite obvious as the vertical difference above the interpolated stream network defines saturated areas. But also for the TI method, where the specific catchment area plays a major role this cannot be modeled as the downslope area always has a larger specific catchment area than a point within this catchment somewhere upslope. Therefore using the aggregated saturated areas of the FHM as validation data resulted in better performance of the applied methods than the classified ones. However, considering the results from the field work, doubts remain if all mapped saturated areas by the FHM behave like saturated areas from the hydrological point of view and are able to generate saturation overland flow.

Another limitation of the FHM is that with a maximum accuracy of 25 m (MICHIELS 2010) it provides coarser information than the modeled saturated areas. These scale discrepancies were tried to be weakened by arranging a buffer around the original FHM. The buffer was selected to be 10 m as this was the smallest buffer possible for the 10 m grid. The performance criteria show a remarkable improvement from the non buffered to the buffered FHM, however this improvement is not sufficient to explain all the disagreement between modeled and mapped saturated areas by inaccuracies during the modeling or of the FHM.

Field survey

Contrary to the FHM, which is a time integrated measurement of saturated areas as it is based on long-term soil characteristics, the field survey provides a time specific measurement. This is a limiting factor for validating long-term mean wetness conditions provided by the FHM and also the static modeled saturated areas with the TI or VDG. The problem of the time specific character of the field survey was already noticeable during the month of accomplishing. In the Zastlerbach catchment there was not yet a snow cover, whereas when the field survey was conducted in the other two catchments a snow cover existed. This was problematic as the snow covered indicator plants which played a leading role in the field survey. Additional, in the higher elevations of the Eyach and Acher catchment there was already a snow cover up to 30 cm where there was no forest, while in a warmer period the snow was melting again and much wetter conditions occurred. Therefore it was difficult to get uniform results.

In addition, the characteristic shapes of the saturated areas were different. In the Zastlerbach catchment most saturated areas are clearly defined due to the steep slopes at their border, as already noticed by GÜNTNER et al. (2004). Therefore the field survey in the Zastlerbach catchment was less complicated than in the other catchments where the saturated areas had a more gradual transition into areas with no saturation. Also the size of some saturated areas was larger in these two catchments, so that not the whole area could be mapped but only sample points of the area

5.3 Quality of the applied methods

TI

Different slope methods

The results show that the global slope method provided the worst results while being also complicated to calculate. The method requires a stream network which was calculated based on the LIDAR DEM. Thus, the same problems occur when calculating the flow direction as discussed above. Another problem is that the stream network delineated with a CIT normally does not fit same good in the whole catchment. Whereas at some areas in the catchment a specific CIT fits to the mapped river at another part of the area it does not. Consequential, the delineated stream network especially for the 1 m grid was not free of little errors, even though obvious mistakes were eliminated as shown in chapter 4.1.

An additional problem occurs because for all river cells the slope is not defined. This problem was solved by one time excluding river cells from the validation data and the other time adding the river cells as high values to the TI. However, with both methods the performance of the slope method was worse than the local ones. This results from the fact that in high gentle elevations, especially at catchment borders the global slope method gives in general steeper slopes than the local slope methods. However, in these regions many saturated areas are located. Another reason is that the flow path to calculate the distances needed for the global slope method is routed by the D8 flow algorithm. With it, sharp breaklines of slopes within a hillslope evolve which do not seem to be realistic. A third reason could be that the concept of global slope is wrong and saturated areas are more controlled by the local topography. This was also the impression of the field survey, where sharp slope changes from a steep to a gentle hillslope often coincided with saturated areas.

Summarizing, it can be concluded that due to the additional data needed for calculating it, the more complicated way of calculation, and the worse performance of the TI with global method, it is more appropriate to apply local slope methods for calculating the TI.

However, also for the local slope method a problem occurs mentioned in chapter 4.1. For the original DEM there would be slopes calculated that have the value of zero and so the TI would not be defined. This problem was questioned in ROSIN (2010) and a method is recommended where a constant value of 2° should be added to all calculated slope angles. The idea is that the replacement of only the value zero by a constant value would result in an inconsistent shift and adding a smaller value than 2° would lead to too high values of the TI. Nevertheless, in this study only the values of zero were adjusted by a small value of 0.01°. With such a low value the inconsistent shift should be negligible and the high values of TI can assumed to be not wrong. But areas such flat might lead to saturated areas. However, according to ROSIN 2010 this might lead to some bias in the method applied in this study.

Between the local slope methods only slight differences occur. For the steeper two catchments, Acher and Zastlerbach, the method of TARBOTON (1997) performed better, whereas for the more gentle Eyach catchment the method of ZEVENBERGEN and THORNE (1987) performed better. Hence, a guess would be that for steeper catchments the steepest slope approach might perform better, whereas for gentle slopes an averaging approach might be the most favorable choice. However, much more results would be needed from other catchments to examine that.

Different flow algorithms

The result that the most divergent flow algorithm performs the best was quite surprising as in all comparable studies introduced in chapter 1.1.2 some level of convergence was implemented in the best performing method. For the Zastlerbach catchment GÜNTNER et al. (2004) found the best TI as a combination of a local averaged downward slope and the MD flow algorithm with a convergence factor of 10 and a CIT of 60,000 m². As they also applied the FHM provided by the FVA for validation with the same finding of the threshold values for the TI all circumstances are similar except for the DEM on which the calculations of the TI are based. In their study the DEM was quite coarser with a grid size of 50 m. Therefore, the reason for the different preferred flow algorithm has to be due to the different grid sizes.

That the TI is sensitive to the grid size is well shown in the two studies of WOLOCK and PRICE (1994) and ZHANG and MONTGOMERY (1994). However, there they applied a method of calculating the TI and compared the results obtained for different grid sizes. Their findings where that with decreasing grid size the average value of the TI also decreases, due to an decrease of the average specific catchment and an increase of the average slope. These findings can be confirmed by this study as the thresholds applied for distinguishing saturated from non saturated cells decreased for all the three catchments for all used methods with decreasing grid size.

But this does not explain the change to the preferred divergent flow algorithm for the finer grids. A possible explanation would be the following: Coarser grid sizes always smooth the DEM. Thereby, the smoothing can also be considered as a manipulation of the DEM to a more divergent shape. Whereas in a finer grid flow is routed by micro topography and is collected by little rills flow for a coarser grid is more routed in a planar way downwards. A good example of that is the problem discussed above for flow routing with a 1 m grid. The flow routing along forest tracks or streets can be interpreted as micro convergence shapes within in the topography. While a forest track is an extreme example it is easy imaginable that these micro convergence shapes also occur in a less impressive way for normal hillslopes. On the opposite, coarser grid sizes average these micro convergence shapes and flow is routed in a more divergent way. In the example of the forest track not all flow is routed concentrated along the street but the whole hillslope is routed in a planar way across the forest track downwards. As coarser DEMs can after the previous interpretation be considered as more divergent DEMs there is a need of some convergence degree in the flow algorithm to keep the flow in its gravimetric driven natural convergence behavior. Contrary, for a high resolution DEM, which can be considered as a more convergent DEM, at least for subsurface flow there is need of a divergent degree in the flow algorithm, With this explanation it could be so explained that the MD method with no additional convergence factor performs better than with convergence factor, and also better than MDinf or D8.

This theory could also explain why the flow algorithm with no special regarding of river cells performs best. The river might be routed automatically in its given drainage system, due to the more convergence characteristic of a finer DEM. However, this would only explain a similar good performance but not a better one. Many saturated areas coincide with the springs of creeks. When there is no CIT the area around the origin of these first order streams is more probably mapped as saturated areas, whereas with the definition of a CIT the mapped saturated areas are more limited as flow is routed along the rivers. Also valley bottoms further below are often mapped as saturated areas so a divergent flow algorithm can help to locate them. However, the circumstances that rivers of higher order are excluded from the validation for all the three catchments in a more or less way might lead to a preference of no special regarding of rivers. According to the findings of McGlynn and Seibert (2003) and Mourier et al. (2008) saturated areas which coincident directly with rivers occur more probable for low order rivers than for high order rivers. Summarized there are the following circumstances which are probably the reason why TIs without a CIT performed better than with it: The more convergent character of the finer DEM, the advantage of modeling saturated areas around first order streams, and the exclusion of high order streams for validation.

VDG

For calculating the VDG the same problems occur than for calculating the global slope as here also an accurate stream network is needed. This could be the explanation why also the VDG performs best for the 10 m grid, where these problems are less, than for the 1 m grid.

As the results show that each of the three different variations of VDG performs best at different times, no trend can be concluded if a finer or coarser stream network performs better. Additional, it has to be mentioned that the interpolated plane on the basis of the stream network with a high CIT has more a fitting parameter character than it is comparable to the groundwater table. An obvious result and non surprising fact is that with VDG only saturated areas near to the stream network can be mapped and the saturated areas located in the gentle heights are nearly never mapped. As the gentle heights build an upper limitation for VDG, regarding the studies to McGlynn and Seibert (2003) and Mourier et al. (2008) again high order streams build the lower limitation for VDG. Therefore this method should only be applied exclusive for low order streams where it is a priori known that saturated areas only occur in valley bottoms. Another possibility for its application could be a combination with the TI as was done by Rosin (2010).

Performance criteria

In this study the applied objective functions evaluating the performance of the modeled saturated areas have quite a simple approach as they compare result directly on a cell-to-cell basis. However, one could argue that when comparing two predictors for one object there will always be some degree of agreement by chance. Therefore, there have been recent studies, like GRABS et al. (2009), where they use the Cohen`s Kappa statistic which includes this by chance agreement in the calculation of the agreement between different predictors. However, a finding of ROSIN (2010) is that this statistic is not appropriate for saturated areas and should not be used, but simple agreement measures. Additional, the fact that the threshold for delineating saturated areas was not arbitrarily selected so that a best fit occurs but based on the validation data, and also the fact that the agreement was normalized on the total cells of modeled saturated cells, led to the simple agreement measures applied in this study.

Different catchments

A reason to perform this study in three different catchments was to evaluate if the methods are sensitive to varying conditions. The results indicate that the VDG method is sensitive to the different catchments as shown in figure 29. This can be explained by its limitations that are already discussed in chapter 5.3. The limitations could also explain why the method performs best for the Acher catchment, where most high order streams are excluded from the validation and worst for the Eyach catchment, where many saturated areas occur at gentle heights. Additional, it is not only the performance of the VDG that varies between the catchments but also the thresholds vary much and thus it seems be difficult to apply this method for study areas where no validation data is available.

The performance of the TI method for the Eyach and Zastlerbach catchment is almost the same and a little worse for the Acher catchment (but is still in the same order of magnitude). Therefore it is difficult to see the impact of the different geology and soils among the catchment. However, these results indicate that the TI can be applied for the range of different conditions within the three catchments also for other ungauged catchments. Thereby it would be important to have one method to define the threshold that delineates saturated areas from non saturated areas. The results show that this seems to be possible as all thresholds are close to each other even though different amounts of saturated areas occur in the catchments. The low value for the Acher catchment could be explained by the low occurrence of river cells in the validation. Even though having the highest amount of saturated areas, the Eyach catchment has comparable value to the Zastlerbach catchment. This could be explained by the more gentle slopes of the catchment compared to the others. Hence, a guess would be that the threshold for the TI correlates with the mean slope of a catchment. However, the three thresholds obtained do not provide enough data volume to be sure and to be able to formulate a concrete method.

5.4 General discussion

All problems of the TI discussed above do more explain inaccuracies of the method but do not consider if there are conceptual errors included. Regarding for example the validation results in the Eyach catchment (figure 30) inaccuracies in calculating of the TI can explain a non perfect match in the area around the highmoor. But how do the big areas of disagreement in other gentle heights or in the lower hillslopes occur? The same problem occurs for the Acher catchment, where most of the saturated areas in the gentle heights are not modeled, but lower hillslope areas are overestimated by the TI. How can it be explained that nearly none of the scattered saturated areas mapped by the FHM in the Zastlerbach catchment are modeled by the TI? For these cases the distances between mapped and modeled saturated areas are too large to be explained by inaccuracies. Here conceptual errors of the TI have to be the reason, assuming a correct mapping by the FHM.

In chapter 2 the high precipitations due to orographic effects are shown for the Acher and Zastlerbach catchment. Therefore it can be assumed that the water balance within the catchments is inhomogeneous and an adjustment of the TI should lead to better performance. This was done with implementing an elevation gradient for the water balance by GÜNTNER et al. (2004). However, this resulted only in little improvement. Nevertheless the results of the Eyach and Acher catchment strongly confirm that this is a conceptual problem and further research should consider it.

Another explanation for underestimating gentle heights by overestimating lower hillslopes could also be that the TI is too much influenced by the specific catchment and less weighting of it could lead to better performance. Another indicator for this could be the bad performance of TI for the different saturation classes compared to the aggregated saturated areas. Especially, in the Eyach catchment the lower part of a hillslope was sometimes mapped as a transitional area by the FHM, whereas the upper part was mapped as a more saturated area. This is nearly impossible to model with the weighting of the specific catchment as it is now implemented in the TI.

Another general mismatch are the scattered little saturated areas, mainly in the Zastlerbach catchment. These might rather originate from the underground, more precisely the geology, than from the topography. The intersection of fractures and faults in the crystalline bedrock with the terrain surface can lead to an emergence of deep groundwater from the fissured aquifer in springs and thus to an evolving of saturated areas (GÜNTNER et al. 2004). Therefore, an implementation of characteristics originated by the geology in the modeling of saturated areas by the TI promises an improvement even though it does not seem to be a trivial application.

In some cases it can be seen that valley bottoms having the same values of TI within one catchment sometimes are mapped as saturated areas by the FHM and sometimes not. An explanation for that could be influence of anthropogenic manipulation on natural flow systems (see chapter 5.1). Implementing them better therefore might promise a better modeling of saturated areas. Another reason for the different behavior of areas with the same TI could be the different soils. If there is a clayey layer and therefore quite impermeable layer in the soil for the one area this might lead to a saturated area, whereas for another area, with the same TI, a sandy soil is more unlikely to generate a saturated area. Therefore, the implantation of soil characteristics might also improve the modeled saturated areas. However, such attempts by GÜNTNER et al. (2004) did only slightly improve the performance which they explained by a lack of detailed soil data. The different soil behavior could also be another reason for the above mentioned phenomenon where the FHM maps lower parts of a hillslopes with a less wetness degree than higher ones.

In total, it can be concluded that the hereby found best method of TI for a finer DEM of 10 m grid size decreases earlier inaccuracies for coarser DEMs resulting in a slight improvement of the performance. However, one has to confess that there is a limit of performance in the basic method of the TI. The results indicate that there are conceptual errors in modeling saturated areas that need to be solved before being able to evaluate the spatial pattern of saturated areas correctly. The best TI method found in this study might provide an appropriate base for that.

6 Conclusion

Is it possible to evaluate saturated areas solely with topographic information?

This was the central question formulated in the objectives of this study and the question can be answered with yes as well as no. Approximately, half of the spatial patterns of saturated areas could be modeled only with the topographic information for three different catchments, whereby the agreement is on a comparable level for all catchments. Some of the disagreement between modeled and mapped saturated areas can be explained by problems occurred during modeling, and also the validation with non hydrologic data might cause misinterpretation. However, it seems that there is a limit of obtainable performance and that there are saturated areas originated by more influences than topography only. Consequential, when there is a need for an entire and precise prediction of the spatial pattern of saturated areas the central questions has to be a negated.

The aim of this study was to analyze if with the new level of quality in the input data, the LIDAR DEM, also a new level of performance can be reached. For one catchment a comparable previous study (GÜNTNER et al. 2004), where they used an input data with worse quality, was available. However, the results of this study show only a slight improvement and the performance of the models in this study is more in the same level than in a higher quality. Thereby, it is not the highest resolution of 1 m that leads to best performance in this study, but a coarsened resolution of 10 m.

Another aim of the study was to find if there is one best method that can be applied also for other catchments or can be applied as a good basis for further research towards better performance. Two different approaches and many variations of them were tested and the results indicate that there is one most preferable method.

Even though for the Acher catchment the VDG performs a little better than the TI it is more limited in its applicability. It should be applied as an exclusive method only for study areas, where it is known a priori that saturated areas only occur along rivers. Combining it with the TI might be reasonable under considering its limitation. However, the results of this study show that it is be difficult to find a reliable threshold for delineating saturated areas for study sites with no validation data.

The more stable and in average better performing method is the TI. Fortunately, the results indicate that there is one flow algorithm method that performs best for all the three catchments. This is the MD method with a convergence factor of 1.1 and no special regarding of rivers for the 10 m grids. Tests have shown that an even lower convergence factor up to 0.1 might result in a slight improvement so the recommendation would be to apply a convergence factor somewhere between. That no special treatment for river cells performed best might be due to the lack of high order streams in the validation. Therefore in cases where they are included a very high CIT might be helpful. Concerning the slope calculating methods the finding is that it should be a local one, whereas no clear recommendation between them can be given, as two times the steepest downward slope performed better and one time the averaging approach, regarding also a part of the upslope area. The thresholds of the best TIs for the three catchments indicate that they might correlate with the mean catchment slope. Therefore, it seems to be possible that with further results of other catchments a method can be found to define a reliable threshold for study areas with no validation data. Consequential, it would so be possible to apply the TI also for ungauged catchment as predictor for the spatial patterns of saturated areas.

For now this method could be applied in cases where only a rough estimation of saturated areas is needed. For example an engineering office could apply it as an uncomplicated and standardized way to get an idea about the location and amount of saturated areas and implement them in a flood routing model. Although that would be a non perfect estimation it would be better than not considering this information at all and therefore should lead to more reliable results.

While the findings of this study might be somehow unsatisfactory at the first place, the results still lead to a correct modeling of the spatial patterns of saturated areas. Since this study shows that there have to be more influencing factors than the topography only on the origin of saturated areas or that there might be conceptual errors within the applied methods further research might focus on finding and implementing these in modeling. For this purpose it is of great value to have one best method that provides a good basis for further development, so further research can focus solely on finding additional improvement. Thereby the results of this study indicate the following points which might improve the modeling of the spatial pattern of saturated areas:

- Mapping of anthropogenic manipulations of natural flow systems and implementing it in the DEM.
- A review of the TI as the results indicate that there might be an overdependence on the specific catchment in its calculation.
- Considering of different water supplies within a catchment.
- Finding a way to implement geologic features like fractures in the calculation.
- Considering different soil types within the catchment.

Overall, it can be concluded that the correct modeling of spatial patterns of saturated areas is not as simple as expected and only better information of the topography is not sufficient for an entire and precise prediction. More factors have to be considered and implemented in the modeling. This provides a further challenge for research so let us accept and overcome it.

Bibliography

BETSON, R. P. (1964). *What is watershed runoff?* Journal of Geophysical Research 69: 1341-1551.

BEVEN, K. J. (1997). *TOPMODEL: A critique*. Hydrological Processes 11(9): 1069-1085.

BEVEN, K. J. and KIRKBY, M. J. (1979). *A physically based, variable contributing area model of basin hydrology*. Hydrological Sciences Bulletin 24(1): 43-69.

BEVEN, K. J., LAMB, R., QUINN, P., ROMANOWICZ, R. and FREER, J. (1995). *TOPMODEL*. In: V. P. SINGH (ed.). Computer Models of Watershed Hydrology. Water Resource Publications. Colorado**:** 627-668.

BRENNER, C. (2006). *Aerial Laser Scanning – Systems, Processing, Applications*. International Summer School Digital Recording and 3D Modelling, 24-29 April 2006. Aghios Nikolaos, Crete, Greece: 244.

BURT, T. P. and BUTCHER, D. P. (1985). *Topographic controls of soil moisture distributions*. Journal of Soil Science 36(3): 469-486.

CONRAD, O. (2007) *SAGA - Entwurf, Funktionsumfang und Anwendung eines Systems für Automatisierte Geowissenschaftliche Analysen*. University of Göttingen. electronic doctoral dissertation: 233

DUNNE, T. and BLACK, R. D. (1970a). *An experimental investigation of runoff production in permeable soils*. Water Resources Research 6: 478-490.

DUNNE, T. and BLACK, R. D. (1970b). *Partial area contributions to storm runoff in a small New England watershed.* Water Resources Research 6(5): 1296-1311.

DUNNE, T., MOORE, T. R. and TAYLOR, C. H. (1975). *Recognition and prediction of runoff-producing zones in humid regions.* Hydrological Sciences Bulletin 20(3): 305-327.

ERSKINE, R. H., GREEN, T. R., RAMIREZ, J. A. and MACDONALD, L. H. (2006). *Comparison of grid-based algorithms for computing upslope contributing area*. Water Resources Research 42(9): W09416.

ETZRODT, N., ZIMMERMANN, R. and CONRAD, O. (2002). *Upscaling water cycle parameters using geomorphometric terrain parameters and topographic indices derived from interferometric DEM*. A. WILSON (ED.). Proceedings of the 3rd International Symposium on Retrieval of Bio- and Geophysical Parameters from SAR Data for Land Applications, 11-14 September, 2001. Sheffield, UK: 251-254.

EVANS, I. S. (1980). *An integrated system of terrain analysis and slope mapping.* Zeitschrift fuer Geomorphologie N.F., Supplementband 36: 274-295.

FREEMAN, T. G. (1991). *Calculating catchment area with divergent flow based on a regular grid*. Computers & Geosciences 17(3): 413-422.

FVA *digitalisierte forstliche Standortskartierung*. Freiburg, Abteilung Waldökologie - Forstliche Versuchs- und Forschungsanstalt Baden-Württemberg (FVA): date of issue, december 2009.

GAJSKI, D. (2004) *Rasterbasierte Geländeoberflächenanalysen*. Technischen Universität Wien. Dissertation: 167

GRABS, T., SEIBERT, J., BISHOP, K. and LAUDON, H. (2009). *Modeling spatial patterns of saturated areas: A comparison of the topographic wetness index and a dynamic distributed model*. Journal of Hydrology 373(1-2): 15-23.

GÜNTNER, A. (1997). *Anwendung des Niederschlag-Abfluss-Modells TOPMODEL im Brugga-Einzugsgebiet*. Diplomarbeit am Institut für Hydrologie, Albert-Ludwigs-Univeristät Freiburg i. Br.: 119.

GÜNTNER, A., SEIBERT, J. and UHLENBROOK, S. (2004). *Modeling spatial patterns of saturated areas: An evaluation of different terrain indices*. Water Resources Research 40(5): -.

GÜNTNER, A., UHLENBROOK, S., LEIBUNDGUT, C. and SEIBERT, J. (1999). *Estimation of saturation excess overland flow areas: comparison of topographic index calculations with field mapping*. In: B. DIEKKRÜGER, M. J. KIRKBY and U. SCHRÖDER (ed.). Regionalization in Hydrology. IAHS. 254. Braunschweig, Germany**:** 203-220.

HEERDEGEN, R. G. and BERAN, M. A. (1982). *Quantifying source areas through land surface curvature and slope*. Journal of Hydrology 57(3-4): 359-373.

HEWLETT, J. D. and HIBBERT, A. R. (1967). *Factors affecting the response of small watersheds to precipitation in humid areas.* In: W. E. SOPPER and H. W. LULL (ed.). Forest Hydrology. Pergamon Press. New York**:** 275-291.

HEWLETT, J. D. and TROENDLE, C. A. (1975). *Non-point and diffused water sources: a variable source area problem.* In: Symposium on Watershed Management, American Society of Civil Engineers: 21-46.

HJERDT, K. N., MCDONNELL, J. J., SEIBERT, J. and RODHE, A. (2004). *A new topographic index to quantify downslope controls on local drainage*. Water Resources Research 40(5): -.

HOLMGREN, P. (1994). *Multiple flow direction algorithms for runoff modelling in grid based elevation models: An empirical evaluation*. Hydrological Processes 8(4): 327-334.

HORTON, R. E. (1933). *The role of infiltration in the hydrologic cycle.* American Geophysical Union fourteenth annual meeting., June, 1933. Washington D. C., National Research Council of the National Academy of Sciences.: 446-460.

HORTON, R. E. (1945). *Erosional Developement of streams and their drainage basins; hydrophysical approach to quantitative morphology*. Bulletin Of The Geological Society Of America 56: 275-370.

KIRKBY, M. J. and WEYMAN, D. R. (1974). *Measurement of contributing area in very small drainage basins*. Seminar Paper Series B, No. 3, Department of Geography, University of Bristol. .

KRAUS, K. and PFEIFER, N. (1998). *Determination of terrain models in wooded areas with airborne laser scanner data*. ISPRS Journal of Photogrammetry and Remote Sensing 53(4): 193-203.

LINDENBERGER, J. (2006). *15 Jahre Erfahrung mit Laserscanning in der Praxis*. 6. Vermessungsingenieurtag. Hochschule für Technik Stuttgart (HfT): 30.

MCGLYNN, B. L. and SEIBERT, J. (2003). *Distributed assessment of contributing area and riparian buffering along stream networks*. Water Resources Research 39(4): 2-1 - 2-7.

MEROT, P., EZZAHAR, B., WALTER, C. and AUROUSSEAU, P. (1995). *Mapping waterlogging of soils using digital terrain models*. Hydrological Processes 9: 27-34.

MEROT, P., SQUIVIDANT, H., AUROUSSEAU, P., HEFTING, M., BURT, T., MAITRE, V., KRUKE, M., BUTTURINI, A., THENAIL, C. and VIAUD, V. (2003). *Testing a climato-topographic index for predicting wetlands distribution along an European climate gradient*. Ecological Modelling 163: 51-71.

MICHIELS, H.-G. (2010). *Qualität der digitalierten forstlichen Standortskartierung der FVA*, Abteilung Waldökologie - Forstliche Versuchs- und Forschungsanstalt Baden-Württemberg (FVA), Freiburg. email correspondence, March, 26th.

MOORE, I. D., GRAYSON, R. B. and LADSON, A. R. (1991). *Digital terrain modelling: A review of hydrological, geomorphological, and biological applications*. Hydrological Processes 5(1): 3-30.

MORRIS, D. G. and HEERDEGEN, R. G. (1988). *Automatically derived catchment boundaries and channel networks and their hydrological applications*. Geomorphology 1(2): 131-141.

MOURIER, B., WALTER, C. and MEROT, P. (2008). *Soil distribution in valleys according to stream order*. Catena 72(3): 395-404.

MURPHY, P. N. C., OGILVIE, J. and ARP, P. (2009). *Topographic modelling of soil moisture conditions: a comparison and verification of two models*. European Journal of Soil Science 60(1): 94-109.

O'CALLAGHAN, J. F. and MARK, D. M. (1984). *The extraction of drainage net-works from digital elevation data*. Comput. Vision Graphics Image Process 28: 328–344.

PLANCHON, O. and DARBOUX, F. (2002). *A fast, simple and versatile algorithm to fill the depressions of digital elevation models*. Catena 46(2-3): 159-176.

QUINN, P., BEVEN, K., CHEVALLIER, P. and PLANCHON, O. (1991). *The prediction of hillslope flow paths for distributed hydrological modelling using digital terrain models*. Hydrological Processes 5: 59-79.

QUINN, P. F., BEVEN, K. J. and LAMB, R. (1995). *The ln(a/tan beta) index: How to calculate it and how to use it within the TOPMODEL framework*. Hydrological Processes 9(2): 161-182.

RAGAN, R. M. (1968). *An experimental investigation of partial area contributions*. Berne Symposium, International Association of Science and Hydrology.

RODHE, A. and SEIBERT, J. (1999). *Wetland occurrence in relation to topography: a test of topographic indices as moisture indicators*. Agricultural and Forest Meteorology 98-9: 325-340.

ROSIN, C. (2010) *Development, evaluation, and application of dominant runoff generation processes in hydrological modeling*. University of British Columbia. PhD thesis, Doctor of Philosophy in Forestry: 146

SCHLEYER, A. (2001). *Das Laserscan-DGM von Baden-Württemberg*. S. R. E. FRITSCH D. Photogrammetric Week 2001. Institut für Photogrammetrie, Universität Stuttgart, Wichmann Verlag Heidelberg: 217-225.

SEEMANN, D. (2007). *Forstliche Standortskartierung in Baden-Württemberg*. Auszug aus der Arbeitsanweisung für die Forstliche Standortskartierung in Baden-Württemberg: Stand April 2007 Version 1.13, FVA Baden-Württemberg Abteilung Waldökologie: 36.

SEIBERT, J. and MCGLYNN, B. L. (2007). *A new triangular multiple flow direction algorithm for computing upslope areas from gridded digital elevation models*. Water Resources Research 43(4): -.

SHANLEY, J. B., KENDALL, C., SMITH, T. E., WOLOCK, D. M. and MCDONNELL, J. J. (2001 in press). *Controls on old and new water contributions to stream flow at some nested catchments in Vermont, USA.* Hydrological Processes 15.

SØRENSEN, R. and SEIBERT, J. (2007). *Effects of DEM resolution on the calculation of topographical indices: TWI and its components*. Journal of Hydrology 347(1-2): 79-89.

SØRENSEN, R., ZINKO, U. and SEIBERT, J. (2006). *On the calculation of the topographic wetness index: evaluation of different methods based on field observations*. Hydrology and Earth System Sciences 10(1): 101-112.

TARBOTON, D. G. (1997). *A new method for the determination of flow directions and upslope areas in grid digital elevation models*. Water Resources Research 33: 309-319.

THOMPSON, J. C. and MOORE, R. D. (1996). *Relations between topography and water table depth in a shallow forest soil*. Hydrological Processes 10(11): 1513-1525.

UHLENBROOK, S. and DIDSZUN, J. (2005). *Sättigungsflächenabfluss, Fallbeispiel Haldenbächle, Südschwarzwald*. (ed.). In: Bronstert, A. (Ed.): Abflussbildung – Prozessbeschreibung und Fallbeispiele. Forum für Hydrologie und Wasserbewirtschaftung. 13.05**:** 62-68.

WABOA (2007). *Wasser- und Bodenatlas Baden-Württemberg, 3. Lieferung. Umweltministerium Baden-Würtemmberg, Landesanstalt für Umwelt, Messungen und Naturschutz Baden-Württemberg*.

WALTER, M. T., WALTER, M. F., BROOKS, E. S., STEENHUIS T. S., BOLL J., WEILER K. (2000). *Hydrologically sensitive areas : Variable source area hydrology implications for water quality risk assessment*. Journal of soil and water conservation 55(3): 277-284.

WOLOCK, D. M. and PRICE, C. V. (1994). *Effects of digital elevation model map scale and data resolution on a topography-based watershed model*. Water Resour. Res. 30(11): 3041-3052.

ZEVENBERGEN, L. W. and THORNE, C. R. (1987). *Quantitative analysis of land surface topography*. Earth Surface Processes and Landforms 12: 47-56.

ZHANG, W. and MONTGOMERY, D. R. (1994). *Digital elevation model grid size, landscape representation, and hydrologic simulations*. Water Resour. Res. 30(4): 1019-1028.

ZHAOLIJIAN, LAIZULONG, LIYINGCHENG, XUEYANLI, LIAOMING, WUZHUOLEI, LIUPEI and LIUXIAOLONG (2008). *Application and analyses of airborne LIDAR technology in topographic survey of tidal flat and coastal zone*. ISPRS Congress. The international archives of the photogrammetry, remote sensing and spatial information sciences. Volume XXXVII, Commission III, Part B3b. Beijing 2008: 233-236.

ZOLLINGER, P. (2010). *Qualität der LIDAR DEMs in Baden-Württemberg.*, Fernerkundung - Landesamt für Geoinformation und Landentwicklung Baden-Württemberg (LGL), Karlsruhe. email correspondance, March, 12th, .

URL

[1] http://www.laserdata.at/saga_packages.html, 23/03/2010

[2] http://www.klimadiagramme.de, 31/03/2010

Annex

A.1 Results of validation for the Eyach catchment; grid size 10 m

method	TI - thresholds t	TI - thresholds s	k_a [%]	k_s [%]	k_t [%]	k_{s+t} [%]	k_{as} [%]	bk_s [%]	bk_t [%]	bk_{s+t} [%]	bk_{as} [%]
MD_h4_C25_St	9.97	10.80	67.74	24.24	22.49	23.18	44.39	27.94	24.52	25.86	49.37
MD_h4_C25_Sz	9.96	10.77	67.94	24.96	22.61	23.53	44.87	28.55	24.64	26.17	49.72
MD_h4_C25_Sg	9.82	10.50	65.44	22.24	17.07	19.12	36.09	25.70	19.29	21.83	41.00
MD_h4_C50_St	9.99	10.84	67.77	24.25	22.51	23.19	44.49	27.93	24.58	25.89	49.50
MD_h4_C50_Sz	9.98	10.80	68.02	24.88	22.86	23.65	45.05	28.46	24.92	26.30	49.93
MD_h4_C50_Sg	9.83	10.54	65.56	22.36	17.27	19.29	36.40	25.82	19.57	22.05	41.37
MD_h4_C100_St	9.99	10.87	67.80	24.26	22.76	23.34	44.46	27.89	24.87	26.05	49.48
MD_h4_C100_Sz	9.99	10.83	68.05	24.81	23.11	23.77	45.06	28.35	25.16	26.41	49.94
MD_h4_C100_Sg	9.84	10.56	65.61	22.48	17.50	19.48	36.43	25.93	19.82	22.24	41.42
MD_h8_C25_St	9.90	10.76	67.32	23.44	22.02	22.58	43.25	27.15	24.05	25.26	48.19
MD_h8_C25_Sz	9.89	10.72	67.46	23.88	22.11	22.80	43.62	27.56	24.27	25.55	48.45
MD_h8_C25_Sg	9.74	10.44	64.99	21.29	16.49	18.40	34.90	24.70	18.66	21.06	39.81
MD_h8_C50_St	9.91	10.80	67.32	23.34	22.06	22.56	43.29	27.00	24.12	25.24	48.24
MD_h8_C50_Sz	9.90	10.76	67.47	23.76	22.20	22.81	43.66	27.35	24.33	25.51	48.49
MD_h8_C50_Sg	9.76	10.48	65.09	21.48	16.72	18.61	35.12	24.88	18.91	21.28	40.03
MD_h8_C100_St	9.92	10.82	67.31	23.27	22.17	22.60	43.23	26.92	24.26	25.30	48.20
MD_h8_C100_Sz	9.91	10.78	67.47	23.69	22.29	22.84	43.62	27.27	24.41	25.53	48.47
MD_h8_C100_Sg	9.77	10.49	65.09	21.43	16.80	18.64	35.12	24.86	19.01	21.33	40.05

method	TI - thresholds		k_a	k_s	k_t	k_{s+t}	k_{as}	bk_s	bk_t	bk_{s+t}	bk_{as}
	t	s	[%]	[%]	[%]	[%]	[%]	[%]	[%]	[%]	[%]
MDinf_h1_C25_Sz	9.90	10.74	67.79	24.44	22.51	23.26	44.50	28.10	24.69	26.02	49.33
MDinf_h1_C25_Sg	9.76	10.46	65.32	21.98	16.98	18.96	35.73	25.40	19.05	21.57	40.57
MDinf_h1_C50_St	9.93	10.82	67.64	23.89	22.53	23.06	44.11	27.54	24.66	25.78	49.06
MDinf_h1_C50_Sz	9.92	10.78	67.80	24.32	22.61	23.27	44.56	27.96	24.83	26.06	49.40
MDinf_h1_C50_Sg	9.77	10.50	65.42	22.09	17.19	19.14	35.97	25.49	19.31	21.76	40.83
MDinf_h1_C100_St	9.94	10.83	67.63	23.80	22.58	23.06	44.08	27.47	24.73	25.80	49.05
MDinf_h1_C100_Sz	9.93	10.80	67.80	24.20	22.72	23.30	44.53	27.87	24.96	26.09	49.38
MDinf_h1_C100_Sg	9.78	10.51	65.44	22.13	17.28	19.21	35.98	25.56	19.38	21.83	40.85
MDinf_h4_C0_St	9.95	10.88	67.63	23.51	22.62	22.96	44.16	27.21	24.73	25.70	49.21
MDinf_h4_C0_Sz	9.94	10.84	67.78	23.76	22.79	23.17	44.58	27.47	25.03	25.98	49.54
MDinf_h4_C0_Sg	9.78	10.54	65.53	21.43	16.84	18.67	35.43	24.94	19.08	21.41	40.44
MDinf_h4_C25_St	9.91	10.77	67.49	23.69	22.25	22.81	43.71	27.40	24.35	25.54	48.65
MDinf_h4_C25_Sz	9.90	10.73	67.63	24.08	22.32	23.01	44.12	27.74	24.49	25.75	48.96
MDinf_h4_C25_Sg	9.75	10.45	65.20	21.65	16.84	18.75	35.45	25.07	18.89	21.34	40.30
MDinf_h4_C50_St	9.92	10.81	67.51	23.59	22.36	22.84	43.80	27.26	24.49	25.57	48.74
MDinf_h4_C50_Sz	9.92	10.77	67.66	23.96	22.47	23.05	44.17	27.58	24.69	25.82	49.02
MDinf_h4_C50_Sg	9.77	10.49	65.29	21.71	17.08	18.92	35.66	25.10	19.18	21.53	40.53
MDinf_h4_C100_St	9.93	10.83	67.51	23.57	22.45	22.88	43.76	27.25	24.59	25.63	48.71
MDinf_h4_C100_Sz	9.92	10.79	67.65	23.88	22.57	23.08	44.14	27.52	24.78	25.85	49.01
MDinf_h4_C100_Sg	9.77	10.51	65.31	21.77	17.18	19.00	35.67	25.20	19.29	21.64	40.55
MDinf_h8_C0_St	9.94	10.87	67.57	23.47	22.54	22.91	43.96	27.19	24.67	25.65	49.01
MDinf_h8_C0_Sz	9.94	10.84	67.70	23.64	22.74	23.09	44.33	27.33	24.91	25.86	49.28
MDinf_h8_C0_Sg	9.78	10.53	65.49	21.31	16.84	18.62	35.29	24.82	19.03	21.33	40.30
MDinf_h8_C25_St	9.90	10.77	67.44	23.60	22.24	22.77	43.57	27.31	24.34	25.50	48.52
MDinf_h8_C25_Sz	9.90	10.73	67.55	23.94	22.22	22.89	43.90	27.61	24.39	25.65	48.75
MDinf_h8_C25_Sg	9.75	10.45	65.12	21.51	16.74	18.63	35.23	24.95	18.82	21.25	40.09
MDinf_h8_C50_St	9.92	10.81	67.45	23.49	22.32	22.78	43.62	27.14	24.47	25.51	48.58
MDinf_h8_C50_Sz	9.91	10.77	67.59	23.84	22.44	22.99	43.97	27.46	24.65	25.75	48.82
MDinf_h8_C50_Sg	9.77	10.49	65.23	21.62	17.03	18.86	35.48	25.03	19.15	21.48	40.36
MDinf_h8_C100_St	9.93	10.83	67.46	23.46	22.42	22.83	43.60	27.15	24.59	25.59	48.57
MDinf_h8_C100_Sz	9.92	10.79	67.58	23.69	22.54	22.99	43.93	27.33	24.73	25.75	48.79
MDinf_h8_C100_Sg	9.77	10.51	65.26	21.68	17.15	18.95	35.51	25.11	19.29	21.60	40.41

A.2 Results of validation for the Eyach catchment; grid size 5 m

method	TI - thresholds t	TI - thresholds s	k_a [%]	k_s [%]	k_t [%]	k_{s+t} [%]	k_{as} [%]	bk_s [%]	bk_t [%]	bk_{s+t} [%]	bk_{as} [%]
D8_St	8.53	10.03	62.61	16.27	15.29	15.67	31.01	19.07	17.03	17.82	35.04
D8_Sz	8.50	9.97	62.47	15.45	15.28	15.35	30.74	18.16	16.95	17.42	34.67
D8_Sg	8.34	9.68	61.27	13.15	12.79	12.93	25.11	15.40	14.55	14.88	28.88
MD_h1_C0_St	9.43	10.39	66.65	21.60	21.63	21.62	41.61	25.19	23.87	24.39	46.83
MD_h1_C0_Sz	9.42	10.34	66.74	21.31	21.96	21.71	41.90	24.86	24.14	24.42	47.06
MD_h1_C0_Sg	9.30	10.11	65.07	19.91	17.39	18.38	35.24	23.33	19.85	21.22	40.51
MD_h1_C25_St	9.36	10.20	66.17	21.70	20.88	21.20	40.08	25.26	23.16	23.98	45.11
MD_h1_C25_Sz	9.34	10.15	66.27	21.50	21.21	21.33	40.37	25.03	23.52	24.11	45.34
MD_h1_C25_Sg	9.24	9.95	64.41	19.95	17.04	18.19	34.02	23.29	19.49	20.98	39.04
MD_h1_C50_St	9.38	10.25	66.26	21.60	21.17	21.34	40.32	25.17	23.43	24.11	45.36
MD_h1_C50_Sz	9.36	10.20	66.36	21.38	21.48	21.44	40.62	24.92	23.75	24.20	45.59
MD_h1_C50_Sg	9.26	10.00	64.54	19.96	17.33	18.36	34.38	23.33	19.80	21.19	39.44
MD_h1_C100_St	9.38	10.27	66.31	21.63	21.32	21.44	40.40	25.19	23.55	24.19	45.46
MD_h1_C100_Sz	9.37	10.22	66.39	21.40	21.60	21.52	40.68	24.91	23.83	24.25	45.68
MD_h1_C100_Sg	9.27	10.02	64.57	19.95	17.42	18.42	34.48	23.32	19.88	21.23	39.56
MD_h4_C0_St	9.22	10.20	65.47	20.39	19.66	19.95	38.45	23.93	21.97	22.74	43.49
MD_h4_C0_Sz	9.20	10.13	65.46	19.95	19.88	19.90	38.47	23.44	22.17	22.66	43.44
MD_h4_C0_Sg	9.10	9.90	63.86	18.47	15.68	16.78	31.90	21.74	18.04	19.49	36.86
MD_h4_C25_St	9.16	10.05	65.06	20.28	19.03	19.52	37.22	23.73	21.34	22.27	42.09
MD_h4_C25_Sz	9.34	10.15	66.27	21.50	21.21	21.33	40.37	25.03	23.52	24.11	45.34
MD_h4_C25_Sg	9.05	9.78	63.28	18.31	15.39	16.54	30.98	21.49	17.66	19.17	35.73
MD_h4_C50_St	9.18	10.09	65.13	20.20	19.21	19.59	37.43	23.65	21.53	22.35	42.35
MD_h4_C50_Sz	9.15	10.03	65.12	19.78	19.41	19.56	37.40	23.17	21.63	22.23	42.23
MD_h4_C50_Sg	9.07	9.82	63.39	18.29	15.62	16.67	31.33	21.48	17.89	19.30	36.14
MD_h4_C100_St	9.19	10.12	65.19	20.22	19.35	19.69	37.55	23.70	21.67	22.46	42.49
MD_h4_C100_Sz	9.16	10.05	65.17	19.79	19.58	19.66	37.52	23.21	21.79	22.35	42.35
MD_h4_C100_Sg	9.07	9.84	63.45	18.33	15.73	16.75	31.47	21.53	17.99	19.38	36.30
MD_h8_C0_St	9.11	10.11	64.54	19.38	18.15	18.63	35.97	22.81	20.52	21.41	40.83
MD_h8_C0_Sz	9.08	10.04	64.46	18.96	18.22	18.51	35.75	22.31	20.53	21.22	40.53
MD_h8_C0_Sg	8.99	9.81	62.96	17.11	14.46	15.50	29.48	20.20	16.76	18.11	34.24
MDinf_h1_C0_St	9.13	10.13	64.91	19.91	18.77	19.22	36.90	23.37	21.09	21.98	41.78
MDinf_h1_C0_Sz	9.10	10.07	64.90	19.56	18.94	19.18	36.87	22.94	21.26	21.92	41.69
MDinf_h1_C0_Sg	9.00	9.82	63.31	17.79	14.94	16.06	30.36	20.90	17.24	18.68	35.15
MDinf_h1_C25_St	9.09	10.03	64.71	19.97	18.32	18.96	36.35	23.37	20.60	21.68	41.11
MDinf_h1_C25_Sz	9.06	9.97	64.69	19.57	18.48	18.90	36.30	22.92	20.77	21.60	41.01
MDinf_h1_C25_Sg	8.97	9.74	62.95	17.86	14.84	16.02	30.15	20.95	17.09	18.60	34.78
MDinf_h1_C50_St	9.11	10.07	64.77	19.92	18.53	19.07	36.48	23.32	20.85	21.81	41.28
MDinf_h1_C50_Sz	9.08	10.01	64.75	19.53	18.67	19.00	36.43	22.88	21.00	21.73	41.18
MDinf_h1_C50_Sg	8.99	9.78	63.04	17.91	14.99	16.14	30.38	20.99	17.29	18.75	35.07
MDinf_h1_C100_St	9.11	10.09	64.79	19.82	18.64	19.10	36.53	23.24	20.97	21.85	41.34
MDinf_h1_C100_Sz	9.09	10.03	64.77	19.43	18.80	19.05	36.49	22.79	21.11	21.76	41.24
MDinf_h1_C100_Sg	9.00	9.80	63.06	17.85	15.08	16.16	30.46	20.95	17.38	18.78	35.18
MDinf_h4_C0_St	9.11	10.12	64.69	19.58	18.45	18.89	36.30	23.03	20.79	21.66	41.17
MDinf_h4_C0_Sz	9.09	10.05	64.63	19.15	18.56	18.79	36.16	22.50	20.86	21.50	40.96
MDinf_h4_C0_Sg	9.00	9.81	63.09	17.37	14.64	15.71	29.79	20.47	16.95	18.33	34.57
MDinf_h8_C0_St	9.11	10.11	64.54	19.38	18.15	18.63	35.97	22.81	20.52	21.41	40.83
MDinf_h8_C0_Sz	9.08	10.04	64.46	18.96	18.22	18.51	35.75	22.31	20.53	21.22	40.53
MDinf_h8_C0_Sg	8.99	9.81	62.96	17.11	14.46	15.50	29.48	20.20	16.76	18.11	34.24

A.3 Results of validation for the Eyach catchment; grid size 1 m

method	TI - thresholds		k_a	k_s	k_t	k_{s+t}	k_{as}	bk_s	bk_t	bk_{s+t}	bk_{as}
	t	s	[%]	[%]	[%]	[%]	[%]	[%]	[%]	[%]	[%]
D8_St	5.18	6.81	61.58	14.94	13.98	14.36	27.71	17.37	15.56	16.28	31.41
D8_Sz	5.15	6.69	61.26	13.86	13.81	13.83	26.93	16.19	15.38	15.70	30.57
D8_Sg	5.24	6.60	60.58	12.49	12.65	12.58	25.04	14.64	14.30	14.43	28.70
MD_h1_C0_St	7.36	8.65	62.02	16.02	14.45	15.07	28.83	18.86	16.57	17.47	33.30
MD_h1_C0_Sz	7.34	8.58	61.78	14.79	14.54	14.64	28.23	17.54	16.62	16.98	32.68
MD_h1_C0_Sg	7.41	8.49	60.80	12.95	13.22	13.11	25.43	15.52	15.35	15.42	29.92
MD_h1_C25_St	7.07	8.23	62.43	17.27	14.57	15.64	29.93	20.29	16.58	18.04	34.26
MD_h1_C25_Sz	7.05	8.17	62.18	16.20	14.57	15.21	29.33	19.14	16.55	17.57	33.63
MD_h1_C25_Sg	7.12	8.09	61.21	14.46	13.20	13.70	26.52	17.20	15.23	16.01	30.87
MD_h1_C50_St	7.20	8.40	62.16	16.85	14.38	15.35	29.13	19.82	16.38	17.74	33.45
MD_h1_C50_Sz	7.18	8.33	61.91	15.71	14.42	14.93	28.50	18.61	16.39	17.27	32.80
MD_h1_C50_Sg	7.25	8.26	60.94	13.92	13.13	13.44	25.70	16.62	15.14	15.72	30.02
MD_h1_C100_St	7.27	8.50	62.05	16.59	14.37	15.25	28.77	19.51	16.43	17.65	33.12
MD_h1_C100_Sz	7.25	8.43	61.80	15.42	14.44	14.83	28.14	18.27	16.47	17.18	32.47
MD_h1_C100_Sg	7.32	8.36	60.84	13.72	13.14	13.37	25.42	16.38	15.20	15.67	29.77
MD_h4_C0_St	6.91	8.36	61.34	15.36	13.23	14.07	27.02	18.05	15.23	16.34	31.22
MD_h4_C0_Sz	6.89	8.28	61.06	14.03	13.29	13.58	26.35	16.62	15.26	15.80	30.53
MD_h4_C0_Sg	6.95	8.20	60.16	12.00	12.28	12.17	23.75	14.40	14.28	14.33	27.95
MD_h4_C25_St	6.66	7.96	61.59	16.26	13.03	14.31	27.83	19.09	14.98	16.60	31.96
MD_h4_C25_Sz	6.63	7.89	61.32	15.09	13.03	13.84	27.14	17.83	14.94	16.08	31.24
MD_h4_C25_Sg	6.70	7.83	60.43	13.10	12.05	12.46	24.58	15.66	14.01	14.66	28.70
MD_h4_C50_St	6.77	8.14	61.45	16.00	13.08	14.23	27.32	18.75	15.02	16.49	31.43
MD_h4_C50_Sz	6.75	8.06	61.18	14.75	13.11	13.76	26.64	17.42	15.01	15.96	30.71
MD_h4_C50_Sg	6.82	7.99	60.29	12.76	12.15	12.39	24.07	15.24	14.10	14.55	28.17
MD_h4_C100_St	6.83	8.23	61.35	15.78	13.10	14.15	26.99	18.53	15.06	16.43	31.10
MD_h4_C100_Sz	6.81	8.15	61.07	14.51	13.14	13.68	26.30	17.17	15.07	15.90	30.38
MD_h4_C100_Sg	6.88	8.08	60.20	12.58	12.20	12.35	23.79	15.06	14.17	14.52	27.89
MDinf_h1_C0_St	6.52	8.10	60.54	14.51	11.82	12.88	24.93	17.03	13.78	15.06	28.92
MDinf_h1_C0_Sz	6.49	8.01	60.21	13.07	11.83	12.32	24.12	15.49	13.75	14.44	28.07
MDinf_h1_C0_Sg	6.57	7.93	59.39	10.90	11.03	10.98	21.79	13.14	13.00	13.06	25.78
MDinf_h1_C25_St	6.34	7.76	60.76	15.19	11.66	13.05	25.65	17.83	13.58	15.26	29.62
MDinf_h1_C25_Sz	6.30	7.68	60.43	13.86	11.61	12.50	24.81	16.41	13.50	14.65	28.74
MDinf_h1_C25_Sg	6.39	7.62	59.61	11.73	10.77	11.15	22.53	14.11	12.73	13.28	26.50
MDinf_h1_C50_St	6.43	7.91	60.62	14.81	11.71	12.93	25.19	17.39	13.63	15.11	29.12
MDinf_h1_C50_Sz	6.40	7.83	60.29	13.43	11.70	12.38	24.36	15.90	13.58	14.50	28.26
MDinf_h1_C50_Sg	6.48	7.77	59.47	11.26	10.89	11.04	22.06	13.57	12.85	13.13	26.00
MDinf_h1_C100_St	6.47	8.00	60.56	14.74	11.75	12.93	24.97	17.30	13.68	15.11	28.90
MDinf_h1_C100_Sz	6.44	7.91	60.23	13.34	11.75	12.38	24.14	15.80	13.65	14.50	28.04
MDinf_h1_C100_Sg	6.53	7.85	59.42	11.24	10.96	11.07	21.88	13.53	12.93	13.17	25.81
MDinf_h4_C0_St	6.52	8.09	60.54	14.51	11.83	12.89	24.94	17.03	13.79	15.07	28.93
MDinf_h4_C0_Sz	6.48	8.00	60.22	13.07	11.84	12.33	24.13	15.49	13.77	14.44	28.08
MDinf_h4_C0_Sg	6.56	7.93	59.40	10.90	11.04	10.99	21.81	13.14	13.02	13.07	25.79
MDinf_h4_C25_St	6.33	7.75	60.76	15.19	11.67	13.06	25.66	17.83	13.59	15.26	29.63
MDinf_h4_C25_Sz	6.30	7.67	60.43	13.87	11.63	12.51	24.83	16.41	13.51	14.65	28.76
MDinf_h4_C25_Sg	6.38	7.62	59.62	11.74	10.79	11.17	22.55	14.12	12.75	13.29	26.52
MDinf_h4_C50_St	6.42	7.91	60.62	14.82	11.73	12.95	25.21	17.39	13.65	15.13	29.14
MDinf_h4_C50_Sz	6.39	7.82	60.29	13.43	11.72	12.39	24.38	15.90	13.60	14.51	28.28
MDinf_h4_C50_Sg	6.47	7.76	59.48	11.27	10.91	11.05	22.08	13.57	12.87	13.15	26.02

A.4 Results of validation for the Zastlerbach catchment; grid size 10 m

method	TI - thresholds		k_a	k_s	k_t	k_{s+t}	k_{as}	bk_s	bk_t	bk_{s+t}	bk_{as}
	t	s	[%]	[%]	[%]	[%]	[%]	[%]	[%]	[%]	[%]
D8_St	10.21	10.21	91.60	25.58	0.00	25.41	25.58	36.11	0.00	35.87	36.04
D8_Sz	10.15	10.16	91.54	25.00	0.00	24.84	25.05	35.15	0.00	34.92	35.15
D8_Sg	9.88	9.88	91.81	18.43	0.00	18.31	18.40	27.52	0.00	27.35	27.45
MD_h1_C0_St	10.71	10.72	93.13	39.09	0.00	38.84	39.24	52.31	0.00	51.97	52.39
MD_h1_C0_Sz	10.65	10.66	93.13	39.06	0.00	38.80	39.22	52.04	0.00	51.70	52.15
MD_h1_C0_Sg	10.48	10.48	93.52	35.37	0.00	35.15	35.48	47.87	0.00	47.58	47.97
MD_h1_C25_St	10.09	10.09	92.55	33.96	0.00	33.74	33.97	45.22	0.00	44.93	45.22
MD_h1_C25_Sz	10.04	10.04	92.51	33.61	0.00	33.39	33.67	44.59	0.00	44.30	44.58
MD_h1_C25_Sg	9.96	9.96	93.00	29.77	0.00	29.59	29.69	40.45	0.00	40.21	40.34
MD_h1_C50_St	10.20	10.21	92.65	34.86	0.00	34.64	34.95	46.85	0.00	46.55	46.83
MD_h1_C50_Sz	10.16	10.16	92.61	34.55	0.00	34.32	34.61	45.94	0.00	45.64	45.94
MD_h1_C50_Sg	10.08	10.08	93.10	30.84	0.00	30.66	30.75	41.98	0.00	41.72	41.89
MD_h1_C100_St	10.30	10.30	92.69	35.15	0.00	34.92	35.28	47.26	0.00	46.96	47.33
MD_h1_C100_Sz	10.25	10.26	92.68	35.06	0.00	34.83	35.23	46.49	0.00	46.19	46.58
MD_h1_C100_Sg	10.16	10.17	93.13	30.99	2.22	30.82	31.06	41.91	0.00	41.66	42.03
MD_h4_C0_St	10.41	10.42	92.84	36.47	0.00	36.23	36.62	48.73	0.00	48.41	48.76
MD_h4_C0_Sz	10.35	10.36	92.82	36.33	0.00	36.09	36.46	48.12	0.00	47.81	48.20
MD_h4_C0_Sg	10.18	10.19	93.25	32.70	0.00	32.50	32.73	44.15	0.00	43.88	44.18
MD_h4_C25_St	10.00	10.00	92.24	31.21	0.00	31.01	31.25	42.59	0.00	42.31	42.59
MD_h4_C25_Sz	9.94	9.95	92.22	31.02	0.00	30.82	31.07	41.99	0.00	41.72	41.95
MD_h4_C25_Sg	9.85	9.85	92.62	25.94	0.00	25.78	25.90	36.05	0.00	35.83	35.98
MD_h4_C50_St	10.10	10.10	92.30	31.79	0.00	31.58	31.84	43.53	0.00	43.25	43.54
MD_h4_C50_Sz	10.04	10.04	92.25	31.27	0.00	31.07	31.32	42.52	0.00	42.24	42.52
MD_h4_C50_Sg	9.94	9.95	92.64	26.24	0.00	26.08	26.14	36.90	0.00	36.67	36.78
MD_h4_C100_St	10.15	10.16	92.35	32.19	0.00	31.98	32.30	44.18	0.00	43.89	44.23
MD_h4_C100_Sz	10.10	10.10	92.31	31.78	0.00	31.57	31.88	43.15	0.00	42.87	43.21
MD_h4_C100_Sg	10.00	10.00	92.73	27.04	0.00	26.88	27.01	37.88	0.00	37.65	37.86
MD_h8_C0_St	10.31	10.32	92.55	33.92	0.00	33.70	34.04	45.60	0.00	45.30	45.68
MD_h8_C0_Sz	10.25	10.26	92.51	33.60	0.00	33.38	33.71	44.90	0.00	44.61	44.98
MD_h8_C0_Sg	10.07	10.07	92.94	29.58	0.00	29.40	29.61	40.08	0.00	39.84	40.10
MDinf_h1_C0_St	10.27	10.28	92.48	33.33	0.00	33.11	33.46	44.73	0.00	44.44	44.79
MDinf_h1_C0_Sz	10.20	10.21	92.44	32.94	0.00	32.72	33.04	43.91	0.00	43.62	43.91
MDinf_h1_C0_Sg	10.04	10.05	92.81	28.31	0.00	28.14	28.33	38.53	0.00	38.30	38.54
MDinf_h1_C25_St	10.00	10.01	92.03	29.32	0.00	29.13	29.36	40.41	0.00	40.14	40.40
MDinf_h1_C25_Sz	9.95	9.96	91.99	28.95	0.00	28.76	29.02	39.63	0.00	39.37	39.63
MDinf_h1_C25_Sg	9.81	9.82	92.43	24.10	0.00	23.95	24.06	33.77	0.00	33.57	33.72
MDinf_h1_C50_St	10.08	10.08	92.09	29.86	0.00	29.67	29.91	41.13	0.00	40.87	41.12
MDinf_h1_C50_Sz	10.02	10.03	92.03	29.37	0.00	29.18	29.42	40.27	0.00	40.00	40.29
MDinf_h1_C50_Sg	9.90	9.90	92.47	24.41	0.00	24.26	24.37	34.24	0.00	34.03	34.19
MDinf_h1_C100_St	10.13	10.13	92.13	30.21	0.00	30.02	30.38	41.76	0.00	41.48	41.87
MDinf_h1_C100_Sz	10.08	10.08	92.07	29.69	0.00	29.49	29.81	40.77	0.00	40.50	40.88
MDinf_h1_C100_Sg	9.94	9.95	92.52	24.91	0.00	24.76	24.94	34.89	0.00	34.68	34.95
MDinf_h4_C0_St	10.27	10.28	92.47	33.23	0.00	33.01	33.34	44.61	0.00	44.32	44.68
MDinf_h4_C0_Sz	10.20	10.21	92.42	32.80	0.00	32.58	32.91	43.81	0.00	43.53	43.86
MDinf_h4_C0_Sg	10.04	10.04	92.80	28.24	0.00	28.07	28.20	38.49	0.00	38.26	38.42
MDinf_h8_C0_St	10.27	10.28	92.46	33.17	0.00	32.96	33.26	44.56	0.00	44.27	44.60
MDinf_h8_C0_Sz	10.20	10.21	92.41	32.74	0.00	32.52	32.83	43.71	0.00	43.42	43.74
MDinf_h8_C0_Sg	10.04	10.04	92.80	28.24	0.00	28.07	28.19	38.49	0.00	38.26	38.42

A.5 Results of validation for the Zastlerbach catchment; grid size 5 m

method	TI - thresholds t	s	k_a [%]	k_s [%]	k_t [%]	k_{s+t} [%]	k_{as} [%]	bk_s [%]	bk_t [%]	bk_{s+t} [%]	bk_{as} [%]
D8_St	9.33	9.34	90.77	18.31	0.00	18.19	18.34	26.68	0.00	26.50	26.66
D8_Sz	9.29	9.30	90.74	18.00	0.00	17.88	18.05	26.22	0.00	26.04	26.20
D8_Sg	9.15	9.16	90.83	14.30	0.00	14.21	14.27	21.62	0.00	21.48	21.58
MD_h1_C0_St	9.80	9.81	92.63	34.75	0.00	34.51	34.87	45.97	0.00	45.66	46.06
MD_h1_C0_Sz	9.75	9.76	92.63	34.79	0.00	34.55	34.94	45.92	0.00	45.61	46.02
MD_h1_C0_Sg	9.68	9.69	92.90	33.61	0.00	33.39	33.66	44.64	0.00	44.35	44.68
MD_h1_C25_St	9.35	9.36	91.78	27.25	0.00	27.06	27.28	37.30	0.00	37.05	37.28
MD_h1_C25_Sz	9.31	9.32	91.77	27.15	0.00	26.97	27.17	36.99	0.00	36.73	36.94
MD_h1_C25_Sg	9.30	9.31	92.08	25.64	0.00	25.47	25.59	35.25	0.00	35.02	35.20
MD_h1_C50_St	9.45	9.46	91.89	28.19	0.00	28.00	28.24	38.77	0.00	38.50	38.77
MD_h1_C50_Sz	9.41	9.42	91.89	28.22	0.00	28.03	28.25	38.66	0.00	38.39	38.65
MD_h1_C50_Sg	9.40	9.40	92.16	26.41	0.00	26.24	26.35	36.71	0.00	36.48	36.65
MD_h1_C100_St	9.54	9.54	92.03	29.46	0.00	29.26	29.60	39.94	0.00	39.67	40.06
MD_h1_C100_Sz	9.49	9.50	92.03	29.46	0.00	29.26	29.59	39.77	0.00	39.50	39.91
MD_h1_C100_Sg	9.47	9.47	92.31	27.74	0.00	27.57	27.82	38.06	0.00	37.82	38.17
MD_h4_C0_St	9.54	9.55	92.11	30.13	0.00	29.93	30.29	40.64	0.43	40.36	40.70
MD_h4_C0_Sz	9.49	9.50	92.11	30.10	0.00	29.90	30.23	40.56	0.00	40.29	40.61
MD_h4_C0_Sg	9.43	9.44	92.34	28.38	0.00	28.20	28.45	38.46	0.49	38.22	38.52
MD_h4_C25_St	9.22	9.23	91.47	24.54	0.00	24.37	24.57	34.06	0.00	33.83	34.05
MD_h4_C25_Sz	9.18	9.18	91.44	24.24	0.00	24.07	24.27	33.56	0.00	33.34	33.54
MD_h4_C25_Sg	9.16	9.16	91.72	22.32	0.00	22.18	22.26	31.31	0.00	31.11	31.25
MD_h4_C50_St	9.31	9.32	91.56	25.33	0.43	25.16	25.35	35.28	0.43	35.04	35.26
MD_h4_C50_Sz	9.26	9.27	91.54	25.10	0.00	24.93	25.15	34.84	0.00	34.60	34.84
MD_h4_C50_Sg	9.24	9.25	91.82	23.24	0.00	23.09	23.19	32.70	0.00	32.49	32.66
MD_h4_C100_St	9.37	9.38	91.68	26.27	0.00	26.09	26.42	36.43	0.00	36.18	36.52
MD_h4_C100_Sz	9.32	9.33	91.65	26.10	0.00	25.92	26.19	35.98	0.43	35.74	36.02
MD_h4_C100_Sg	9.30	9.30	91.92	24.13	0.00	23.98	24.20	33.81	0.00	33.60	33.88
MD_h8_C0_St	9.44	9.45	91.81	27.46	0.00	27.27	27.54	37.50	0.00	37.24	37.50
MD_h8_C0_Sz	9.39	9.39	91.78	27.19	0.43	27.01	27.30	37.08	0.86	36.84	37.12
MD_h8_C0_Sg	9.32	9.33	92.01	25.32	0.00	25.15	25.32	34.87	0.00	34.65	34.84
MDinf_h1_C0_St	9.40	9.41	91.74	26.90	0.00	26.72	27.00	36.79	0.00	36.54	36.81
MDinf_h1_C0_Sz	9.35	9.36	91.72	26.67	0.00	26.49	26.77	36.38	0.00	36.14	36.45
MDinf_h1_C0_Sg	9.29	9.30	91.93	24.57	0.00	24.41	24.61	33.87	0.00	33.65	33.90
MDinf_h1_C25_St	9.19	9.20	91.31	23.10	0.43	22.95	23.13	32.27	0.43	32.05	32.24
MDinf_h1_C25_Sz	9.15	9.16	91.29	22.91	0.43	22.76	22.93	31.93	0.00	31.71	31.92
MDinf_h1_C25_Sg	9.11	9.12	91.54	20.56	0.00	20.42	20.53	29.08	0.00	28.89	29.05
MDinf_h1_C50_St	9.26	9.26	91.37	23.59	0.00	23.43	23.61	33.08	0.43	32.86	33.04
MDinf_h1_C50_Sz	9.21	9.22	91.34	23.36	0.00	23.20	23.36	32.69	0.00	32.47	32.64
MDinf_h1_C50_Sg	9.18	9.18	91.59	21.03	0.00	20.90	20.99	29.91	0.00	29.72	29.84
MDinf_h1_C100_St	9.31	9.31	91.47	24.49	0.00	24.32	24.58	34.35	0.00	34.12	34.38
MDinf_h1_C100_Sz	9.26	9.27	91.44	24.22	0.00	24.05	24.31	33.85	0.00	33.62	33.90
MDinf_h1_C100_Sg	9.22	9.22	91.69	21.95	0.00	21.81	21.96	31.21	0.00	31.01	31.21
MDinf_h4_C0_St	9.40	9.40	91.72	26.72	0.00	26.54	26.81	36.57	0.00	36.32	36.61
MDinf_h4_C0_Sz	9.35	9.36	91.70	26.51	0.00	26.33	26.61	36.24	0.00	35.99	36.29
MDinf_h4_C0_Sg	9.29	9.30	91.91	24.38	0.00	24.22	24.41	33.64	0.00	33.43	33.66
MDinf_h8_C0_St	9.39	9.40	91.70	26.54	0.00	26.36	26.63	36.41	0.00	36.16	36.42
MDinf_h8_C0_Sz	9.35	9.35	91.68	26.33	0.43	26.16	26.39	36.04	0.00	35.80	36.06
MDinf_h8_C0_Sg	9.29	9.30	91.89	24.20	0.00	24.04	24.21	33.42	0.00	33.21	33.42

A.6 Results of validation for the Zastlerbach catchment; grid size 1 m

method	TI - thresholds t	TI - thresholds s	k_a [%]	k_s [%]	k_t [%]	k_{s+t} [%]	k_{as} [%]	bk_s [%]	bk_t [%]	bk_{s+t} [%]	bk_{as} [%]
D8_St	6.80	6.81	89.88	9.12	0.00	9.06	9.13	13.80	0.02	13.71	13.80
D8_Sz	6.77	6.78	89.87	8.98	0.00	8.92	8.99	13.62	0.02	13.53	13.62
D8_Sg	6.80	6.81	89.89	9.13	0.02	9.07	9.14	13.89	0.02	13.80	13.90
MD_h1_C0_St	8.03	8.04	91.18	21.77	0.05	21.63	21.88	30.55	0.07	30.35	30.61
MD_h1_C0_Sz	8.01	8.02	91.17	21.74	0.00	21.59	21.85	30.53	0.05	30.33	30.59
MD_h1_C0_Sg	8.01	8.02	91.32	21.92	0.00	21.78	22.00	30.85	0.00	30.65	30.89
MD_h1_C25_St	7.70	7.71	90.65	17.14	0.02	17.03	17.13	24.29	0.02	24.13	24.26
MD_h1_C25_Sz	7.69	7.69	90.64	17.03	0.02	16.92	17.03	24.16	0.02	24.00	24.14
MD_h1_C25_Sg	7.72	7.73	90.83	17.58	0.02	17.47	17.56	25.09	0.00	24.92	25.04
MD_h1_C50_St	7.80	7.81	90.73	17.87	0.02	17.75	17.86	25.61	0.05	25.45	25.58
MD_h1_C50_Sz	7.78	7.79	90.72	17.75	0.02	17.64	17.75	25.49	0.02	25.32	25.46
MD_h1_C50_Sg	7.81	7.81	90.90	18.23	0.00	18.11	18.20	26.31	0.02	26.14	26.27
MD_h1_C100_St	7.86	7.87	90.83	18.75	0.00	18.63	18.75	26.78	0.00	26.60	26.75
MD_h1_C100_Sz	7.84	7.85	90.82	18.68	0.02	18.55	18.66	26.69	0.02	26.51	26.65
MD_h1_C100_Sg	7.87	7.88	91.01	19.08	0.00	18.95	19.05	27.42	0.00	27.24	27.38
MD_h4_C0_St	7.80	7.81	90.80	18.43	0.04	18.31	18.52	26.25	0.05	26.08	26.31
MD_h4_C0_Sz	7.78	7.79	90.79	18.36	0.02	18.24	18.45	26.17	0.00	26.00	26.22
MD_h4_C0_Sg	7.78	7.79	90.90	18.15	0.02	18.03	18.21	26.02	0.02	25.85	26.06
MD_h4_C25_St	7.50	7.51	90.35	14.43	0.00	14.33	14.43	20.90	0.02	20.76	20.88
MD_h4_C25_Sz	7.48	7.49	90.33	14.29	0.02	14.20	14.29	20.74	0.02	20.60	20.73
MD_h4_C25_Sg	7.50	7.51	90.48	14.44	0.00	14.35	14.43	21.11	0.02	20.97	21.09
MD_h4_C50_St	7.61	7.62	90.45	15.32	0.02	15.22	15.32	22.36	0.02	22.21	22.34
MD_h4_C50_Sz	7.60	7.60	90.43	15.19	0.00	15.09	15.19	22.22	0.00	22.07	22.20
MD_h4_C50_Sg	7.62	7.62	90.57	15.24	0.04	15.14	15.22	22.48	0.07	22.33	22.45
MD_h4_C100_St	7.66	7.67	90.52	16.00	0.02	15.90	16.00	23.31	0.04	23.16	23.29
MD_h4_C100_Sz	7.64	7.65	90.51	15.88	0.02	15.77	15.88	23.17	0.04	23.02	23.16
MD_h4_C100_Sg	7.66	7.67	90.65	15.83	0.00	15.73	15.82	23.30	0.00	23.15	23.27
MDinf_h1_C0_St	7.64	7.65	90.47	15.52	0.02	15.42	15.57	22.45	0.05	22.30	22.49
MDinf_h1_C0_Sz	7.62	7.63	90.46	15.42	0.04	15.32	15.47	22.33	0.02	22.18	22.37
MDinf_h1_C0_Sg	7.62	7.63	90.56	15.16	0.05	15.06	15.18	22.07	0.07	21.93	22.10
MDinf_h1_C25_St	7.42	7.43	90.19	13.05	0.02	12.97	13.06	19.17	0.02	19.05	19.17
MDinf_h1_C25_Sz	7.40	7.40	90.18	12.92	0.02	12.84	12.93	19.02	0.02	18.89	19.01
MDinf_h1_C25_Sg	7.41	7.42	90.31	12.93	0.04	12.85	12.92	19.17	0.04	19.04	19.15
MDinf_h1_C50_St	7.51	7.51	90.24	13.51	0.02	13.43	13.52	19.89	0.02	19.76	19.88
MDinf_h1_C50_Sz	7.49	7.49	90.23	13.38	0.02	13.30	13.38	19.73	0.02	19.60	19.72
MDinf_h1_C50_Sg	7.50	7.51	90.35	13.31	0.00	13.22	13.29	19.77	0.00	19.65	19.75
MDinf_h1_C100_St	7.55	7.56	90.30	14.05	0.02	13.96	14.06	20.78	0.00	20.64	20.76
MDinf_h1_C100_Sz	7.53	7.54	90.29	13.92	0.00	13.83	13.92	20.62	0.00	20.49	20.61
MDinf_h1_C100_Sg	7.55	7.55	90.42	13.80	0.00	13.71	13.78	20.60	0.02	20.47	20.57
MDinf_h4_C0_St	7.64	7.65	90.47	15.51	0.05	15.40	15.56	22.43	0.07	22.29	22.47
MDinf_h4_C0_Sz	7.62	7.63	90.46	15.40	0.07	15.30	15.44	22.31	0.05	22.16	22.35
MDinf_h4_C0_Sg	7.62	7.63	90.56	15.14	0.02	15.04	15.16	22.06	0.02	21.91	22.08
MDinf_h4_C25_St	7.50	7.51	90.35	14.43	0.00	14.33	14.43	20.90	0.02	20.76	20.88
MDinf_h4_C25_Sz	7.48	7.49	90.33	14.29	0.02	14.20	14.29	20.74	0.02	20.60	20.73
MDinf_h4_C25_Sg	7.41	7.42	90.31	12.91	0.04	12.83	12.89	19.16	0.02	19.04	19.14
MDinf_h4_C50_St	7.50	7.51	90.24	13.51	0.02	13.42	13.51	19.90	0.05	19.77	19.89
MDinf_h4_C50_Sz	7.48	7.49	90.23	13.38	0.02	13.29	13.38	19.74	0.04	19.61	19.72
MDinf_h4_C50_Sg	7.50	7.50	90.35	13.31	0.00	13.22	13.29	19.80	0.00	19.67	19.78

A.7 Results of validation for the Acher catchment; grid size 10 m

method	TI - thresholds		k_a	k_s	k_t	k_{s+t}	k_{as}	bk_s	bk_t	bk_{s+t}	bk_{as}
	t	s	[%]	[%]	[%]	[%]	[%]	[%]	[%]	[%]	[%]
D8_St	9.64	10.11	85.47	22.63	4.13	16.24	27.15	27.49	5.04	19.74	32.37
D8_Sz	9.61	10.07	85.41	22.36	3.99	16.02	26.77	27.20	4.93	19.51	31.95
D8_Sg	9.55	9.88	85.71	14.21	4.73	10.93	18.18	18.58	5.72	14.12	23.17
MD_h1_C0_St	10.05	10.50	87.45	32.92	8.12	24.35	40.37	39.63	9.51	29.22	47.66
MD_h1_C0_Sz	10.03	10.46	87.47	33.19	8.37	24.62	40.31	39.81	9.73	29.42	47.60
MD_h1_C0_Sg	9.96	10.30	87.89	27.32	7.84	20.57	33.89	34.27	9.57	25.71	41.58
MD_h1_C25_St	9.84	10.19	86.35	26.95	6.06	19.73	33.20	32.74	7.16	23.90	39.46
MD_h1_C25_Sz	9.82	10.15	86.30	26.87	5.83	19.60	32.80	32.72	6.90	23.80	39.02
MD_h1_C25_Sg	9.78	10.04	86.61	20.56	6.06	15.54	26.13	26.42	7.33	19.81	32.69
MD_h1_C50_St	9.92	10.28	86.45	26.63	6.83	19.79	34.16	32.60	8.08	24.13	40.68
MD_h1_C50_Sz	9.89	10.25	86.40	26.53	6.85	19.73	33.74	32.56	8.22	24.15	40.33
MD_h1_C50_Sg	9.85	10.13	86.73	20.52	6.63	15.71	27.35	26.46	7.96	20.05	34.22
MD_h1_C100_St	9.94	10.32	86.53	26.61	6.93	19.81	35.05	32.68	8.16	24.21	41.78
MD_h1_C100_Sz	9.91	10.29	86.50	26.76	7.07	19.96	34.56	32.85	8.36	24.39	41.32
MD_h1_C100_Sg	9.87	10.16	86.82	20.71	6.59	15.82	28.32	26.79	8.04	20.29	35.44
MD_h4_C0_St	9.84	10.28	86.90	30.16	7.14	22.20	36.67	35.92	8.50	26.44	43.24
MD_h4_C0_Sz	9.81	10.24	86.91	30.21	7.23	22.27	36.64	35.89	8.45	26.41	43.23
MD_h4_C0_Sg	9.75	10.08	87.25	23.54	6.63	17.69	29.40	29.40	7.95	21.97	36.01
MD_h4_C25_St	9.69	10.03	86.18	26.05	5.76	19.04	32.05	31.58	7.00	23.09	38.23
MD_h4_C25_Sz	9.66	10.00	86.14	25.83	5.65	18.86	31.76	31.42	6.78	22.91	37.92
MD_h4_C25_Sg	9.62	9.89	86.39	18.85	5.86	14.35	24.71	24.42	7.18	18.45	31.00
MD_h4_C50_St	9.75	10.13	86.30	26.40	6.53	19.54	32.82	32.12	7.69	23.68	39.19
MD_h4_C50_Sz	9.72	10.10	86.27	26.19	6.72	19.46	32.58	31.91	7.98	23.64	38.96
MD_h4_C50_Sg	9.68	9.97	86.55	19.61	6.88	15.20	25.72	25.29	8.29	19.40	32.14
MD_h4_C100_St	9.78	10.17	86.36	26.37	6.83	19.62	33.37	32.07	8.07	23.77	39.84
MD_h4_C100_Sz	9.75	10.13	86.31	26.01	6.72	19.34	33.11	31.77	8.00	23.56	39.58
MD_h4_C100_Sg	9.70	10.00	86.60	19.58	6.90	15.19	26.34	25.26	8.32	19.39	32.84
MD_h8_C0_St	9.76	10.20	86.57	28.50	6.17	20.78	34.46	34.13	7.36	24.88	40.66
MD_h8_C0_Sz	9.73	10.16	86.55	28.52	6.24	20.82	34.26	34.11	7.41	24.89	40.42
MD_h8_C0_Sg	9.67	9.99	86.89	21.63	5.91	16.19	26.73	27.13	7.18	20.22	32.99
MDinf_h1_C0_St	9.75	10.18	86.46	27.86	5.83	20.25	33.83	33.44	6.92	24.28	40.02
MDinf_h1_C0_Sz	9.71	10.14	86.45	27.84	6.01	20.30	33.62	33.41	7.01	24.29	39.78
MDinf_h1_C0_Sg	9.66	9.98	86.80	20.89	5.77	15.65	26.18	26.33	6.88	19.59	32.32
MDinf_h1_C25_St	9.64	10.01	86.13	26.02	5.53	18.94	31.54	31.53	6.51	22.89	37.48
MDinf_h1_C25_Sz	9.61	9.97	86.09	26.02	5.52	18.93	31.16	31.54	6.40	22.85	37.13
MDinf_h1_C25_Sg	9.57	9.85	86.26	18.70	5.06	13.97	23.61	23.95	6.23	17.81	29.55
MDinf_h1_C50_St	9.70	10.09	86.25	26.69	5.76	19.46	32.34	32.35	6.92	23.56	38.53
MDinf_h1_C50_Sz	9.67	10.06	86.22	26.59	5.76	19.40	32.05	32.23	6.85	23.46	38.22
MDinf_h1_C50_Sg	9.62	9.92	86.43	19.65	5.52	14.75	24.76	25.08	6.68	18.71	30.89
MDinf_h1_C100_St	9.72	10.13	86.27	26.49	5.95	19.39	32.60	32.16	7.10	23.50	38.78
MDinf_h1_C100_Sz	9.69	10.09	86.23	26.40	5.85	19.30	32.32	32.01	6.92	23.34	38.48
MDinf_h1_C100_Sg	9.64	9.95	86.46	19.62	5.71	14.80	25.13	25.03	6.87	18.74	31.24
MDinf_h4_C0_St	9.74	10.18	86.44	27.75	5.74	20.14	33.73	33.36	6.78	24.18	39.92
MDinf_h4_C0_Sz	9.71	10.13	86.42	27.74	5.86	20.18	33.51	33.35	6.89	24.21	39.67
MDinf_h4_C0_Sg	9.65	9.98	86.79	20.82	5.82	15.62	26.03	26.32	6.91	19.60	32.19
MDinf_h8_C0_St	9.74	10.18	86.42	27.68	5.58	20.05	33.65	33.32	6.65	24.11	39.86
MDinf_h8_C0_Sz	9.71	10.13	86.40	27.64	5.76	20.08	33.37	33.25	6.79	24.11	39.55
MDinf_h8_C0_Sg	9.65	9.98	86.76	20.73	5.60	15.49	25.89	26.26	6.84	19.53	32.08

A.8 Results of validation for the Acher catchment; grid size 5 m

method	TI - thresholds		k_a	k_s	k_t	k_{s+t}	k_{as}	bk_s	bk_t	bk_{s+t}	bk_{as}
	t	s	[%]	[%]	[%]	[%]	[%]	[%]	[%]	[%]	[%]
D8_St	8.76	9.26	84.35	16.78	4.43	12.45	20.66	20.94	5.60	15.56	25.43
D8_Sz	8.72	9.21	84.30	16.58	4.37	12.29	20.32	20.72	5.45	15.36	25.08
D8_Sg	8.70	9.12	84.20	11.51	3.51	8.69	14.99	15.29	4.58	11.51	19.48
MD_h1_C0_St	9.27	9.70	86.37	28.13	6.68	20.60	34.07	33.94	7.86	24.79	40.49
MD_h1_C0_Sz	9.24	9.65	86.42	28.40	6.81	20.83	34.35	34.25	7.94	25.02	40.76
MD_h1_C0_Sg	9.23	9.59	86.56	24.71	7.40	18.61	31.38	30.39	8.69	22.73	37.90
MD_h1_C25_St	9.07	9.42	85.50	22.58	6.10	16.79	28.58	28.43	7.11	20.94	34.80
MD_h1_C25_Sz	9.03	9.38	85.53	22.72	6.34	16.97	28.75	28.65	7.31	21.16	35.07
MD_h1_C25_Sg	9.04	9.33	85.63	18.75	6.32	14.37	25.26	24.65	7.35	18.55	31.64
MD_h1_C50_St	9.15	9.53	85.56	22.75	6.41	17.01	29.03	28.52	7.40	21.11	35.23
MD_h1_C50_Sz	9.12	9.48	85.57	22.88	6.55	17.15	29.05	28.67	7.52	21.21	35.47
MD_h1_C50_Sg	9.12	9.43	85.72	18.91	6.84	14.65	26.00	24.64	7.94	18.75	32.37
MD_h1_C100_St	9.19	9.57	85.64	22.83	6.43	17.07	29.80	28.60	7.48	21.19	36.12
MD_h1_C100_Sz	9.15	9.53	85.64	22.91	6.50	17.15	29.75	28.71	7.53	21.27	36.14
MD_h1_C100_Sg	9.16	9.48	85.81	19.08	6.96	14.81	26.82	24.75	8.09	18.87	33.30
MD_h4_C0_St	9.06	9.51	85.78	24.78	6.00	18.19	30.18	30.23	7.06	22.10	36.23
MD_h4_C0_Sz	9.02	9.45	85.79	24.84	6.05	18.24	30.30	30.29	7.08	22.14	36.39
MD_h4_C0_Sg	9.02	9.39	85.88	20.79	6.18	15.63	26.81	25.99	7.31	19.40	32.86
MD_h4_C25_St	8.88	9.24	85.20	21.00	5.70	15.63	26.55	26.17	6.67	19.32	32.32
MD_h4_C25_Sz	8.83	9.18	85.20	20.95	5.85	15.65	26.60	26.23	6.84	19.42	32.39
MD_h4_C25_Sg	8.85	9.15	85.25	16.73	5.57	12.79	22.65	21.85	6.69	16.50	28.48
MD_h4_C50_St	8.96	9.35	85.28	21.47	5.88	16.00	27.09	26.95	6.85	19.89	33.11
MD_h4_C50_Sz	8.91	9.30	85.29	21.42	6.04	16.02	27.17	26.92	7.08	19.96	33.23
MD_h4_C50_Sg	8.92	9.26	85.37	17.33	5.90	13.30	23.43	22.63	6.94	17.10	29.47
MD_h4_C100_St	8.99	9.40	85.32	21.61	5.88	16.09	27.39	27.14	6.83	20.01	33.46
MD_h4_C100_Sz	8.95	9.34	85.32	21.59	6.03	16.12	27.40	27.14	7.01	20.08	33.51
MD_h4_C100_Sg	8.96	9.30	85.42	17.51	6.09	13.49	23.86	22.85	7.18	17.32	29.97
MD_h8_C0_St	8.98	9.42	85.43	22.89	5.61	16.82	27.79	28.17	6.65	20.62	33.62
MD_h8_C0_Sz	8.93	9.36	85.42	22.78	5.71	16.79	27.79	28.08	6.76	20.60	33.68
MD_h8_C0_Sg	8.93	9.30	85.47	18.69	5.31	13.97	23.85	23.80	6.44	17.68	29.68
MDinf_h1_C0_St	8.97	9.41	85.34	22.38	5.45	16.44	27.28	27.64	6.41	20.19	33.10
MDinf_h1_C0_Sz	8.92	9.35	85.35	22.37	5.50	16.45	27.34	27.65	6.50	20.23	33.21
MDinf_h1_C0_Sg	8.92	9.29	85.40	18.23	5.36	13.69	23.33	23.27	6.47	17.34	29.14
MDinf_h1_C25_St	8.82	9.21	85.05	20.51	5.49	15.24	25.39	25.59	6.49	18.88	30.89
MDinf_h1_C25_Sz	8.78	9.15	85.04	20.45	5.51	15.21	25.31	25.54	6.52	18.86	30.84
MDinf_h1_C25_Sg	8.79	9.10	85.04	15.95	4.91	12.06	20.96	20.74	6.06	15.56	26.44
MDinf_h1_C50_St	8.89	9.29	85.12	20.96	5.43	15.51	25.82	26.23	6.43	19.28	31.54
MDinf_h1_C50_Sz	8.84	9.23	85.11	20.91	5.54	15.52	25.78	26.23	6.49	19.30	31.51
MDinf_h1_C50_Sg	8.85	9.18	85.12	16.56	5.08	12.51	21.47	21.58	6.22	16.17	27.16
MDinf_h1_C100_St	8.93	9.35	85.15	21.07	5.53	15.62	26.04	26.37	6.49	19.39	31.79
MDinf_h1_C100_Sz	8.88	9.29	85.15	21.07	5.61	15.64	26.02	26.40	6.63	19.46	31.83
MDinf_h1_C100_Sg	8.89	9.23	85.18	16.79	5.34	12.75	21.91	21.86	6.42	16.41	27.66
MDinf_h4_C0_St	8.96	9.40	85.33	22.28	5.49	16.38	27.23	27.55	6.46	20.15	33.03
MDinf_h4_C0_Sz	8.91	9.34	85.33	22.26	5.42	16.35	27.22	27.55	6.42	20.13	33.08
MDinf_h4_C0_Sg	8.91	9.28	85.39	18.15	5.48	13.68	23.26	23.19	6.64	17.35	29.07
MDinf_h8_C0_St	8.95	9.40	85.31	22.14	5.50	16.30	27.11	27.44	6.48	20.08	32.93
MDinf_h8_C0_Sz	8.91	9.34	85.31	22.10	5.45	16.26	27.10	27.42	6.49	20.07	32.98
MDinf_h8_C0_Sg	8.91	9.28	85.36	17.98	5.38	13.53	23.07	23.04	6.55	17.22	28.87

Eidesstattliche Erklärung

Hiermit erkläre ich, dass die Arbeit selbständig und nur unter Verwendung der angegebenen Hilfsmittel angefertigt wurde.

Ort, Datum

Volker Rothmund